



UNIVERSITÀ
DEGLI STUDI
FIRENZE

DOTTORATO DI RICERCA IN
NEUROSCIENZE

CICLO XXXVI

COORDINATORE Prof.ssa Maria Pia Amato

**Behavioural, pupillometric and imaging
evidence of experience-dependent changes in
visual perception**

Settore Scientifico Disciplinare BIO /09

Dottoranda

Dott.ssa Acquafredda Miriam

Tutore

Prof.ssa Paola Binda

Coordinatore

Prof.ssa Maria Pia Amato

(firma)

Anni 2020/2023

Summary

This thesis presents four experiments involving adult human participants, where we combined a range of techniques (psychophysics, pupillometry and neuroimaging) to explore the many ways in which sensory processing adapts to the context, as set by behavioural goals (attention) or experience (sensory deprivation).

Chapter 1 (General Introduction) presents our main methodological tools: binocular rivalry, the classical paradigm to investigate ocular dominance and binocular vision; pupillometry, a non-invasive technique to index the strength of visual representations; monocular deprivation, a standard paradigm to boost or suppress visual cortical representations; and functional MRI (magnetic resonance imaging), which allowed us to study the functional connectivity of the visual brain at rest.

In chapter 2, we analyzed the reliability of a set of indices that may be extracted from binocular rivalry and have been traditionally associated with a variety of perceptual and cognitive functions. On the one hand, our findings advise caution when interpreting the association between stable psychological characteristics (e.g., personality traits) and the rate of switching or the probability of fused percepts, given the state-dependent variability of these parameters. On the other hand, they provide strong support for the use of binocular rivalry to track ocular dominance, given the excellent stability and reliability of this parameter. Chapter 3 proceeded to using this binocular rivalry-based index of ocular dominance for investigating the effects of endogenous cueing. We combined this with a pupillometry measurement, to objectively index the dominance of the two stimuli during rivalry. We found that attention biases binocular rivalry dynamics, boosting the dominance of the cued stimulus; however, it does not enhance the associated pupil response. These results are consistent with two interpretations. One possibility is that attention biases rivalry dynamics without affecting the perceptual representation of the stimuli, but merely shifting the decision criterion that participants use for reporting their percepts. Another possibility is that attention does affect the perceptual representation of the cued stimulus, but only when there is competition between the two stimuli (e.g., during mixed percept, when we do see a transient pupil-size modulation); once one of the two stimuli has gained exclusive perceptual dominance, there is no more room for attention to enhance or suppress visual representations. Preliminary evidence against this second possibility was acquired in Chapter 4, which used the same

combined paradigm to investigate the perceptual consequences of short-term sensory deprivation. Two hours of monocular deprivation reliably boosted the dominance of the stimuli in the deprived eye, replicating previous studies and altering rivalry dynamics in a way that was qualitatively similar to the effects of endogenously cueing attention. However, contrary to what was found with attention cueing, here we observed that the perceptual boost was accompanied by a measurable change in the associated pupil responses. Thus, sensory deprivation had an effect on the dynamics of binocular rivalry that, unlike the effect of attention cueing, was faithfully reflected by the pupil-size modulations. This supports the concept that short-term sensory deprivation reliably, although transiently, affects the strength of visual representations, boosting visually evoked responses to stimuli in the deprived eye in a way that is reflected in perception as well as in basic visually evoked responses like pupil-size modulations.

Chapter 5 showed that the effects of sensory deprivation extend beyond perceptual dynamics and visually evoked responses, influencing the functional connectivity of the visual brain at rest. In a series of fMRI tests, we found that 2h of monocular deprivation were sufficient to reduce the functional connectivity of the visual cortex with the ventral pulvinar, while leaving the connectivity with the lateral geniculate nucleus unaltered. We propose that this reflects a reconfiguration of the flow of information within the visual system, which could change the way bottom-up sensory evidence (sensory input) is combined with top-down predictions (what we expect to see, which may be carried through cortico-pulvino-cortical connections). As discussed in Chapter 6 (general discussion), this provides initial evidence for the pathway through which contextual factors could affect sensory evidence – without interfering with the first swipe of signals from the periphery through the sensory cortex but modulating the recurrent exchange of information across brain areas, which combines sensory data with a priori information.

Table of Contents

1	Chapter 1 – General Introduction	7
1.1	Binocular rivalry and competition between eyes.....	7
1.2	Binocular rivalry and competition between stimuli	8
1.3	Binocular rivalry and attention	9
1.4	Pupil size as a marker of perceptual strength	10
1.5	Ocular dominance plasticity shapes perception	12
2	Chapter 2 - Measuring the reliability of binocular rivalry	16
2.1	Introduction	16
2.2	Materials & Methods.....	18
2.2.1	Participants	18
2.2.2	Ethics statement	18
2.2.3	Apparatus, stimuli and procedure	18
2.2.4	Descriptive statistics	21
2.2.5	Measurement reliability: test-retest reliability and internal consistency	22
2.2.6	Hypothesis testing	23
2.3	Results.....	24
2.4	Discussion	34
3	Chapter 3 - Attention Cueing in Rivalry: Insights from Pupillometry	38
3.1	Introduction	38
3.2	Materials and Methods	39
3.2.1	Participants	39
3.2.2	Ethics statement	40
3.2.3	Apparatus, stimuli, and procedures.....	40
3.2.4	Eye tracking data acquisition and analysis.....	43
3.2.5	Statistical approach.....	45
3.2.6	Control experiment.....	46
3.3	Results	46
3.3.1	Analysis of mixed percepts	59
3.4	Discussion	62
4	Chapter 4 – Pupil size as an index of ocular dominance plasticity	65
4.1	Introduction	65
4.2	Methods.....	66
4.2.1	Subjects.....	66
4.2.2	Apparatus, stimuli and procedures.....	67
4.2.3	Monocular deprivation	68
4.2.4	Eye tracking data acquisition and analysis	69
4.2.5	Statistical approach.....	70
4.3	Results.....	71
4.4	Discussion	76

5	Chapter 5 - Short-term monocular deprivation in adult humans alters functional brain connectivity measured with ultra-high field Magnetic Resonance Imaging	78
5.1	Introduction	78
5.2	Materials and Methods	80
5.2.1	Participants and ethics statement	80
5.2.2	Short-term monocular deprivation	80
5.2.3	Binocular rivalry	80
5.2.4	MR system and sequences.....	81
5.2.5	fMRI preprocessing	82
5.2.6	ROI definition	83
5.2.7	Analysis performed on data acquired at TR = 3s.....	83
5.2.8	Analysis performed on data acquired at TR = 1s.....	85
5.2.9	Diffusion tensor imaging preprocessing and analysis	85
5.3	Results.....	86
5.4	Discussion	94
6	Chapter 6 – General discussion.....	98
6.1	Conclusions and future direction	101
7	Appendix.....	102
7.1	Extended data from Chapter 3	102
7.2	Extended data from Chapter 5	106
8	Bibliography	111

Table of Figures

Figure 2-1.	Experimental set-ups and parameters of rivalry dynamics.....	20
Figure 2-2.	Ocular dominance: variability across sessions and within-session.	25
Figure 2-3.	Mean durations of exclusive dominance phases: variability across-sessions and within-session.	28
Figure 2-4.	Mixed percept proportions: variability across-sessions and within-session.....	30
Figure 2-5.	Consistency of binocular rivalry parameters across set-ups (Experiment 4).	32
Figure 2-6.	Comparison of the ratio of test-retest reliability and internal consistency.....	34
Figure 3-1-	Dichoptic stimulation and rivalry dynamics.	42
Figure 3-2	Pupil modulations track perceptual alternations.....	47
Figure 3-3	Attention cueing affects perceptual alternations but not pupil modulations.....	49
Figure 3-4	Pupil time courses are comparable across cueing conditions.....	53
Figure 3-5	Effects of attention cueing vs. enhancing contrast.....	56
Figure 3-6	Effects of attention cueing on mixed percepts.....	61
Figure 4-1	Experimental procedure and indices of perceptual alternations before monocular deprivation. ...	72
Figure 4-2	Monocular deprivation effects on perceptual dominance and pupil modulations.	75
Figure 5-1	vPulv and LGN functional connectivity patterns	87
Figure 5-2	vPulv and LGN functional connectivity with the visual cortex.....	89
Figure 5-3	vPulv and LGN effective connectivity with V1 assessed with Dynamic Causal Modeling.....	91
Figure 5-4	vPulv and LGN effective connectivity with V1 assessed with a cross-correlation analysis	92
Figure 5-5	Mean optic radiation profiles	94
Figure 7-1	Pupil size modulations in rivalry and simulation conditions.....	102
Figure 7-2	Pupil modulations track perceptual alternations comparably across cueing conditions irrespectively of whether and how pupil traces are baseline corrected.....	103
Figure 7-3	Fourier amplitude spectra for the seed regions of interest	107

Figure 7-4 V1 and dPulv functional connectivity patterns	108
Figure 7-5 V1 and dPulv functional connectivity with visual and intraparietal regions.....	109

Table of Tables

Table 2-1. Comparison of test-retest reliability and internal consistency.....	27
Table 3-1 The effects of cueing on proportions and pupil size.	51
Table 3-2 Contrast enhancement effects.	57
Table 3-3 The effects of cueing on proportions and pupil size in the control experiment.	58
Table 7-1 Three-way ANOVA for attention cueing results	105
Table 7-2 Signal-to-noise ratios for the seed regions of interest.....	106

Table of Equations

Equation 2-1	21
Equation 2-2	22
Equation 3-1	41
Equation 3-2	43
Equation 3-3	45
Equation 3-4	45
Equation 4-1	68
Equation 4-2	68
Equation 4-3	69
Equation 4-4	70
Equation 5-1	81
Equation 5-2	84
Equation 5-3	84
Equation 5-4	84
Equation 5-5	84

1 Chapter 1 – General Introduction

2
3 If two observers were shown identical images, they would be very unlikely to have identical
4 perceptual experiences. Even when the same observer is repeatedly exposed to the same
5 image, their perceptual experience would exhibit variability.

6 This is because our perception of the environment is not merely a reflection of the external
7 world but is rather a dynamic and subjective construction of reality. It constitutes an active
8 process influenced by past experiences, expectations, and attentional mechanisms. As such,
9 the study of perception extends far beyond the mere processing of sensory input and delves
10 into the intricate neural mechanisms that give rise to our conscious experiences. Throughout
11 this dissertation, I will focus on how these modulatory signals shape visual perception.

12 13 1.1 Binocular rivalry and competition between eyes

14
15 A paradigmatic example of how perception goes beyond mirroring the external reality is the
16 phenomenon of binocular rivalry. Binocular rivalry is a form of visual bistability that arises
17 when incompatible images are presented to the two eyes. Despite the absence of any physical
18 change in the stimuli, individuals experience perceptual alternations between the two stimuli
19 at irregular intervals (Brascamp et al., 2015). The most interesting aspect of binocular rivalry
20 is having unchanging physical stimulation and varying awareness, which allows for a
21 comparison of neural events between moments that differ only for the contents of
22 consciousness, not the physical input. This property gained binocular rivalry the title of
23 “window into consciousness” (Leopold & Logothetis, 1999) and it has been useful for studying
24 a variety of brain functions.

25 Despite the interest it received, the nature of the competitive interactions that mediate
26 binocular rivalry is partially unresolved (Tong, 2001). The core assumption is that rivalry arises
27 from mutual inhibition between monocular neurons. When one monocular input is stronger
28 than the other, it activates an inhibitory neuron that can entirely suppress inputs from the
29 other eye. However, the response to the dominating input progressively adapts and thereby
30 generates progressively weaker inhibition; this eventually leads to the other eye breaking
31 suppression and becoming dominant. The underlying circuit may be identified in inhibitory
32 feedback signals from V1 to monocular layers of the lateral geniculate nucleus (Lehky, 1988),

33 but it could be applied equally well to competitive lateral interactions among monocular V1
34 neurons as has been proposed in Blake's model (Blake, 1989). This eye-based competition
35 framework is supported by several bits of behavioral evidence (Blake et al., 1980; Fox & Check,
36 1972; Wales & Fox, 1970). For example, if a left-eye vertical grating is dominant and a right-
37 eye horizontal grating is suppressed, a sudden exchange of the two monocular patterns leads
38 to the perception of the left-eye horizontal grating (Blake et al., 1980), strongly suggesting that
39 the dominant/suppressed state is attached to the eye, not to the stimulus, consistent with the
40 predictions of interocular competition. This model has undergone evaluation also through
41 neurophysiological and neuroimaging studies, revealing a strong alignment between neural
42 activity and subjective perception (Tong, 2001). In line with pioneering EEG studies (COBB et
43 al., 1967; Lansing, 1964), subsequent MEG investigations demonstrated that binocular rivalry
44 induces extensive neural modulations not only in the occipital cortex but also in temporal and
45 frontal regions (Tononi, 1998). Functional MRI studies aimed to identify the source of these
46 rivalry-related responses and suggested that the competition underlying binocular rivalry is
47 already resolved by the time visual information reaches the extra-striate cortex (Tong et al.,
48 1998), and its resolution may be achieved within the primary (or striate) visual cortex, at a
49 level where representations are still monocular (Tong & Engel, 2001). This model posits a
50 direct connection between perceptual dominance during binocular rivalry and eye-of-origin
51 strength, which implies that binocular rivalry should be an ideal tool to assess eye dominance
52 (see Ooi & He, 2020). In chapter two, we put this assumption to a test, examining the many
53 different parameters that can be used to capture the dynamics of perceptual alternations
54 (dominance proportions, speed of rivalry alternations, occurrence of mixed percepts) and
55 assessing their reliability.

56

57 1.2 Binocular rivalry and competition between stimuli

58

59 The eye-based competition model is well supported by several bits of experimental evidence,
60 but it has also been challenged by some experimental observations (Lehmkuhle & Fox, 1975;
61 Wade & Wenderoth, 1978). One of these is the phenomenon of interocular grouping rivalry,
62 which occurs when presenting two different but complementary images to the two eyes,
63 which are perceptually bound into a coherent picture (Kovacs et al., 1996). This interocular
64 grouping would not be predicted by any eye competition model, which would predict only the

65 alternation of monocular percepts. Based on this and other findings, an alternative model was
66 formulated a pattern-competition model (Leopold & Logothetis, 1999; Logothetis et al., 1996)
67 where reciprocal inhibition occurs between different patterns rather than between monocular
68 channels. There was also a proposal for a hybrid model, where inhibitory interactions could
69 take place both between monocular neurons (interocular competition) and between pattern-
70 selective neurons (pattern competition;(Tong et al., 2006)).

71 Irrespectively of the elements competing for perceptual dominance, eye- or pattern-selective,
72 the competition has been traditionally related to physical strength: the physically stronger
73 stimulus, the one triggering the greater sensory responses, wins. Stimulus strength was first
74 related by Levelt (LEVELT, 1966)to stimulus features as density, luminance contrast, and
75 sharpness of image contours and later joined by color contrast and motion coherence
76 (Brascamp et al., 2015).

77 However, recent studies have shown that the competition between the rivalling stimuli can
78 be biased beyond physical strength, by cognitive factors like training (Dieter et al., 2016),
79 reward (Marx & Einhauser, 2015; Wilbertz et al., 2017), emotional content (Alpers et al., 2011)
80 and attention.

81

82 1.3 Binocular rivalry and attention

83

84 Exogenous attention, often referred to as stimulus-driven attention, is the result of salient
85 external stimuli that automatically capture our awareness (K. N. Nguyen et al., 2020). In the
86 context of binocular rivalry, exogenous attention can dramatically influence the duration and
87 dominance of one image over the other (Chong et al., 2005; Ooi & He, 1999) and initiate a
88 perceptual alternation (Paffen & Van der Stigchel, 2010). Moreover, drawing attention away
89 from the rivalry stimuli can slow down the perceptual alternation rate (Alais, van Boxtel, et al.,
90 2010; Brascamp & Blake, 2012; Paffen et al., 2006) or even abolish the alternations altogether
91 (Zhang et al., 2011). Endogenous attention, on the other hand, is driven by internal goals,
92 intentions, or cognitive processes. In the context of binocular rivalry, endogenous attention
93 can be voluntarily directed toward one of the rival images, amplifying its dominance (Chong
94 et al., 2005; Hancock & Andrews, 2007; Meng & Tong, 2004; Ooi & He, 1999).

95 The observation that not only the physically stronger stimulus wins, but also the one where
96 we direct our (endogenous or exogenous) attention, led to revising the definition of stimulus
97 strength in the context of binocular rivalry.

98 One possibility is that attention acts by amplifying the sensory responses to the attended
99 stimuli, increasing their perceptual or “effective” strength (for a review see Carrasco & Barbot,
100 2019) in rivalry like in the standard non-rivalrous situations; supporting evidence mainly
101 comes from behavioural measures, which rely exclusively on introspection. This is problematic
102 because perceptual reports do not reflect only the dynamic construction of perception but
103 also depend on an additional factor, decision. Every time we perceive a stimulus, we categorize
104 it in our minds; this phenomenon is called perceptual decision-making and attention has been
105 convincingly shown to drive this process (Rangelov & Mattingley, 2020; Yang, 2017). Our
106 recent work, described in Chapter 3, aimed at investigating whether endogenous attention
107 affects perception by altering the effective strength of the cued stimulus, or rather by biasing
108 the decision criteria that guide its categorization. We did so by combining binocular rivalry
109 and the relative behavioural reports of perceptual dominance, with the use of a non-invasive,
110 objective measure of the content of perception: pupil size.

111

112 1.4 Pupil size as a marker of perceptual strength

113

114 Two muscles are responsible for changing the size of the pupil: the iris sphincter muscle, which
115 constricts the pupil, and the iris dilator muscle, which dilates it (Kardon, 2005; McDougal &
116 Gamlin, 2008). When luminance increases, the pupil constricts. This pupillary light response
117 (PLR) is largely supported by a subcortical reflex pathway. Luminance information from the
118 retina is relayed to the midbrain pretectal nucleus, which in turn projects to the Edinger-
119 Westphal nucleus, which finally induces contraction of the pupillary sphincter (McDougal &
120 Gamlin, 2014). A separate circuit supports pupil dilation, as produced by luminance
121 decrements as well as changes in arousal levels. Noradrenaline released from the Locus
122 Coeruleus stimulates α -adrenoceptors with an excitatory influence on the iris dilator muscle
123 and an inhibitory influence on the Edinger–Westphal nucleus. The net result of these effects
124 is a pupil dilation response that, in conditions of constant illumination, accompanies the
125 increase of sympathetic tone (Steinhauer et al., 2004).

126 Besides these subcortical circuits, pupil responses are likely to be modulated by cortical
127 signals, given that they are not only set by the physical strength of the visual input, but also
128 affected by the way it is selected, processed, and interpreted (for reviews, Binda & Murray,
129 2015; Mathôt, 2018; Mathôt & Van der Stigchel, 2015). A prominent example of this
130 phenomenon is the attentional modulation of pupillary light responses (Binda et al., 2013a,
131 2014; Binda & Murray, 2015; Bombeke et al., 2016; Ebitz et al., 2014; Mathôt et al., 2013;
132 Mathôt et al., 2014; Olmos-Solis et al., 2018; Unsworth & Robison, 2016). Several studies have
133 shown that covertly attending to a brighter or darker stimulus is sufficient to trigger a pupil
134 response, just like (although much weaker than) directly looking at something that is bright
135 or dark (Binda et al., 2013a, 2014; Binda & Murray, 2015b; Bombeke et al., 2016; Ebitz et al.,
136 2014; Mathôt et al., 2013, 2014; Naber et al., 2013; Olmos-Solis et al., 2018; Unsworth &
137 Robison, 2016). This effect is so robust that it can even be used to decode whether people are
138 covertly attending to something bright or dark, with around 90% accuracy on a single-trial
139 level (Mathôt et al., 2016). Neurophysiological studies have shown similar effects (Ebitz &
140 Moore, 2017; C.A. Wang & Munoz, 2016). Ebitz and his group in 2017 stimulated frontal eye
141 field neurons to trigger a covert shift of attention to the receptive field of these neurons; next,
142 they flashed a stimulus either within, or outside of, the stimulated receptive field. Crucially,
143 they observed a stronger pupillary light response to stimuli flashed within the stimulated
144 receptive field, compared to outside of the stimulated receptive field—a result that echoes
145 behavioral studies (Binda & Murray, 2015a; Olmos-Solis et al., 2018). Other results suggest
146 that pupillary constrictions may even be induced in the absence of visual stimulation, by
147 merely asking participants to mentally visualize a bright scene (Laeng & Sulutvedt, 2014) or
148 by stimuli that evoke the idea of bright objects, like pictures of the sun (Binda et al., 2013b)
149 or words conveying brightness (Mathôt et al., 2017).

150 Pupil size changes have also been observed during binocular rivalry, where stimuli of different
151 luminance or contrast perceptually alternate, and pupil size follows the brightness of the
152 currently dominant stimulus: constricting when seeing bright, dilating when seeing dark.
153 Initial work on binocular rivalry and pupil changes dates back to 1966, when Lowe and
154 colleagues showed that the same monocular light flash elicited a smaller pupil response when
155 delivered to the suppressed eye than the dominant eye (LOWE & OGLE, 1966). This idea was
156 followed up by demonstrating that pupil size depended on the characteristics of the dominant
157 percept: during the intervals where the grating of higher luminance or contrast was dominant,

158 pupil size was smaller than in intervals when the other grating was dominant (Einhäuser et al.,
159 2008; Fahle et al., 2011; Naber et al., 2011). A second component of pupil modulations
160 systematically accompanied rivalrous perception, irrespectively of the luminance of the
161 stimuli (Einhäuser et al., 2008; Fahle et al., 2011). Both in binocular rivalry and other types of
162 perceptual rivalry (Necker cube, auditory rivalry, visual plaids), pupil traces show a transient
163 dilation around the time of perceptual switch, which may be informative of the duration of
164 the subsequent dominance phase. This pupil response has been related to the activation of
165 the Locus Coeruleus and the consequent noradrenaline release. This release would
166 consolidate the behavioural decision (Einhäuser et al., 2008) either by enhancing cortical
167 responsivity to the dominant stimulus (HURLEY et al., 2004) or by favouring its processing and
168 integration with a priori knowledge (Murphy et al., 2021; Reimer et al., 2014, 2016). These
169 studies suggest that pupil size could keep track of both sensory and cognitive processing
170 (Binda & Murray, 2015a). Even though attention-related pupillary responses happen on a very
171 small scale, in the order of 0.1 mm or less, these pupil modulations might be the marker of
172 the ubiquity of top-down influences on sensory processing (Binda & Murray, 2015a), including
173 complex ones such as attention and contextual modulation of perception.

174 In Chapter 4, we applied the lessons learned from applying pupillometry to the study of
175 attention during binocular rivalry, to the investigation of another factor: monocular
176 deprivation.

177

178 1.5 Ocular dominance plasticity shapes perception

179

180 In the wake of the ground-breaking research conducted by Hubel and Wiesel in the 1960s
181 (Hubel & Wiesel, 1965; Wiesel & Hubel, 1963) ocular dominance plasticity has emerged as a
182 fundamental model for neural adaptability. Hubel and Wiesel recorded the visual cortex
183 activity in cats at various developmental stages, including those with normal vision and those
184 subjected to monocular deprivation through eyelid suture (Wiesel & Hubel, 1963). Their
185 investigations revealed that monocular deprivation disrupted the establishment of ocular
186 dominance columns in the primary visual cortex (V1). This disruption was evident both
187 anatomically, with a reduction in the cortical area representing the deprived eye, and
188 functionally, leading to persistent effects throughout the animal's life, resulting in a condition
189 known as amblyopia (Levi & Carkeet, 1993), characterized by decreased visual acuity and

190 diminished responsiveness to stimuli in the deprived eye. However, the efficacy of this
191 manipulation was contingent on the timing of monocular deprivation. Applying the same or
192 even longer periods of MD to adult animals had negligible effects (HENSCH & QUINLAN, 2018).
193 This introduced the concept of a 'critical period' during which the application of MD is most
194 impactful.

195 Notably, over the past few decades, various interventions were found to effectively reopen
196 windows of plasticity throughout adulthood. This suggests that a form of plasticity remains
197 viable in the adult visual cortex, featuring effects and mechanisms that are partly distinct from
198 those supporting developmental plasticity (He et al., 2006; Kalogeraki et al., 2014; Sale et al.,
199 2007; Spolidoro et al., 2011; Vetencourt et al., 2008).

200

201 In adult humans, functional changes have been observed with a short-term version of a visual
202 deprivation paradigm (Binda & Lunghi, 2017; Kwon et al., 2009; Lunghi, Berchicci, et al., 2015;
203 Lunghi et al., 2011, 2013; Zhang et al., 2009; J. Zhou et al., 2013, 2014). Two hours of
204 monocular contrast deprivation are followed by a counterintuitive transient boost of the
205 deprived eye – opposite to the amblyopia induced by several days of monocular deprivation
206 during the critical period. This effect has been dubbed “homeostatic plasticity” to distinguish
207 it from the “Hebbian plasticity” that is characteristic of the critical period and to foreshadow
208 the possible underlying mechanisms: automatic regulation of cortical excitability aimed at
209 keeping response levels at an approximately constant level in the face of reduced stimulation.
210 This counterintuitive “homeostatic plasticity” effect has been reported several times, mainly
211 (but not exclusively) using binocular rivalry as a behavioural index of eye dominance. Two
212 hours of monocular deprivation (through the application of a translucent patch over the
213 dominant eye) transiently but strongly affect the dynamics of binocular rivalry: after
214 deprivation, the deprived eye dominates rivalrous perception for twice as long as the non-
215 deprived eye and the effect may last for up to 90-180 minutes after eye-patch removal (Binda
216 et al., 2018; Lunghi et al., 2011, 2013). The shift in ocular drive is compatible with a boost in
217 perceptual strength of the stimulus shown to the deprived eye (Lunghi et al., 2011). This
218 hypothesis has been supported by EEG and fMRI studies, that showed an increase of visual
219 evoked responses elicited by the stimulus shown to the deprived eye (Binda et al., 2018;
220 Lunghi, Berchicci, et al., 2015). However, it is interesting to note that these physiological
221 indices of the boost of the deprived eye are not directly related to the behavioural effect,

222 because they were acquired in conditions that are very different from those used in
223 behavioural testing. Visual evoked responses (EEG or fMRI) were recorded by presenting
224 stimuli passively, in absence of any perceptual report; in addition, stimuli for VEP and fMRI
225 measurements were delivered monocularly, i.e., separately to each eye (Binda et al., 2018;
226 Lunghi, Berchicci, et al., 2015). All this contrasts with the conditions of the behavioural
227 experiments, where participants were continuously engaged in reporting their perception,
228 which tracked the competitive interactions between the stimuli presented to the two eyes. In
229 Chapter 4, we combined binocular rivalry with pupillometry, aiming at providing a sensitive,
230 non-invasive, and direct measure of short-term monocular deprivation on the effective
231 strength of the deprived eye – collected simultaneously with the behavioural test.

232

233 The analysis of the physiological effects of short-term monocular deprivation has allowed an
234 extensive description of the characteristics of the deprived eye boost (Binda et al., 2018;
235 Lunghi, Berchicci, et al., 2015). Pattern-onset visual evoked potentials (VEPs) before and after
236 monocular deprivation showed opposite effects for the two eyes (Lunghi, Berchicci, et al.,
237 2015). The amplitude of the C1 component of the VEP responses, typically reflecting the
238 earliest stage of visual processing in V1 (F. Di Russo et al., 2002), and the peak in alpha band
239 after monocular deprivation were enhanced for the deprived eye but reduced for the non-
240 deprived eye. Moreover, the amplitude of later components, such as P1 and P2, were equally
241 altered by monocular deprivation, suggesting that the variations in cortical excitability
242 propagate to extra-striate areas and may vary feed-back projection to V1.

243 Coherent observations came from the analysis of BOLD responses in the visual cortex. Binda
244 and colleagues (Binda et al., 2018) performed ultra-high field fMRI during the presentation of
245 high contrast dynamic visual stimuli, delivered separately to the two eyes, before and after 2
246 hours of monocular contrast deprivation. They found a paradoxical increase of the BOLD
247 responses for the eye that was deprived of contrast vision and a decrease for the eye exposed
248 to normal visual experience. This effect has been related to contrast gain-control mechanisms
249 that, to compensate for the reduced incoming signal in the patched eye, would boost the
250 neuronal responses of the deprived eye (Castaldi et al., 2020) or increase of inhibition of the
251 non-deprived eye (Gong et al., 2023; Lyu et al., 2020).

252 Crucially, these modulations were not only observed in the visual cortex, but also in the ventral
253 Pulvinar, a nucleus of the visual thalamus (Kurzawski et al., 2022). On the other hand, there

254 was no modulation of responsiveness before/after modulation in an adjacent thalamic
255 nucleus: the Lateral Geniculate Nucleus, which provides the main feedforward input to V1.
256 This indicates that short-term monocular deprivation has a cortical origin and may propagate
257 to the ventral Pulvinar through the dense cortico-pulvino-cortical connections (Arcaro et al.,
258 2018; Benarroch, 2015; Sherman, 2005; Shipp, 2003). These connections have been related
259 to the modulation of bottom-up and top-down cortical pathways integrating visual inputs and
260 predictions (Bridge et al., 2016; Galuske et al., 2019; Jaramillo et al., 2019; Kanai et al., 2015;
261 Z. Liu et al., 2012).

262 This could suggest a radical reinterpretation of the short-term monocular deprivation
263 phenomenon; rather than reflecting a homeostatic regulation of V1 responses, it could be
264 linked to the predictive processing of sensory information and more specifically to a revision
265 of internally generated predictions triggered by systematically incoherent sensory information
266 (one eye failing to transduce the signals expected based on the other eye input and based on
267 the observer's own actions). In line with this hypothesis, there is mounting evidence that,
268 even in absence of any contrast deprivation, a mismatch between perception and
269 expectations is sufficient to trigger ocular dominance plasticity (Bai et al., 2017; Kim et al.,
270 2017; Ramamurthy & Blaser, 2018; Steinwurz et al., 2023).

271 In Chapter 5, we tested the hypothesis that the distorted sensory experience induced by
272 monocular patching has modulatory effects not only on visual evoked responses but also on
273 the thalamo-cortical circuitry supporting the integration of sensory and prediction signals.

274
275
276
277
278
279
280
281
282
283
284
285
286
287
288
289
290

291 2 Chapter 2- Measuring the reliability of binocular rivalry

292

293 2.1 Introduction

294

295 Binocular rivalry is a form of perceptual bi-stability that occurs when the two eyes are
296 simultaneously presented with incompatible images (Alais, 2005; LEVELT, 1966). Observers
297 track and report their visual perception by indicating periods of complete dominance of the
298 image presented in either eye and periods of mixed percepts, i.e., transient periods of
299 binocular fusion in which either a piecemeal combination or a superimposition/fusion of the
300 two images is perceived. This technique is a widely used tool in visual psychophysics to study
301 various aspects of vision and cognition (Baker, 2010).

302 One characteristic that is often studied with binocular rivalry is ocular dominance, or the
303 degree to which our visual perception relies on the input from either eye (Dieter et al., 2017b;
304 Ding et al., 2018; Handa et al., 2006; Ooi & He, 2001). The dynamics of binocular rivalry
305 provide an elaborated measure of ocular dominance, more quantitative and precise (Ooi &
306 He, 2020), than other sighting eye dominance tests, such as the Porta test (Lederer, 1961;
307 Porta, 1593) or the hole in card test (DURAND, 1910). For example, binocular rivalry made it
308 possible to unveil a form of plasticity in adult humans, consisting of an ocular dominance shift
309 after a brief period (about 2 hours) of monocular deprivation (Han et al., 2020; Lunghi et al.,
310 2011, 2013; M. Wang et al., 2020).

311 Besides ocular dominance, the dynamics of binocular rivalry have been linked to multiple
312 aspects of perceptual and cognitive function. The temporal frequency with which alternative
313 percepts take turns during binocular rivalry (measured by the duration of exclusive dominance
314 phases or its inverse, the switch rate) shows large inter-individual variability (Dieter et al.,
315 2017b; Gallagher & Arnold, 2014; Ooi & He, 2001) and it correlates with switch rates in other
316 forms of perceptual rivalry [(Carter & Pettigrew, 2003), but see (Brascamp et al., 2018) for a
317 recent re-evaluation of this result]. These and other observations suggest that rivalry
318 dynamics may be an intrinsic ultradian rhythm – a stable, trait-like characteristic of every
319 individual. There is evidence of genetic factors affecting this rhythm (Miller et al., 2010;
320 Shannon et al., 2011),—which tends to be similar across monozygotic twins. There is also
321 evidence for the association between the rhythm of perceptual alternations during binocular
322 rivalry and psychological traits or disorders. For instance, binocular rivalry dynamics are slower

323 in individuals with autism (Robertson et al., 2013; Spiegel et al., 2019), in neurotypical
324 individuals with stronger self-reported autistic traits (Dunn & Jones, 2020), and in patients
325 with schizophrenia (Xiao et al., 2018; Ye et al., 2019). Other studies found that rivalry dynamics
326 are slower in people with bipolar disorder and depression (Jia et al., 2015; MILLER et al., 2003;
327 Ngo et al., 2011), but faster in those with anxious personality traits (Jia et al., 2020; Nagamine
328 et al., 2007). Thus, differences in binocular rivalry dynamics may emerge as a potential proxy
329 for complex psychological constructs, such as personality traits and disorders.

330 Given the diverse uses of binocular rivalry, it is important to establish its reliability. Indices
331 such as mean phase duration and proportion of mixed percepts have been shown to be stable
332 within a given experimental session (K. C. Dieter et al., 2017b, 2017a; van Ee, 2005), implying
333 good internal consistency. What is missing is an assessment of their test-retest reliability, i.e.,
334 their stability over experimental sessions performed on different days, which is expected to
335 be high for any trait-like characteristic. For ocular dominance, reliability was recently
336 questioned by Min et al., (2021), who compared different techniques for the assessment of
337 ocular dominance (binocular rivalry, binocular phase combination, and dichoptic masking).
338 The authors report that ocular dominance estimates obtained by parallel-oriented dichoptic
339 masking and binocular phase combination tasks show higher test-retest reliability compared
340 to binocular rivalry, which exhibited poor stability across experimental sessions. In particular,
341 ocular dominance estimated on different days using binocular rivalry showed high variability
342 and no significant correlation across participants. These results partially contradict previous
343 studies, which show that binocular rivalry provides precise and reliable estimates of ocular
344 dominance across days (K. C. Dieter et al., 2017a), and even proposed binocular rivalry as the
345 standard technique to quantify sensory eye dominance in adult humans (see Ooi & He, 2020
346 for review).

347 To address these issues, here we examined the reliability of binocular rivalry dynamics and
348 derived ocular dominance measures using four relatively large datasets, and a variety of
349 methods and stimuli. Inspired by Min et al.'s approach, we separately assessed two aspects
350 of reliability: internal consistency, based on the variability of estimates within a single
351 experimental session, and test-retest reliability, based on the variability across experimental
352 sessions conducted on separate days.

353

354 2.2 Materials & Methods

355

356 2.2.1 Participants

357

358 A total of 118 volunteers with normal or corrected to normal vision participated in the four
359 experiments presented here. All except the authors were naïve to the purposes of the study.
360 Part of these data were collected in the context of past studies, the results of which have been
361 reported previously.

362 40 volunteers (Mean age 28.6 ± 0.72 years, 25 females including authors I.S. and C.L.) took part
363 in experiment 1 (Sarı & Lunghi, 2023).

364 33 volunteers (Mean age 25.8 ± 0.11 years, 18 females including authors M.A. and C.L.) took
365 part in experiment 2 (Acquafredda et al., 2022).

366 34 volunteers (Mean age 23.9 ± 0.79 years, 24 females including authors C.L. and C.S.) took
367 part in experiment 3 (Lunghi & Sale, 2015; Steinwurz et al., 2020).

368 20 volunteers (Mean age 27.5 ± 0.4 years, 14 females including author C.S.) took part in
369 experiment 4 (Unpublished); 7 of these had also participated in experiment 3.

370

371 2.2.2 Ethics statement

372

373 All four experimental protocols were approved by local ethics committees. The “Comité
374 d’éthique de la Recherche de l’université Paris Descartes” approved experiments 1 & 2 (CER-
375 PD:2019-16-LUNGHI) and the “Comitato Etico Pediatrico Regionale—Azienda Ospedaliero-
376 Universitaria Meyer—Firenze” approved experiments 3 & 4 (protocol “Plasticità del Sistema
377 visivo”). All experiments were performed in accordance with the Declaration of Helsinki (DoH-
378 Oct2008). All participants gave written informed consent.

379

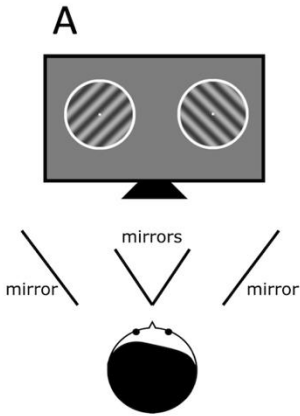
380 2.2.3 Apparatus, stimuli and procedure

381

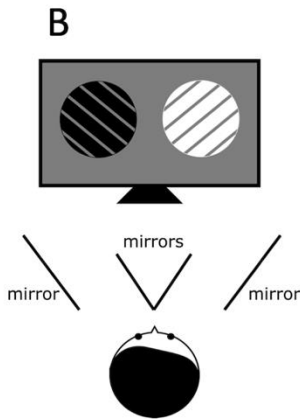
382 A diagram of the experimental setups for the four experiments included in the study is
383 reported in Figure 1 (A-D). All experiments shared the same logic and design, which we
384 describe first, followed by the specific features of each individual experiment.

385

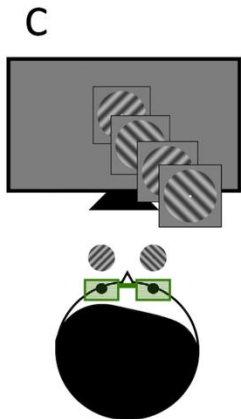
Mirrors, gratings



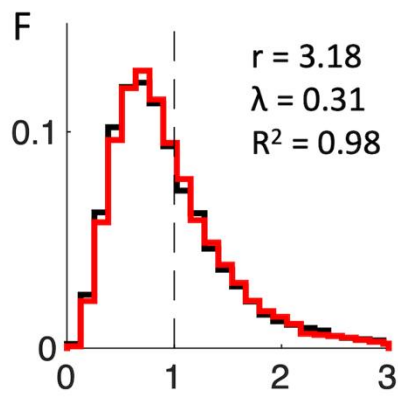
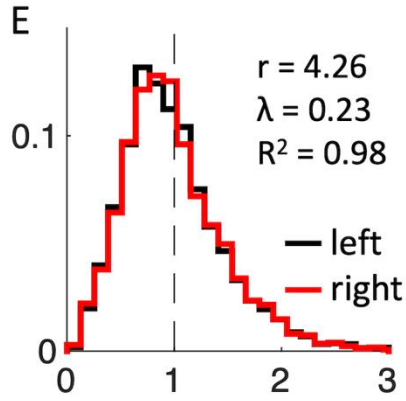
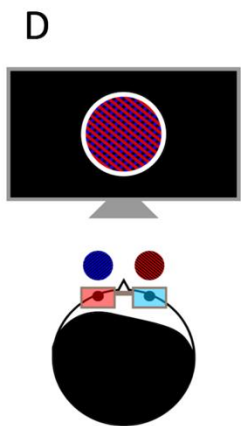
Mirrors, B/W patches



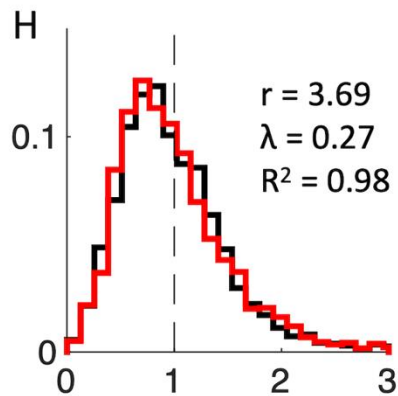
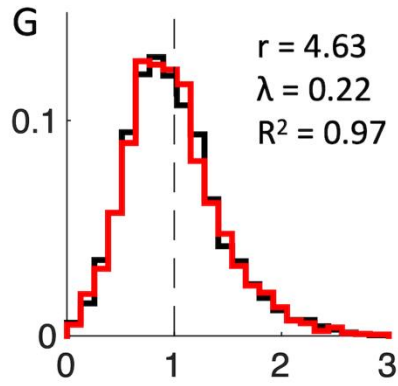
Shutter goggles, gratings



Shutter vs. anaglyph goggles



Probability density



Normalized phase durations

387

388 *Figure 2-1. Experimental set-ups and parameters of rivalry dynamics*

389 *A-D: Schematics of the stimuli and set-ups. E-H: Probability density function of the normalized*
390 *phase durations for exclusive dominance of left and right eyes (respectively black and red*
391 *lines), with best-fitting parameters of the Gamma distribution.*

392

393 For all experiments, participants took part in two experimental sessions, at least 24 hours
394 apart. Each session was divided into 2 trials of 3 minutes each (6 minutes in total), except for
395 experiment 2 where 4 three-minute long trials (12 minutes in total) were tested. Participants
396 viewed the monitor from a 57 cm distance; a chin/forehead rest stabilized head position. The
397 stimuli consisted of small circular gratings presented dichoptically in central view; they were
398 inscribed in a binocular frame to facilitate fusion. Participants reported rivalrous alternations
399 through the computer keyboard, by continuously pressing one of three keys to report
400 exclusive percepts of orthogonally oriented gratings (right-arrow for clockwise and left-arrow
401 for counter-clockwise) or a mixture of those (piecemeal or fusion: down-arrow key). The
402 orientation of gratings presented in either eye was counter-balanced across participants and
403 switched on every trial to avoid adaptation. For experiment 1, the swapping procedure was
404 done every 90 seconds i.e. halfway through a trial.

405

406 Experiments mainly differed in the method used for dichoptic stimulation. Experiments 1 and
407 2 used a mirror stereoscope placed in front of an LCD monitor (BenQ XL2420Z, 1920 x 1080
408 pixels, 144 Hz refresh rate, Taipei, Taiwan). Experiment 3 and the first session of experiment 4
409 used CRS ferromagnetic shutter goggles (Cambridge Research Systems, Kent, United Kingdom)
410 and a CRT monitor (Barco 6551, 800 x 600 pixels, 140 Hz refresh rate, Kortrijk, Belgium). The
411 second session of experiment 4 used anaglyph red-blue goggles and a LED monitor (LG IPS
412 24EA53, 1920 x 1080, 60 Hz refresh rate, Seoul, South Korea).

413 There were also differences in the stimuli used to induce rivalry (recall that these experiments
414 were run for independent studies). In experiments 1 and 3 and in the first session of
415 experiment 4, stimuli were monochromatic sinusoidal gratings (orientation: $\pm 45^\circ$, spatial
416 frequency: 2 cpd, contrast: 50%, size: 3° or 2° in experiments 1 and 3 and experiment 4
417 respectively) presented against a uniform grey background (Experiment 1: luminance 110

418 cd/m², C.I.E. x = 0.305, y = 0.332; Experiment 3 and 4: luminance 37.4 cd/m², C.I.E. x = 0.442,
419 y = 0.537). In the second session of experiment 4, stimuli were red and blue gratings
420 (orientation: ±45°, size: 3°, spatial frequency: 2 cpd, maximum luminance: 0.5 cd/m²),
421 presented against a black uniform background. In experiment 2, stimuli were 3° disks, one
422 white (maximum screen luminance 295 cd/m²) and one black (minimum screen luminance 10
423 cd/m²) shown against a uniform grey background (luminance 152 cd/m²). To discourage
424 binocular fusion, the disks were overlaid with orthogonal grey lines (45° clockwise or
425 counterclockwise, 0.033° or 1 pixel wide, and 0.5° apart).

426

427 2.2.4 Descriptive statistics

428

429 For each binocular rivalry trial, we used our participants' continuous perceptual reports to
430 extract the following parameters.

431 Exclusive dominance phases were defined as periods of time during which participants
432 reported seeing exclusively the image presented to their right or left eye. Phase durations
433 were computed separately for each eye; durations shorter than 0.25 sec were considered
434 keypress errors and discarded from the analysis.

435 We also measured the time spent reporting mixed percepts (fusion or piecemeal
436 combinations of the images presented in the two eyes) and expressed it as a proportion of
437 the total testing time.

438 Ocular dominance was defined as the proportion of exclusive right-eye dominance, according
439 to the following equation:

440

$$441 \quad ODI = \frac{Time_{RE} - Time_{LE}}{Time_{RE} + Time_{LE}}$$

442

443 Equation 2-1

444 where ODI stands for Ocular Dominance Index and Time_{RE} and Time_{LE} are the total amount of
445 time (in seconds) spent seeing through the right eye or left eye respectively. Participants with
446 an ODI > 0.25 or < -0.25 in the first session were excluded from further testing, leaving the
447 sample sizes as reported in the above section. This exclusion criterion was applied because all
448 studies were aimed at investigating the impact of external factors (e.g. short-term monocular
449 deprivation or voluntary attention) on ocular dominance. Participants showing extreme ocular
450 dominance values at baseline were excluded to avoid a possible saturation effect.

451 We checked that the distribution of exclusive dominance phase durations followed a Gamma
452 distribution. First, we normalized phase durations separately for the right and left eye to their
453 mean phase duration. Next, we pooled phase durations from all participants.

454 Finally, these normalized phase duration distributions (Figure1E-H) were fit with a two-
455 parameter Gamma distribution, with shape α and scale β parameters:

456

$$457 \quad f(x|\alpha, \beta) = \frac{1}{\beta^\alpha \Gamma(\alpha)} x^{\alpha-1} e^{-\frac{x}{\beta}} \quad \text{for } x, \alpha, \beta > 0$$

458

459 *Equation 2-2*

460 Where Γ is the gamma function, x the number of dominance phases. Best fit parameters are
461 reported in the text insets of Figure1E-H.

462

463 2.2.5 Measurement reliability: test-retest reliability and internal consistency

464

465 Estimates of internal consistency and test-retest reliability were obtained from the intra-
466 session and the inter-session variability, respectively, of the three main parameters of interest:
467 ocular dominance index, mean phase durations (pooled across eyes) and mixed percept
468 proportions.

469 By internal consistency, we mean the stability of a parameter within a given trial (i.e., a portion
470 of an experimental session that was run without interruptions). Our aim was to compare this
471 with the stability of the same parameter across sessions. The latter was measured as the
472 difference in the parameter estimates from one trial in the first session vs estimates from one
473 trial in the second session. For each trial, we represented perceptual reports as a list of phases,
474 each linked with its duration and type (left eye, right eye, mixed). This list was resampled
475 10,000 times with reinsertion; for each resampling, we estimated the three parameters of
476 interest and computed their difference between the two trials coming from different sessions.
477 Finally, we took the standard deviation across these 10,000 differences as a measure of
478 standard error and combined standard errors across trials by taking the median. We used this
479 value as indicative of internal consistency. By including this step in our analysis, we estimated
480 intra-session variance in a way that (1) does not need the a priori assumption of equal variance
481 on the two sessions, (2) is independent of the means, and (3) is directly comparable to inter-
482 session variance (from which we derived our measure of test-retest reliability). By test-retest

483 reliability, we mean the stability of a parameter across experimental sessions conducted on
484 separate days. To estimate this, we computed inter-session correlations and inter-session
485 differences as visualized in Bland-Altman plots.

486 Inter-session correlations were computed as the Pearson's r of the values obtained for each
487 parameter in the two sessions; vertical and horizontal lines around each data point (leftmost
488 panels of Figures 2-5) showing the bootstrapped standard error of the index obtained for each
489 session.

490 Bland-Altman plots (Altman & Bland, 1983) were generated by plotting, for each parameter,
491 the difference between the two sessions (inter-session difference) against the mean across
492 sessions. We integrated this representation with our measure of internal consistency by
493 showing the bootstrapped standard error of the intersession difference as vertical lines
494 around each data point. Horizontal dashed lines show summary statistics of both test-retest
495 reliability and internal consistency in the form of 95% confidence intervals, allowing for a
496 direct comparison of the two. Dark Blue/Red/Green horizontal dashed lines show the 95%
497 limits of agreement, computed as the mean $\pm 1.96 \times$ standard deviation of the inter-session
498 differences across participants. Light Blue/Red/Green horizontal lines show the 95%
499 confidence interval of the inter-session difference, computed as the $\pm 1.96 \times$ the median
500 bootstrapped standard error across participants. We show these representations in two
501 versions, before and after z-scoring of the data (central and rightmost panels of Figures 2-5,
502 respectively); the latter allows for comparing test-retest reliability and internal consistency
503 across indices (note that x- and y-scales of the rightmost plots are kept consistent across all
504 figures). To facilitate comparison with Min et al. (Min et al., 2021), the z-scored confidence
505 intervals of the ocular dominance indices are also reported in Table 1.

506 2.2.6 Hypothesis testing

507
508 We checked that all variables were normally distributed (Kolgorov-Smirnov test (Limiting
509 form), $p > 0.05$). Statistical significance was evaluated using both p-values and log-transformed
510 JZS Bayes Factors, computed with the default scale factor of 0.707 (Wagenmakers et al., 2012).
511 The Bayes Factor is the ratio of the likelihood of the two models H_1/H_0 given the observed
512 data, where H_1 is the experimental hypothesis (effect present) and H_0 is the null hypothesis
513 (effect absent). A base 10 logarithm of the Bayes Factor ($\log BF$) larger than $|0.5|$ corresponds
514 to a likelihood ratio larger than 3 in favour of either H_1 (when $\log BF > 0.5$) or H_0 (when $\log BF$

515 < -0.5) and this value is conventionally used to indicate substantial evidence in favour of either
516 hypothesis. Comparisons across parameters (Figure 6) were performed using two-tailed,
517 paired-samples t-tests. The p-values were corrected for multiple comparisons with Bonferroni
518 correction.

519 520 2.3 Results

521
522 We measured binocular rivalry in a total of 118 participants with three dichoptic stimulation
523 set-ups and four different stimuli. Dichoptic stimulation was achieved through a mirror
524 stereoscope in experiments 1 and 2 (Figure 1A-B), shutter goggles in experiment 3 (Figure 1C),
525 and anaglyph red/blue goggles in experiment 4 (Figure 1D). In experiments 1-3, data collection
526 was repeated twice with identical stimuli and set-up, on different days, allowing us to gauge a
527 measure of stability and reliability of rivalry indices; in experiment 4, data were acquired with
528 two different set-ups testing the stability of those indices across time and stimulation
529 conditions.

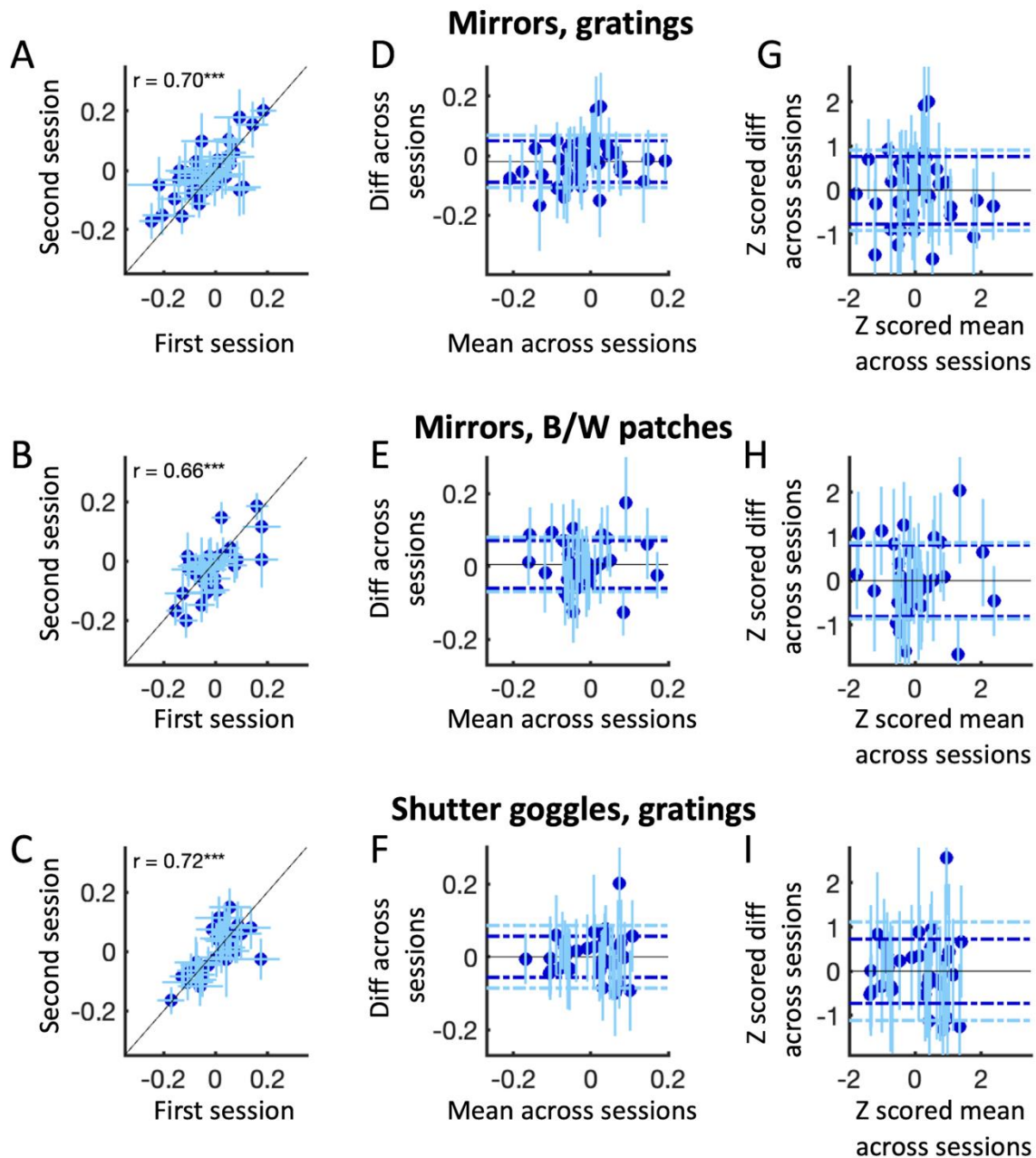
530 Figure 1E-H reports data from experiments 1-4. In all cases, the distribution of the normalized
531 mean durations of exclusive dominance phases was well modelled by the Gamma function (all
532 $R^2 > 0.96$; best-fit parameters are reported as text insets in Figure 1E-H), as expected (LEVELT,
533 1966, 1967). Based on the Gamma-fits we gauged that all four experiments elicited a typical
534 binocular rivalry phenomenon.

535 Next, we focused on three main indices of rivalry dynamics from the first three experiments:
536 ocular dominance (Figure 2), mean phase durations (Figure 3), and mixed percept proportions
537 (Figure 4). Results for the three indices from the fourth experiment are shown in Figure 5.

538 Ocular dominance (computed as in Equation 1) is well correlated across the two sessions of
539 data collection (Experiment 1: $r = 0.70$, $p < 0.001$, $lgBF = 4.42$; Experiment 2: $r = 0.66$, $p < 0.001$,
540 $lgBF = 2.83$; Experiment 3: $r = 0.72$, $p < 0.001$, $lgBF = 4.49$, Figure 2A-C). Inspection of the
541 Bland-Altman plots shows that the confidence intervals of test-retest reliability (horizontal
542 dashed blue lines) are within the confidence intervals of the internal consistency (horizontal
543 dashed cyan lines). In other words, the test-retest reliability (distance of blue symbols from
544 the $y=0$ line) is expected from the internal consistency of the parameter (vertical blue lines
545 representing ± 1 bootstrapped standard error). This means that the variance between sessions

546 is fully explained by the variance within session (internal consistency), indicating that ocular
 547 dominance is not significantly affected by state-dependent day-to-day variations.
 548

Ocular dominance index



549
 550

551 *Figure 2-2. Ocular dominance: variability across sessions and within-session.*

552 *A-C: individual participants' ocular dominance indices for the first (x-axis) and the second*
 553 *session (y-axis). The cyan error bars around data points represent the bootstrapped standard*
 554 *error of a single participant's ocular dominance index within a single session. Continuous black*

555 *lines mark the bisector, indicating no difference between the two sessions. In-text values report*
556 *Pearson's correlation indices and significance (* $p < .05$; ** $p < .01$; *** $p < .001$).*

557 *D-F: Bland–Altman plots where the difference in ocular dominance between the first and*
558 *second sessions is plotted as a function of the mean across two sessions. The horizontal*
559 *continuous black line indicates the mean difference across subjects. The outer horizontal dark*
560 *blue dashed lines indicate the relative 95% limits of agreement, indicative of test-retest*
561 *reliability. Cyan continuous lines around each point show the bootstrapped standard error of*
562 *the single-subject measurements, indicative of internal consistency. Cyan horizontal dashed*
563 *lines indicate the 95% confidence interval of internal consistency across participants. In all*
564 *panels, the three rows report data from experiments 1,2, and 3 respectively.*

565 *G-I: Bland-Altman plots based on z-scored data. All indicators are the same as D-F. The*
566 *continuous black line reports the $y=0$ function.*

567

568 Table 1 reports summary statistics from Figure 2 using similar conventions as in Min et al.,
569 2021 (including z-scoring of the data and reporting 95% limits of agreements and 95%
570 confidence intervals to index test-retest reliability and internal consistency respectively). Our
571 values are not far from the values reported by Min et al (Min et al., 2021) for their binocular
572 rivalry experiments; in particular, measures of internal consistency are comparable across
573 studies or marginally larger. However, our 95% limits of agreements are smaller than those in
574 Min et al. (Min et al., 2021), indicating better test-retest reliability of our ocular dominance
575 indices than any of the measures in Min et al. (Min et al., 2021), both those derived from
576 binocular rivalry and other tasks and paradigms.

577

	Method	Inter-session	Intra-session
Current study	Binocular rivalry: mirrors, gratings (n=40)	±1.53	±1.82
	Binocular rivalry: mirrors, B/W patches (n=33)	±1.62	±1.73
	Binocular rivalry: shutter goggles, gratings (n=34)	±1.46	±2.23
Min et al., 2021	Binocular rivalry: shutter goggles, luminance modulated gratings (n=45)	±2.49	±1.69
	Binocular combination at many contrasts (n=34)	±2.08	±0.59
	Parallel-oriented masking (n=14)	±1.83	±0.50

578

579

580 *Table 2-1. Comparison of test-retest reliability and internal consistency*

581 *The first three rows (pink) show results from our experiments 1-3: the 95% limits of agreement*
582 *of ODI (a measure of test-retest reliability) and the 95% bootstrapped confidence interval (a*
583 *measure of internal consistency). All values are z-scored, as in Min et al., 2021 reported in the*
584 *bottom rows (grey).*

585

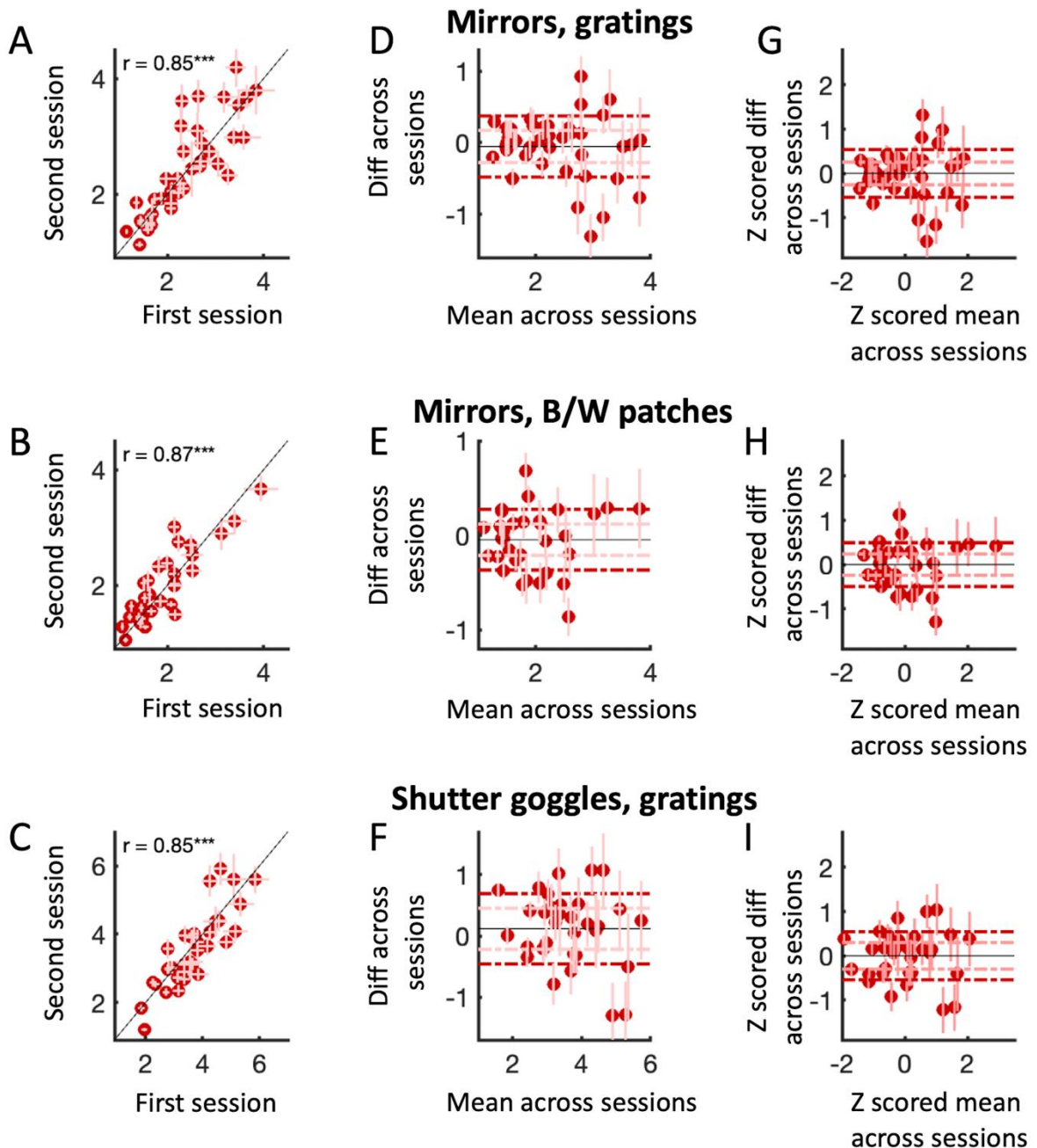
586 Figure 3 uses the same format as Figure 2 to report the mean duration of exclusive dominance
587 phases (pooled across eyes). Again, we found excellent correlations across sessions,
588 irrespectively of the type of stimuli or set-up (Experiment 1: $r = 0.85$, $p < 0.001$, $lgBF = 9.35$;
589 Experiment 2: $r = 0.87$, $p < 0.001$, $lgBF = 8.49$; Experiment 3: $r = 0.85$, $p < 0.001$, $lgBF = 9.45$).
590 However, contrary to what was observed for ocular dominance, the Bland-Altman plots
591 (Figure 3D-F) show that the test-retest reliability (distance of red symbols from the $y=0$ line) is
592 worse than expected from the internal consistency of the parameter (vertical light red lines
593 representing ± 1 bootstrapped standard error), suggesting that a significant portion of the
594 between-sessions variance cannot be explained by the internal fluctuations occurring within
595 the session, but is instead related to external or state-dependent factors.

596

597 Z-scored values in the third column can be compared with the same values computed for ODI
598 (Figure 2 G-I). The spread of the data points indicating the differences across sessions is similar

599 between the two measurements, and their limits of agreement are comparable. However, the
 600 light bars are much shorter for mean phase durations compared to ODI, indicating much
 601 higher internal consistency for mean phase durations than for the ocular dominance index.
 602

Mean phase durations (s)



603
 604
 605
 606

Figure 2-3. Mean durations of exclusive dominance phases: variability across-sessions and within-session.

607 *A-C: individual participants' mean phase durations (s) for the first session (x-axis) and second*
608 *session (y-axis). All indicators are the same as in Figure 2.*

609 *D-F: Bland–Altman plots. All indicators are the same as in Figure 2. Horizontal dark red lines*
610 *mark the 95% confidence interval of test-retest reliability and light red ones mark that of*
611 *internal consistency.*

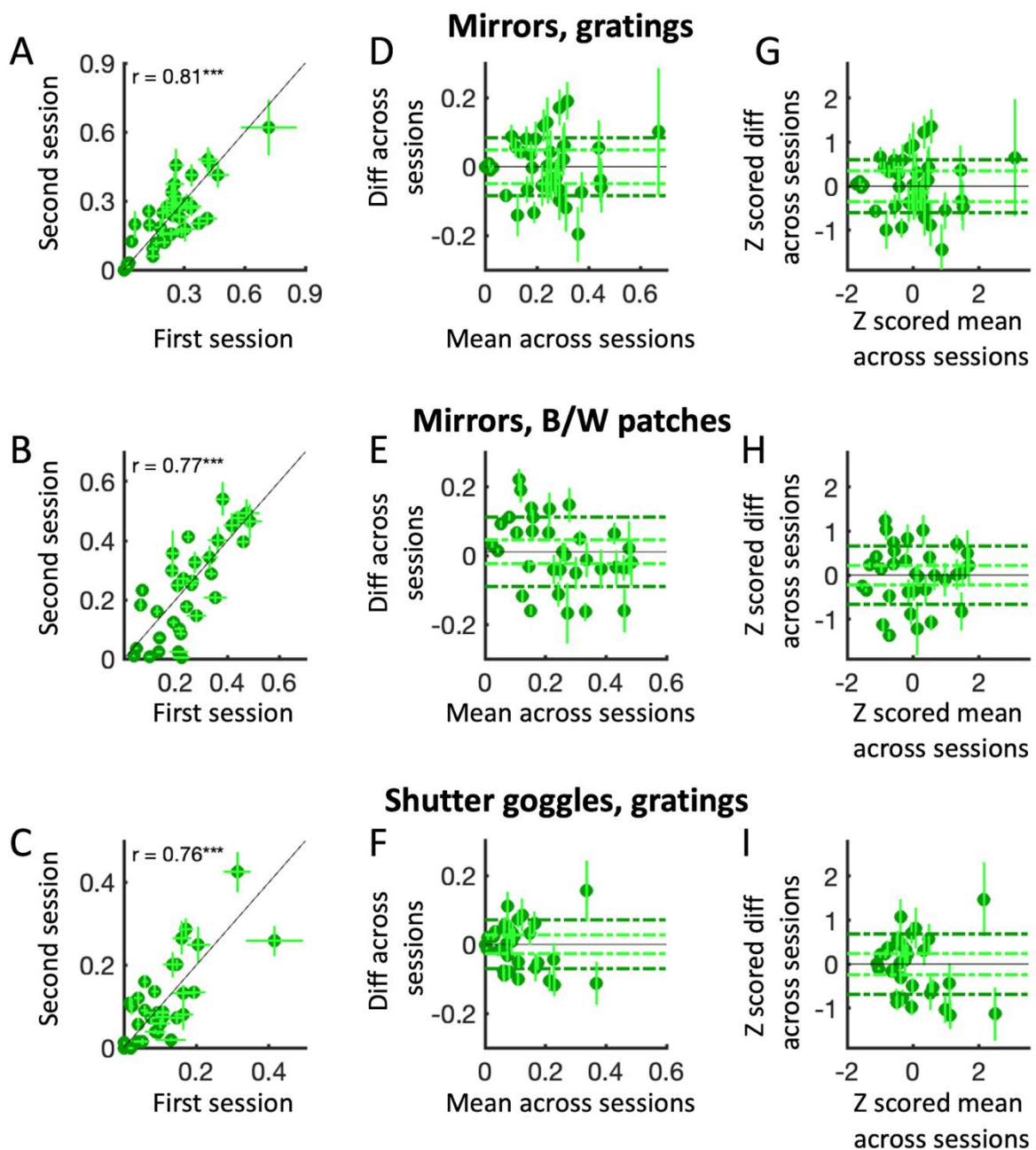
612 *G-I: Bland-Altman plots based on z-scored data. All indicators are the same as D-F.*

613

614 Figure 4 uses the same format as Figures 2 and 3 to report the proportion of mixed percepts.
615 Values are well correlated across sessions (Experiment 1: $r = 0.81$, $p < 0.001$, $\lg BF = 7.74$;
616 Experiment 2: $r = 0.77$, $p < 0.001$, $\lg BF = 5.06$; Experiment 3: $r = 0.76$, $p < 0.001$, $\lg BF = 4.86$).
617 However, as seen for the mean phase durations in Figure 3, the Bland-Altman plots (Figure
618 4D-F) show that the test-retest reliability (distance of blue symbols from the $y=0$ line) is worse
619 than expected from the internal consistency of the parameter (vertical green lines
620 representing ± 1 bootstrapped standard error). The same conclusions hold for the z-scored
621 values plotted in the panels G-I.

622

Mixed proportion



623
624

625 *Figure 2-4. Mixed percept proportions: variability across-sessions and within-session.*

626 *A-C: individual participants' mixed percept proportions for the first session (x-axis) and second*
627 *session (y-axis). All indicators are the same as in Figures 2 and 3. Horizontal dark green lines*
628 *mark the 95% confidence interval of test-retest reliability and light green ones mark that of*
629 *internal consistency*

630 *D-F: Bland–Altman plots. All indicators are the same as in Figures 2 and 3.*

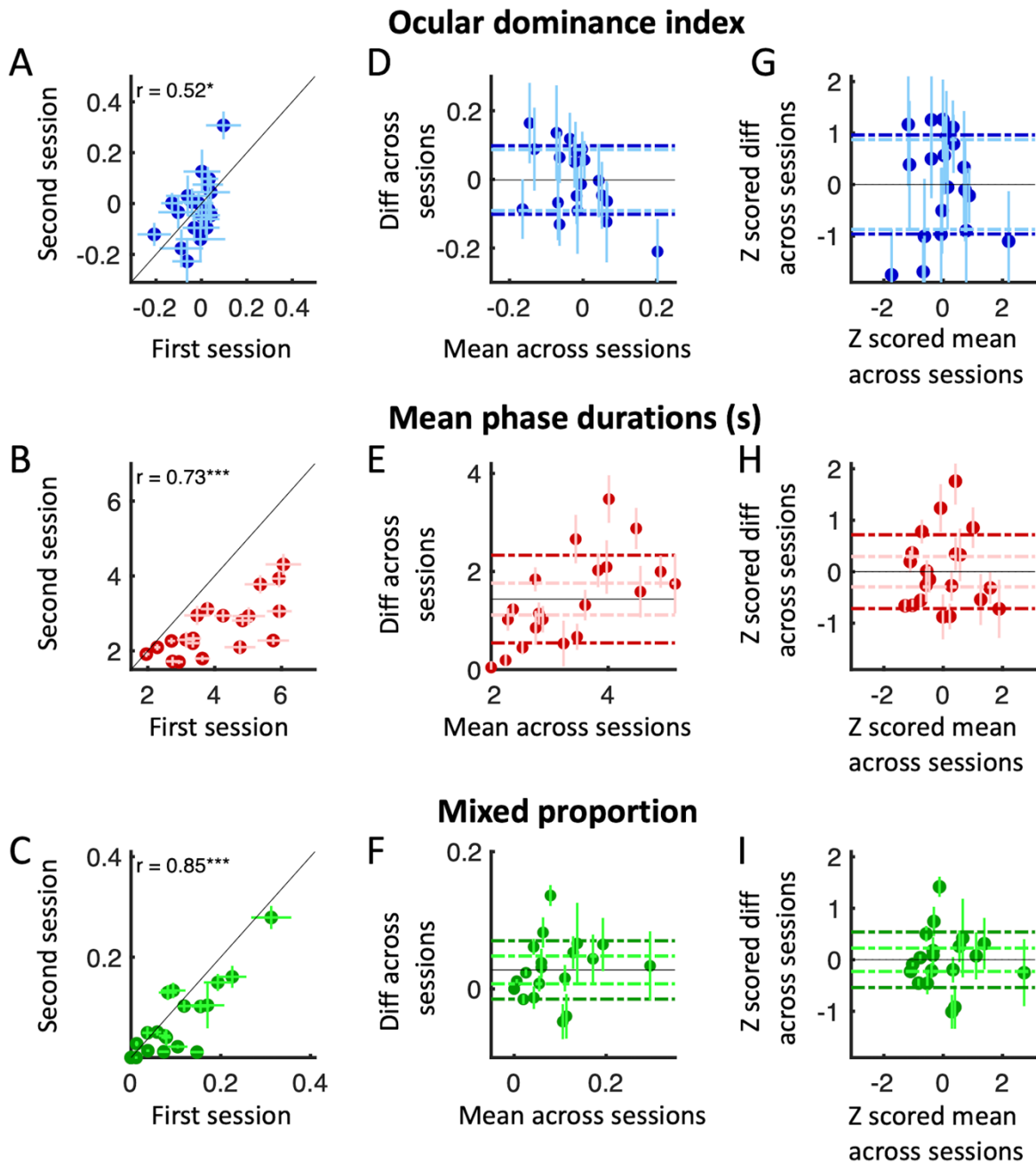
631 *G-I: Bland-Altman plots based on z-scored data. All indicators are the same as D-F.*

632 In our fourth experiment, we asked whether similar conclusions would hold when comparing
633 binocular rivalry dynamics and ocular dominance indices across sessions collected on different
634 days and with different stimulation conditions. We measured rivalry using either the stimulus
635 of experiment 3 (first session: monochromatic gratings delivered via shutter goggles) or a new
636 stimulus (second session: colored gratings delivered via anaglyph glasses). Figure 5A-C shows
637 that rivalry dynamics were still correlated across sessions (ODI: $r = 0.52$, $p = 0.02$, $lgBF = 0.41$;
638 mean phase durations: $r = 0.73$, $p < 0.001$, $lgBF = 2.14$; mixed proportions: $r = 0.85$, $p < 0.001$,
639 $lgBF = 4.01$), although mean phase durations were systematically longer in the first session, as
640 expected from the much lower contrast of the stimuli.

641 Bland-Altman plots show that the main difference across indices is in their internal consistency
642 (better for mixed percept proportions, followed by mean phase durations and worse for ODI),
643 in the face of homogeneously high and fairly similar test-retest reliability. This pattern of
644 results is confirmed by the z-scored data (Figure 5G-I). Thus, the results of experiment 4
645 (comparison across days and experimental set-ups) are in line with the results of experiments
646 1-3 (comparison across days with identical experimental set-ups).

647

Shutter vs. anaglyph goggles, gratings



648
649

650 *Figure 2-5. Consistency of binocular rivalry parameters across set-ups (Experiment 4).*

651 *In all panels, the three rows show data from Experiment 4 for ocular dominance index, mean*
652 *phase duration and mixed percept proportions respectively.*

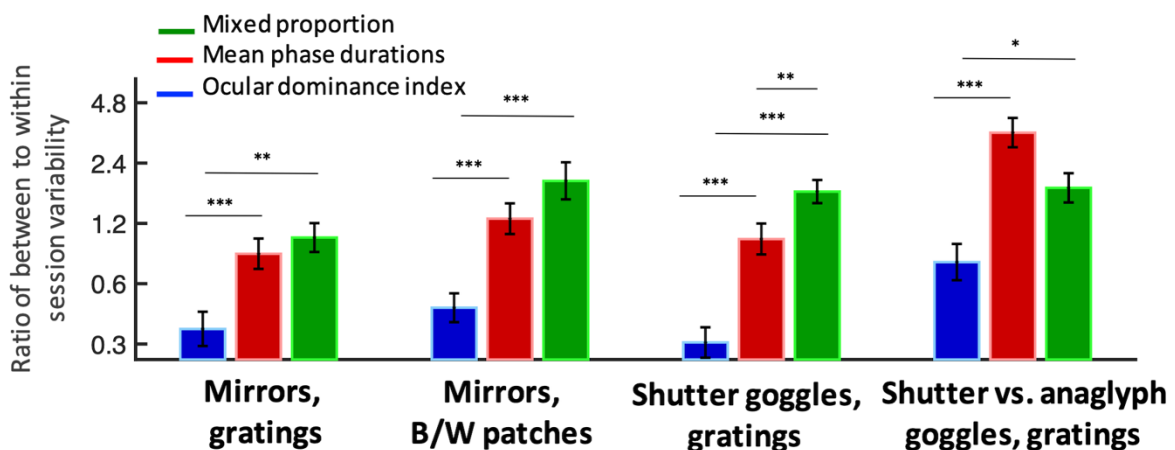
653 *A -C: Individual participants' measurement of interest for the first session (x-axis: shutter*
654 *goggles) and the second session (y-axis: anaglyph goggles). All indicators are the same as in*
655 *Figures 2,3 and 4.*

656 D-F: Bland–Altman plots where the difference in measurement of interest between the first
 657 and second sessions is plotted as a function of the mean across two sessions. All indicators are
 658 the same as in Figures 2,3 and 4.

659 G-I: Bland-Altman plots based on z-scored data. All indicators are the same as D-F.

660

661 Figure 6 illustrates more directly the relationship between internal consistency and test-retest
 662 reliability for the three parameters of interest. For each parameter, we considered each
 663 individual participant’s test-retest reliability (measured as the difference between sessions)
 664 and the same participants’ internal consistency (instability of the measure in each session,
 665 measured as the bootstrapped standard error); we took the ratio of these measures, log-
 666 transformed to distribute normally and finally averaged ratio values across participants. Large
 667 ratio values imply that indices vary more across sessions than within sessions, while small
 668 values imply that intersession differences are largely accounted for by internal (in-
 669)consistency. A two-way ANOVA with within-subjects factor “binocular rivalry parameter”
 670 (three levels: ODI, mean phase durations and mixed percepts) and between-subjects factor
 671 “experiment” (four levels, from 1 through 4) revealed significant effects of parameter
 672 ($F(2,246) = 57.63, p < 0.001$), experiment ($F(3,123) = 10.65, p < 0.001$), and parameter by
 673 experiment interaction ($F(6,246) = 2.15, p = 0.048$). Post-hoc t-tests revealed that, in all
 674 experiments, ODI showed the smallest value; smaller than mean phase durations (Experiment
 675 1: $t = 3.27, p < 0.001$, Experiment 2: $t = 4.88, p < 0.001$, Experiment 3: $t = 5.35, p < 0.001$,
 676 Experiment 4: $t = 5.11, p < 0.001$) and smaller than mixed percept proportions (Experiment 1:
 677 $t = 4.01, p < 0.01$, Experiment 2: $t = 5.48, p < 0.001$, Experiment 3: $t = 7.39, p < 0.001$,
 678 Experiment 4: $t = 2.77, p < 0.05$).



679
 680

681 *Figure 2-6. Comparison of the ratio of test-retest reliability and internal consistency.*
682 *Bar plot of the ratio of test-retest reliability to internal consistency for ocular dominance index*
683 *(blue bars), mean phase duration (red bars) and mixed percept proportion (green bars),*
684 *separately for our four experiments. Ratios were log-transformed before averaging and*
685 *comparing; their means and SEM (shown by the error bars) were transformed back into their*
686 *natural values and visualized on a logarithmic scale; consequently, a value of 2 indicates that,*
687 *on average, the variability between sessions is twice as large as the variability within sessions.*
688 *Asterisks report significance of the post-hoc t-tests (* $p < .05$; ** $p < .01$; *** $p < .001$).*

689

690 2.4 Discussion

691

692 We measured the reliability of three main parameters of binocular rivalry (an index of ocular
693 dominance, the mean of dominance phase durations, and mixed percept proportions), related
694 to two physiological constructs: sensory eye dominance and rivalry switch rate. We measured
695 their stability over time (test-retest reliability) and their stability within each experimental trial
696 (internal consistency).

697 The ocular dominance index showed lower internal consistency than the other two indices:
698 phase durations and mixed percepts. However, this internal noise was sufficient to account
699 for its variability across sessions, implying good stability of this index over time. On the
700 contrary, the high internal consistency of mean phase duration and mixed percept proportions
701 would have predicted higher test-retest reliability than observed. This implies that the test-
702 retest reliability of these measurements is disturbed beyond their internal noise by other
703 external or state-dependent factors.

704 Binocular rivalry is often used to estimate ocular dominance (K. C. Dieter et al., 2017a; Ooi &
705 He, 2020; Xu et al., 2011). In particular, it has been key to reveal a residual form of ocular
706 dominance plasticity in adult humans (Bai et al., 2017; Binda et al., 2017; Chadnova et al.,
707 2017; Lunghi, Berchicci, et al., 2015b; Lunghi, Emir, et al., 2015; Lunghi et al., 2011, 2013; B.
708 N. Nguyen et al., 2021; M. Wang et al., 2020; Xu et al., 2010), with potential translational
709 impact for the treatment of amblyopia (Lunghi et al., 2019; Ooi et al., 2013; J. Zhou et al.,
710 2019). This approach is predicated upon the reliability of the ocular dominance measurements
711 made with binocular rivalry. Min et al., (2021) recently questioned this assumption, reporting
712 that results from binocular rivalry are not particularly stable over time and far worse than

713 other tasks like binocular combination or masking. In the present study, using four
714 independent binocular rivalry experiments, we found strong evidence in support of the
715 stability of ocular dominance indices, which showed excellent test-retest reliability for a
716 variety of methods and stimuli and demonstrated remarkable concordance even when
717 comparing ocular dominance indices obtained with two very different rivalry-inducing stimuli
718 and methods (shutter vs. anaglyph goggles, displaying monochromatic vs. colored stimuli).
719 Using similar metrics as Min et al., 2021, we obtained similar estimates of internal consistency;
720 however, we observed generally better test-retest reliability, implying better stability of our
721 ocular dominance estimates over time (Table 1). We suggest that few differences between our
722 binocular rivalry experiments and the experiment in Min et al., 2021 could account for this
723 discrepancy. One is the larger amount of data per measurement: one session lasted between
724 6 and 12 minutes in our study (2 or 4 trials), but only 3 minutes in Min et al.'s. Another
725 methodological issue concerns the possible impact of perceptual biases and/or adaptation. In
726 all our experiments, we swapped grating orientations across eyes on every trial, to minimize
727 the effects of adaptation and counterbalance the potential impact of subtle non-corrected
728 anisometric refraction errors. In Min et al., most participants were tested without this
729 orientation-swapping step. A third potential difference between our study and Min et al.
730 (2021) concerns the participants' ocular dominance range. In Min et al.'s sample, ocular
731 dominance values range between approximately -0.8 and 0.5, while the largest range in our
732 samples covers values from -0.25 to 0.4. The inclusion of participants with extreme ocular
733 dominance in Min et al.'s sample might be adding to the difference in their reliability
734 estimation and ours, suggesting that binocular rivalry dynamics might be less stable for
735 participants with extreme ocular dominance.

736 We conclude that, provided that some methodological steps are taken, and that participants
737 don't show extreme sensory eye dominance, binocular rivalry provides a robust and stable
738 estimate of ocular dominance, which can be trusted for evaluating its short-term changes like
739 those induced by monocular deprivation.

740 Turning to the other main parameters that may be extracted from binocular rivalry, the mixed
741 percept proportions showed good internal consistency and test-retest reliability. A similar
742 pattern was observed for the mean duration of dominance phases for which we observed high
743 test-retest reliability, comparable to or better than the ocular dominance index, in line with
744 previous reports (Carter & Pettigrew, 2003; K. C. Dieter et al., 2017a, 2017b; van Ee, 2005).

745 Mean phase durations were also well correlated across binocular rivalry measures obtained
746 with different stimuli and methods, despite an overall difference in the average mean phase
747 duration – lower contrast stimuli inducing slower switch rates (Experiment 4). This indicates
748 that some participants have faster/lower switch rates compared to the average across our
749 sample and maintain this behaviour irrespective of the exact stimuli and methods used to
750 induce bistable perception. There is growing evidence that binocular rivalry switch rate
751 reflects a perceptual trait and an internal ultradian rhythm (Carter & Pettigrew, 2003), i.e. a
752 stable and distinctive feature of each individual participant. While our results confirm that
753 part of the variance in this parameter is trait-like, they also highlight the impact of state-
754 dependent factors. When comparing measurements collected on separate days, we found
755 that differences between sessions were larger than could be expected from the internal
756 inconsistency of this parameter. This suggests that a participant’s psychological and/or
757 physiological state contributes to setting their binocular rivalry switch rate while leaving ocular
758 dominance estimates unaffected. This is coherent with evidence showing that, when a
759 binocular rivalry task is repeated over several days, ocular dominance estimates remain stable,
760 while the switch rate is consistently altered by the task repetition (Bao et al., 2018); it is also
761 coherent with our previous observation that switch rates are not predictive of ocular
762 dominance or its plasticity (Steinwurz et al., 2020). Our data offer no elements to understand
763 the nature of these state-dependent variables. We speculate that they could be related to
764 fluctuations in the participant’s motivation and focus on the task, as attention could artificially
765 reduce switch rates (Paffen et al., 2006). In addition, they could be related to fluctuations in
766 other ultradian rhythms that have similar rates as binocular rivalry, such as respiratory rates
767 (0.16-0.33 Hz, (M. A. Russo et al., 2017)) and sympathetic/parasympathetic dynamic balance
768 (e.g. spontaneous fluctuations in pupillary diameter < 1Hz (Reimer et al., 2014) and metabolic
769 factors, given previous indications of a relationship between these factors and
770 cognitive/perceptual function (Animali et al., 2023; Binda & Lunghi, 2017; Pfeffer et al., 2022;
771 Pomè, Burr, et al., 2020).

772

773 In conclusion, our findings provide evidence for the reliability of the two main parameters
774 extracted from binocular rivalry: ocular dominance and switch rate. We show that the switch
775 rate is liable to state-related changes, which limits the possibility of reliably associating this
776 parameter to trait-like characteristics like genetic make-up and psychological traits. On the

777 other hand, we provide evidence that ocular dominance is a trait-like characteristic stable over
778 time, and thereby qualifies binocular rivalry as a valid tool to follow short-term changes of
779 sensory eye-dominance.

780
781
782
783
784
785
786
787
788
789
790
791
792
793
794
795
796
797
798
799
800
801
802
803
804
805
806
807
808
809
810
811
812
813
814
815
816
817
818
819
820
821
822

823
824

825

826 3 Chapter 3- Attention Cueing in Rivalry: Insights from Pupillometry

827

828 3.1 Introduction

829

830 When stimuli in the two eyes are incompatible, binocular fusion fails and perception
831 alternates between the monocular images (Alais & Blake, 2015; Wheatstone, 1838). Rivalry
832 has been shown to depend on attention, as perceptual alternations tend to cease when
833 attention is diverted away. When this happens, neural oscillations in early visual areas are also
834 suppressed (Zhang et al., 2011), consistent with the notion that attention modulates the
835 strength of early neural representations (Carrasco, 2011). These effects are adequately
836 modelled by assuming that attentional resources are automatically driven to the dominant
837 stimulus unless engaged elsewhere; and that attention provides recurrent excitation of the
838 corresponding monocular input, acting synergically with interocular inhibition to maintain the
839 competition between eyes (Li et al., 2017). Besides diverting attention away from the stimuli,
840 cueing attention to one of the rivaling stimuli can affect binocular rivalry, shifting perceptual
841 dominance in favour of the cued percept (Chong et al., 2005; K. C. Dieter et al., 2016; Hancock
842 & Andrews, 2007; Meng & Tong, 2004; Mitchell et al., 2004; Paffen & Alais, 2011; van Ee et
843 al., 2006). However, the neural underpinnings of cueing effects have been less systematically
844 studied and, to the best of our knowledge, no previous study has tested whether attention
845 cueing affects the strength of early visual representations during rivalry. Interocular
846 competition can sometimes be overcome by pattern-based competition, as in interocular
847 grouping rivalry (Alais et al., 2000), where monocular stimuli are complementary, e.g., two
848 half gratings, and perception alternates between images grouped across eyes (Alais et al.,
849 2000). The role of attention in interocular grouping rivalry has not been investigated. In
850 general, attention cueing has more pronounced effects on more complex types of bistable
851 perception, such as Necker cube or bistable structure from motion (Meng and Tong, 2004; van
852 Ee et al., 2005), which could predict stronger attentional modulations in interocular grouping
853 than in binocular rivalry. Here, we propose pupillometry as a method to indirectly index the

854 strength of competing visual representations and objectively quantify the effects of attention
855 cueing on binocular and interocular grouping rivalry.
856 Pupil size is mainly set by retinal illumination through a simple subcortical circuit (Loewenfeld,
857 1993). However light responses are modulated by saliency, attention, brightness illusions and
858 contextual processing (Binda & Murray, 2015b; Laeng et al., 2012; Mathôt, 2018; Wang &
859 Munoz, 2015) indicating that the subcortical circuit is fed with cortical signals (Binda & Gamlin,
860 2017) that represent effective stimulus strength. As long as stimuli are tagged with different
861 luminance, pupil diameter can be used to accurately and precisely track attention in space
862 (Binda et al., 2013; Mathôt et al., 2013; Naber et al., 2013) and perceptual alternations over
863 time (Einhäuser et al., 2008; Fahle et al., 2011; LOWE & OGLE, 1966; Naber et al., 2011; Tortelli
864 et al., 2021a; Turi et al., 2018). Here, we exploited this strategy and used luminance to tag
865 pupil responses to stimuli rivalling in perception (for an alternative approach that did not rely
866 on luminance tagging, see Brascamp et al., 2021. We predicted that, if attention cueing
867 enhances the effective strength of the dominant stimulus, pupil modulations should be
868 amplified. The amplification would provide an objective and time-resolved index of how
869 attention affects binocular and interocular grouping rivalry.

870

871 3.2 Materials and Methods

872 3.2.1 Participants

873

874 We recruited 38 participants (17 males and 21 females including two authors, mean age 26.5
875 6 0.69 years). Sample size was based on a power analysis that determined the minimum
876 number of participants required to detect a medium-sized effect (effect size 0.50, two-tailed
877 a 0.05, power 0.8 = 33 participants; we recruited a few more anticipating data losses that
878 fortunately did not occur). Ten additional participants were recruited for the control
879 experiment (nine females and one male, mean age 27.1 6 0.82 years). All participants had
880 normal or corrected-to-normal visual acuity (ETDRS charts), normal stereopsis (TNO test), and
881 normal color vision (Ishihara plates); balanced ocular dominance (excluding participants with
882 ocular dominance higher than 70%); no self-reported history of eye surgery, other active eye
883 diseases or mental illness.

884

885 3.2.2 Ethics statement

886

887 The experimental protocol was approved by the local ethics committee (Comité d'Éthique de
888 la Recherche de l'Université Paris Descartes, CER-PD:2019–16-LUNGHI) and was performed in
889 accordance with the Declaration of Helsinki (DoH-Oct2008). All participants gave written
890 informed consent and were reimbursed for their time at a rate of 10e/h.

891

892 3.2.3 Apparatus, stimuli, and procedures

893

894 Experiments took place in a dark and quiet room. Visual stimuli were developed in MATLAB
895 (The MathWorks Inc.) using Psychtoolbox-3 (Brainard, 1997) running on a PC (Alienware
896 Aurora R8) and a NVIDIA graphics card (GeForce RTX2080). Visual stimuli were displayed on a
897 53.5-cm-wide monitor, driven at a resolution of 1920 x 1080 pixels. The display was linearized
898 by γ -correction; it was seen through a four-mirror stereoscope which enabled dichoptic
899 viewing of two display areas of $12 \times 8^\circ$ each; a chin rest was used to stabilize head position at
900 57 cm from the display. In each display area, a central red fixation point (0.15° in diameter)
901 surrounded by a square frame ($3.5 \times 3.5^\circ$) was shown against a uniform grey background
902 (luminance: 152 cd/m^2). The mirrors were carefully adjusted at the beginning of each session
903 to ensure accurate alignment of the dichoptically presented squares. Participants were asked
904 to keep their gaze on the fixation point shown at screen center and to refrain from blinking
905 while the stimuli were on. Dichoptic presentations consisted of two sets of stimuli, designed
906 to elicit two forms of rivalry: binocular rivalry and interocular grouping rivalry. For binocular
907 rivalry, visual stimuli consisted of two disks (Fig. 1A), 3° in diameter, one white (maximum
908 screen luminance 295 cd/m^2) and one black (minimum screen luminance 10 cd/m^2). Given the
909 mid-level grey background, the two stimuli had virtually identical Weber contrast of 0.9, but
910 they differed in terms of Michelson (0.3 for the white disk and 0.9 for the black disk).
911 Perception alternated between exclusive dominance of the white and the black disk, or mixed
912 percepts (either piecemeal or fusion). To discourage fusion, the disks were overlaid with thin
913 orthogonal grey lines (45° clockwise or counterclockwise, one pixel wide, corresponding to
914 0.033° , and 0.5° apart, with the same luminance as the background).

915 For interocular grouping rivalry, the same stimuli (white/black disks with thin lines) were split
916 vertically, and the two halves were shown to the two eyes (Fig. 1B). Possible percepts were
917 exclusive dominance of the white or the black disk (grouped interocularly), monocular
918 percepts (half white half black disks, as shown to the left or to the right eye) and fusion or
919 piecemeal percepts. Stimuli were presented continuously for 3-min-long trials. Trials were
920 separated by 60-s-long pauses with only the fixation point shown against the background.
921 During this time, participants reported their perception of afterimages; analyses of this
922 behaviour will be reported in a separate publication. On each trial, a different combination of
923 disk colour and line orientation was presented to each eye; combinations varied pseudo-
924 randomly across trials. Participants continuously reported perception by keeping one of three
925 keys pressed: right or left arrows to report dominance of the stimulus with clockwise or
926 counter-clockwise tilted lines, or the down-arrow key any time dominance of either stimulus
927 was incomplete (i.e., monocular percepts in interocular grouping rivalry, piecemeal and fusion
928 events were not distinguished in our paradigm). We did not exclude data from any trial or
929 participant. We eliminated perceptual phases shorter than 0.3 s (accounting for a total of 1.3%
930 and 0.6% of recording time for binocular rivalry and interocular grouping rivalry, respectively),
931 which we assumed to reflect keypress-errors or very fast switches or return transitions that
932 would not be adequately tracked by the slow dynamics of the pupil. In total, we analyzed ~
933 500 perceptual phases per participant and stimulus type (591.23 ± 25.71 for binocular rivalry
934 and 501.78 ± 23.97 for interocular grouping rivalry, mean ± 1 SE across participants).
935 Dominance phase distributions were adequately captured by a typical γ -distribution (LEVELT,
936 1967) with shape a and scale b parameters for binocular rivalry: $a = 2.62$; $b = 0.32$ and for
937 interocular grouping rivalry: $a = 2.50$ and $b = 0.34$ in Equation 1. The goodness-of-fit
938 (coefficient of determination R^2) was 0.94 for binocular rivalry and 0.97 for interocular
939 grouping:

940

$$941 \quad f(x|\alpha, \beta) = \frac{1}{\beta^\alpha \Gamma(\alpha)} x^{\alpha-1} e^{-\frac{x}{\beta}} \quad \text{for } x, \alpha, \beta > 0$$

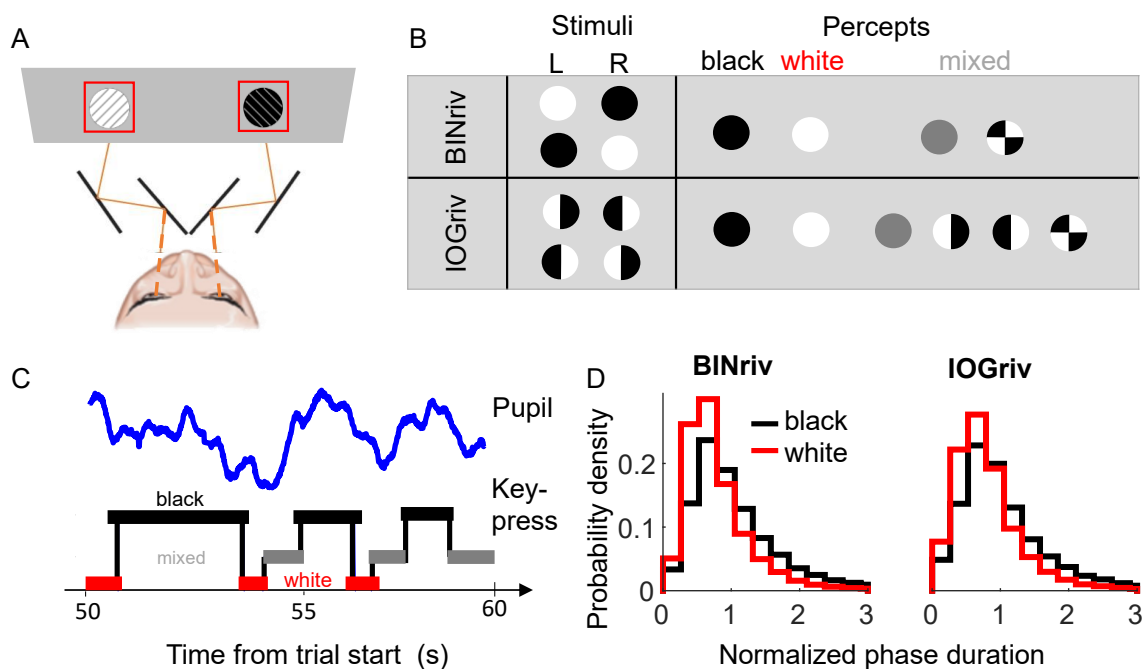
942

943

944 *Equation 3-1*

945 Where Γ is the gamma function and x the number of dominance phases.

946 Binocular rivalry and interocular grouping rivalry were both tested in three conditions: no
 947 attentional cue, black percept cued or white percept cued. In the latter, a “D” or a “B” letter
 948 was displayed at the beginning of the trial cueing participants to endogenously focus their
 949 attention on the black or white disk throughout the rivalrous alternations. We applied a fully
 950 randomized factorial design, where each participant completed 32 trials, divided into eight
 951 sessions of four trials each, one for each combination of rivalry type and attentional cueing,
 952 distributed over two days. We also set up a simulated rivalry stimulus, where a single white,
 953 black or half white and half black disk (the latter simulating mixed percepts) was shown
 954 monocularly to one eye (right or left in separate trials), alternating with phases of 2.5 ± 0.01
 955 s. Four trials of this stimulus were always run at the beginning of the experiment, to help
 956 participants familiarize themselves with the task. Note that this is different from a standard
 957 “replay rivalry” as it involved a standardized alternation between stimuli, and it was merely
 958 intended to measure pupil modulations produced by the physical alternation of luminance
 959 stimuli.
 960



961
 962 *Figure 3-1- Dichoptic stimulation and rivalry dynamics.*

963 *A: Schematics of the stimuli (white or black patches overlaid with orthogonal thin lines),*
 964 *presented dichoptically through a four-mirror stereoscope. B: Schematic representation of*

965 *the possible stimulus configurations (thin lines omitted) and perceptual outcomes for*
966 *binocular rivalry (BINriv) and interocular grouping rivalry (IOGriv).*
967 *C: Example traces from a segment of the experiment, where participants used keypresses to*
968 *report the dominant percept (square wave) and we recorded pupil size modulations (blue*
969 *wave). D: Probability density function of the normalized phase durations for exclusive*
970 *dominance of white or black disk percepts in binocular rivalry and interocular grouping rivalry.*

971 3.2.4 Eye tracking data acquisition and analysis

972
973 During rivalry and simulated rivalry, we monitored pupil diameter and two-dimensional eye
974 position with an infrared camera (EyeLink 1000 system, SR Research) mounted below the
975 monitor screen and behind the stereoscope. EyeLink data were streamed to the main
976 computer through the EyeLink toolbox for MATLAB (Cornelissen et al., 2002) and thereby
977 synchronized with participant's keypresses. Pupil diameter measurements were transformed
978 from pixels to millimeters using an artificial 4-mm pupil positioned at the approximate location
979 of the participant's eye. Pupil and gaze tracking data consisted of 180 x 100 (180 s at 1000 Hz)
980 time points. These included signal losses, eyeblinks and other artifacts, which we cleaned out
981 by means of the following steps (all implemented with in-house MATLAB software):

- 982 - Identification and removal of large artifacts: removal of time-points with unrealistically small
983 or large pupil size (more than 1.5 mm from the median of the trial or <0.2 mm, corresponding
984 to blinks or other signal losses).
- 985 - Identification and removal of finer artifacts: identification of samples where pupil size varied
986 at unrealistically high speeds (> 10 mm per second, beyond the physiological range).
- 987 - Removal of low-frequency oscillations by subtracting a high-pass Butterworth filter with a
988 threshold frequency of 0.1 Hz from each 180 s-long trial.

989 After this cleaning procedure was applied, we verified fixation stability by measuring the
990 dispersion of eye position samples around the mean of each trial as the bivariate confidence
991 ellipse area (BCEA), defined as the following:

992

$$993 \quad BCEA = 2 * k * \sigma_H * \sigma_V * (1 - \rho)^{0.5}$$

994 *Equation 3-2*

995 Where k is the confidence limit for the ellipse, σ_H and σ_V are the standard deviation of eye
996 positions in the horizontal and vertical meridian respectively, ρ is the product-moment
997 correlation of these two position components and $k=1.14$, implying that the ellipse included
998 68% ($1-e^{-k}$) of the distribution. To test for possible differences in eye-movement patterns,
999 we averaged the BCEA values across trials and entered these values in a 2x2 repeated measure
1000 ANOVA with factors: cueing condition (no cue/cueing) and rivalry type (binocular/interocular
1001 grouping rivalry). No main effect or interaction was significant, suggesting that fixation was
1002 equally stable across all conditions and rivalry types (main effect of cueing condition: $F(1,37)$
1003 = .41, $p = .52$, $\log BF = -.64$; main effect of stimulus type: $F(1,37) = .44$, $p = .51$, $\log BF = -.69$;
1004 cueing condition by stimulus type interaction: $F(1,37) = .70$, $p = .41$, $\log BF = -.54$). After
1005 cleaning, pupil data and continuous recordings of perceptual reports were down-sampled to
1006 100 Hz, by taking the median of the retained time points in nonoverlapping time windows. If
1007 no retained sample was present in a window, that window was set to “NaN” (MATLAB code
1008 for “not a number”). Down-sampled pupil traces (to which we re-applied the second step of
1009 the cleaning procedure) were finally parsed into epochs locked to each perceptual switch
1010 (when the participant changed perceptual report) and labeled according to the color of the
1011 dominant stimulus after the switch. Pupil time courses were averaged across epochs for each
1012 participant; further averaging across participants yields traces in Figure 2. In order to minimize
1013 the impact of pupil size changes unrelated to the perceptual switches, we also analyzed data
1014 after subtracting a baseline from each epoch, measured in the -1: 0.5 s interval preceding the
1015 switch. To compare pupil size across dominance phases, stimuli and attention conditions, we
1016 extracted a pupil size index by averaging baseline corrected pupil size in the -0.5:1 s interval
1017 around the switch. Note that shifting the intervals for pupil baseline, or skipping the baseline
1018 correction step, affected the size of pupil modulations but it did not change our conclusion on
1019 the effects of attention and stimulus type (see Appendix Fig. 7-1); also, we verified that
1020 attention cueing did not affect pupil baseline measures (see Appendix Fig. 7-2).

1021 To quantify the effect of attention on both perceptual reports and pupil measurements, we
1022 computed indices of attentional modulation (AMI) for comparing perceptual and pupil
1023 measures in cueing versus in no-cueing trials. Specifically, we used Eq. 3-4, where PROP is the
1024 total dominance time of the white and black disk percepts divided by total testing time and
1025 PUPDIFF is the average pupil size difference between black and white disk dominance phases.
1026

1027
$$AMI_{prop} = (PROP\ percept1_{cued} - PROP\ percept2_{uncued}) -$$

1028
$$(PROP\ percept1_{nocue} - PROP\ percept2_{nocue})$$

1029 *Equation 3-3*

1030
$$AMI_{pup} = PUPDIFF_{cued} - PUPDIFF_{nocue}$$

1031 *Equation 3-4*

1032

1033 For the sake of clarity, we chose to quantify perceptual reports using dominance proportions;
1034 however, the same conclusions could be drawn analyzing mean phase durations instead. To
1035 check for possible differences in the reliability of pupillary modulations across conditions, we
1036 also evaluated the cross-correlation between pupil size and perceptual reports. Previous
1037 studies reported that synchronization with rapid cognitive and perceptual events is more
1038 precise for pupil change rate (the first derivative of pupil size) than for pupil (Brascamp et al.,
1039 2021; de Gee et al., 2020; Murphy et al., 2021), presumably because of the long temporal
1040 impulse-response function of the pupil, which results in a broad autocorrelation of this
1041 measure. In line with these studies, we opted to measure the cross- correlation between
1042 perceptual reports and the pupil-size change rate. For each participant, we averaged the
1043 normalized cross-correlation function across trials and stimulus type. We fit it with a Gaussian
1044 function (constrained to peak at lags smaller than 1.5 s and with SD smaller than 0.2 s) and
1045 compared its peak amplitude across conditions.

1046 3.2.5 Statistical approach

1047

1048 Significance was evaluated using both p-values and log-transformed JZS Bayes factors
1049 computed with the default scale factor of 0.707 (Wagenmakers et al., 2012). The Bayes factor
1050 is the ratio of the likelihood of the two models H1/H0 given the observed data, where H1 is
1051 the experimental hypothesis (effect present) and H0 is the null hypothesis (effect absent). A
1052 base 10 logarithm of the Bayes factor (logBF) larger than |0.5| corresponds to a likelihood
1053 ratio larger than 3 in favor of either H1 (when logBF > 0.5) or H0 (when logBF < -0.5) and this
1054 value is conventionally used to indicate substantial evidence in favor of either hypothesis (Kass
1055 & Raftery, 1995; Keyzers et al., 2020). Bayesian ANOVAs were run in JASP, and the
1056 corresponding Bayes factors represent the change from before posterior inclusion odds
1057 (BF_{inclusion}) computed across matched models. Moreover, following the review reviewed by
1058 Richardson (Richardson, 2011), we report partial eta squares (η^2 , computed in JASP) as effect

1059 size estimates for all factors in our repeated measures ANOVAs. We estimated the internal
1060 consistency of our parameter estimates by split-half reliability. Each parameter was estimated
1061 twice per participant, on half the dataset (odd and even trials) and we evaluated the
1062 correlation of the two sets across participants. Finally, we evaluated the significance of
1063 behavioral attentional effects at the single participant level with a bootstrapping approach, by
1064 resampling (10,000 times, with reinsertion) dominance phases in cueing and no-cueing
1065 conditions, applying Equation 3, computing the proportion of samples where the attentional
1066 modulation index was larger than 0 or smaller than 0 and assigning the significance for $p <$
1067 0.025.

1068 3.2.6 Control experiment

1069

1070 A control experiment was performed after the end of the study, with the aim of estimating
1071 the sensitivity of pupil size measurements to manipulations of stimulus strength. The original
1072 set-up was inaccessible at the time of testing, and we replicated the conditions of the main
1073 experiment as closely as possible in another set-up, using the same eye-tracker (EyeLink 1000
1074 system, SR Research), similar mirror stereoscope and a computer that ensured equal
1075 performance. Specifically, stimuli were generated with the PsychoPhysics Toolbox routines
1076 (Brainard, 1997) and MATLAB (MATLAB r2010a, The MathWorks Inc.) housed in a Mac Pro 4.1,
1077 and displayed on a 52.5-cm-wide LCD screen with maximum screen luminance of 108 cd/m².
1078 Instead of using the maximum and minimum screen output, we reduced luminance levels by
1079 about a factor of 10 to allow for modulations of stimulus contrast. We set the background
1080 luminance to 15 cd/ m² grey and tested six conditions: a no cue and white cued condition in
1081 which stimuli were 28 and 2 cd/ m² or the white and black disk, re-respectively, and four
1082 conditions where the Michelson contrast of the white disk stimulus was increased by 25%,
1083 50%, 100% and 150% (luminance values: 33, 40, 63, and 108 cd/ m²). Each condition was
1084 tested in four trials, and all data were collected over a single session.

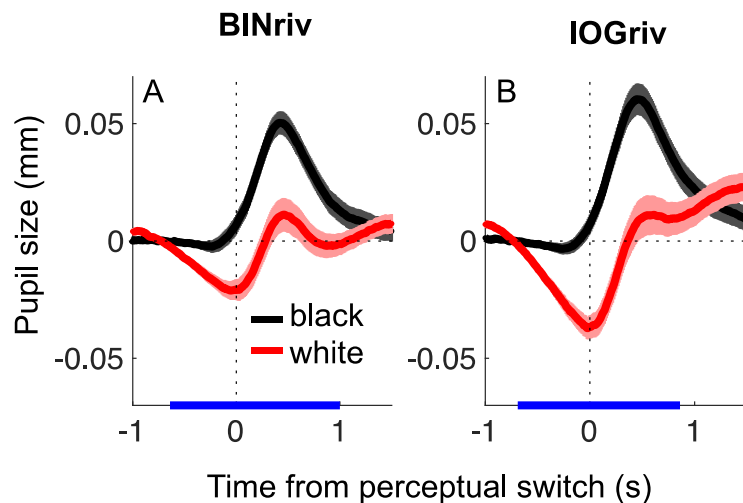
1085

1086 3.3 Results

1087

1088 We analysed perceptual alternations and the associated pupil modulations during binocular
1089 and interocular grouping rivalry, in two conditions: with and without attentional cueing. In
1090 no cueing conditions, pupil diameter reliably tracked perceptual alternations between a white

1091 and a black disk presented dichoptically, either one disk per eye generating binocular rivalry,
1092 or each disk split vertically between eyes generating interocular grouping rivalry (Figure 1).
1093 Despite constant stimulation (hence constant luminance), pupils were relatively dilated when
1094 participants reported seeing black, compared to when they reported seeing white (Figure 2A-
1095 B, black vs red line), in both types of rivalry.



1096

1097

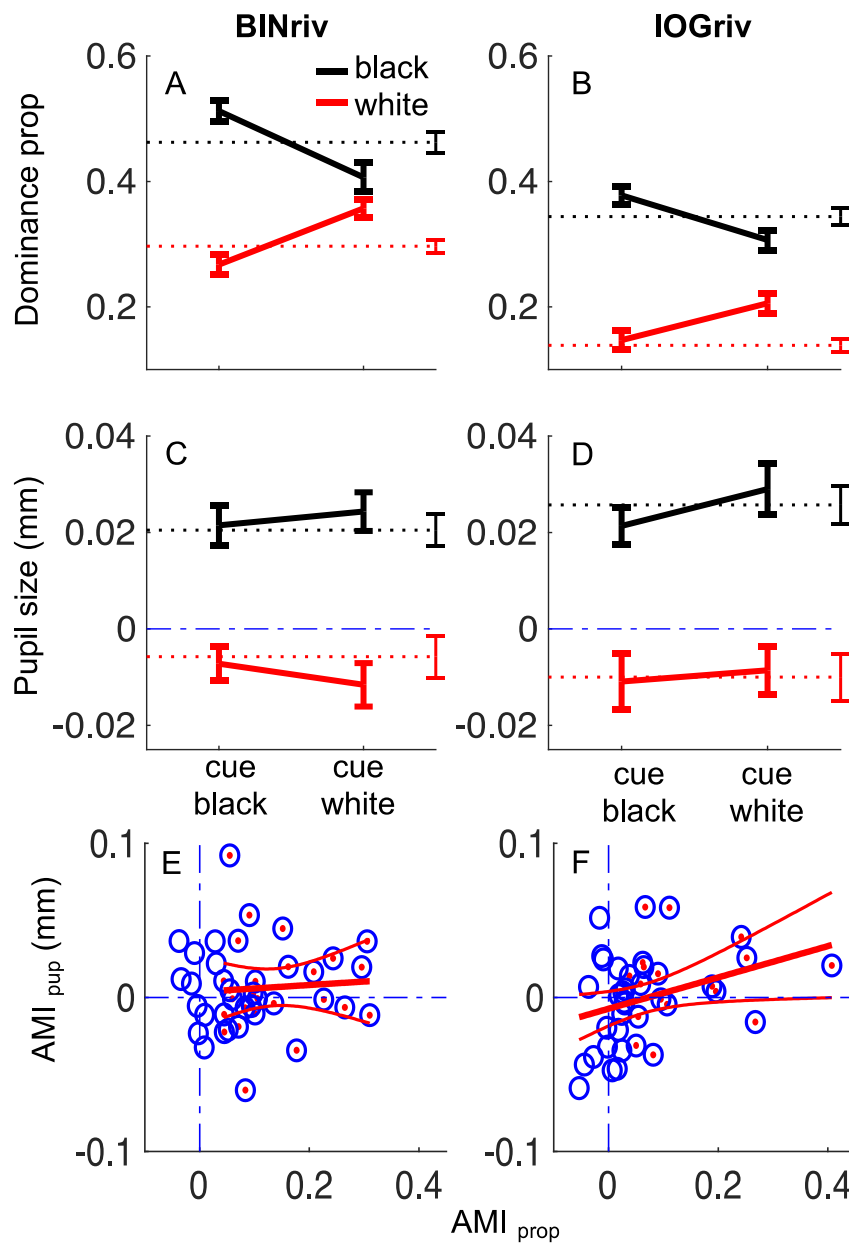
1098 *Figure 3-2 Pupil modulations track perceptual alternations.*

1099 *Baseline subtracted pupil size traces aligned to perceptual switches towards exclusive*
1100 *dominance of a white disk or a black disk percept and averaged across phases, separately for*
1101 *binocular rivalry (A) and interocular grouping rivalry (B). In all panels: shadings report mean*
1102 *± 1 s.e. across participants and the blue marks on the x-axis highlight timepoints where*
1103 *pairwise comparisons between traces are significant (one-tailed t-test, $p < 0.05$ FDR corrected).*
1104 *Observations regarding the latency of the pupillary response and its relative magnitude are*
1105 *reported in Figure 7-1 in the Appendix, where non-baseline subtracted traces are shown.*

1106

1107 The analysis of behavioural reports in the no cueing condition (dotted lines in Figure 3) showed
1108 a net predominance of black disk percepts with respect to the white ones (binocular rivalry:
1109 $t(37) = 8.70$, $p < .001$, $\log BF = 7.77$; interocular grouping rivalry: $t(37) = 12.81$, $p < .001$, $\log BF$

1110 = 12.27). In line with the modified Levelt's propositions and results by Qiu et al., 2020, this
1111 can be explained by the higher Michelson contrast of the black disk stimulus (recall that the
1112 background was set to mid-grey, resulting in identical Weber contrast but different Michelson
1113 contrast for the two disk stimuli). However, dominance of the black percept cannot logically
1114 explain the pupil modulations; moreover, while both black dominance and pupil size
1115 modulations varied across participants, the two were reliably uncorrelated (binocular rivalry:
1116 $r = -.09$, $p = .58$, $\log BF = -.83$, interocular grouping rivalry: $r = -.20$, $p = .22$, $\log BF = -.58$).
1117 Figure 3A-B also shows that exclusive percepts were much rarer in interocular grouping rivalry
1118 compared to binocular rivalry ($t(37) = 12.23$, $p < .001$, $\log BF = 11.68$), reflecting the response
1119 mapping we used; for interocular grouping rivalry, mixed reports included epochs where the
1120 individual monocular images in the left and right eye dominated.
1121 Having established pupil size as a marker of perceptual dominance in both binocular and
1122 interocular grouping rivalry, we proceeded to assess the impact of attention cueing on
1123 perceptual alternations and pupil size modulations (continuous lines in Figure 3).
1124



1125

1126 *Figure 3-3 Attention cueing affects perceptual alternations but not pupil modulations*

1127 *A-B: perceptual dominance for exclusive white (red line) or black (black line) disk percepts,*
 1128 *without attentional cueing (dashed lines) or when the white or the black disk percept were*
 1129 *cued (continuous lines, cueing condition indicated on the abscissa). Error bars report ± 1 s.e.*
 1130 *across participants.*

1131 *C-D: baseline corrected average pupil size computed in a fixed temporal window (between -.5*
 1132 *and 1 s from the perceptual transition) during phases of exclusive dominance of the black*
 1133 *(black line) and the white disk (red line). Results from the no-cueing condition are reported by*

1134 *dashed lines. Continuous lines report the results from the trials where the white or the black*
1135 *percepts were cued (separated on the abscissa). Error bars report ± 1 s.e. across participants.*
1136 *E-F: individual participants' attentional modulation indices for perceptual dominance (x-axis)*
1137 *and pupil size (y-axis), computed with Equations 3-4. Dash-dot blue lines mark the $x=0$ and $y=0$*
1138 *lines, indicating no effect of attention cueing. Each circle reports results from one participant;*
1139 *red dots highlight participants with a significant attentional modulation index for perceptual*
1140 *dominance. Red lines show the best fitting line and its 95% confidence intervals.*

1141 *In all panels, the left column reports results for binocular rivalry and the right for interocular*
1142 *grouping rivalry.*

1143 As expected, perceptual dominance of the cued stimulus was enhanced, resulting in a
1144 significant interaction between dominant percept (white/black) and cued percept
1145 (cueing white/cueing black) on the proportion of exclusive dominance phases (Fig. 3A, B;
1146 Table 1, middle column). We summarized the effect of attention with an attentional
1147 modulation index (Eq. 3 in Materials and Methods), which was in the order of 10% for both
1148 types of rivalry (single participant data are shown on the abscissas of Fig. 3E, F). The effect
1149 was statistically reliable at the group level and, in most cases, at the individual participant
1150 level (boot-strapped attentional modulation indices were significantly higher than zero in
1151 27/38 or 20/38 participants for binocular and interocular grouping rivalry, respectively,
1152 highlighted with a red dot in Fig. 3E, F; it was significantly lower than zero in only 2/38
1153 participants for interocular grouping rivalry and in no participant for binocular rivalry).
1154 Attentional modulation indices were correlated between binocular rivalry and interocular
1155 grouping ($r = 0.61$, $p < 0.001$, $\log BF = 2.63$), suggesting that they measure a relatively stable
1156 feature of our participants. In line with this, we found no indication that interocular grouping
1157 rivalry was more affected by attention than binocular rivalry; if anything, there was a small
1158 effect in the opposite direction (binocular rivalry minus interocular grouping rivalry, $t(37) =$
1159 2.33 , $p = 0.02$, $\log BF = 0.28$).

1160

	Proportions	Pupil size
dominant percept	$F_{(1,37)} = 146.46^*$ $p < 0.001$ $\log BF = 30.54$ $\eta_p^2 = 0.80$	$F_{(1,37)} = 46.09^*$ $p < 0.001$ $\log BF = 22.52$ $\eta_p^2 = 0.55$
rivalry type	$F_{(1,37)} = 82.62^*$ $p < 0.001$ $\log BF = 25.49$ $\eta_p^2 = 0.69$	$F_{(1,37)} = 0.12$ $p = 0.73$ $\log BF = -0.90$ $\eta_p^2 = 0.003$
cued percept	$F_{(1,37)} = 5.37^*$ $p = 0.03$ $\log BF = -0.82$ $\eta_p^2 = 0.13$	$F_{(1,37)} = 1.91$ $p = 0.17$ $\log BF = -0.78$ $\eta_p^2 = 0.05$
dominant percept x rivalry type	$F_{(1,37)} = 0.99$ $p = 0.33$ $\log BF = -0.62$ $\eta_p^2 = 0.03$	$F_{(1,37)} = 0.17$ $p = 0.68$ $\log BF = -0.72$ $\eta_p^2 = 0.005$
dominant percept x cued percept	$F_{(1,37)} = 32.96^*$ $p < 0.001$ $\log BF = 11.33$ $\eta_p^2 = 0.47$	$F_{(1,37)} = 1.78$ $p = 0.19$ $\log BF = -0.53$ $\eta_p^2 = 0.05$
rivalry type x cued percept	$F_{(1,37)} = 0.08$ $p = 0.77$ $\log BF = -0.78$ $\eta_p^2 = 0.002$	$F_{(1,37)} = 1.92$ $p = 0.17$ $\log BF = -0.54$ $\eta_p^2 = 0.05$
dominant percept x rivalry type x cued percept	$F_{(1,37)} = 5.45^*$ $p = 0.02$ $\log BF = -0.11$ $\eta_p^2 = 0.13$	$F_{(1,37)} = 0.03$ $p = 0.85$ $\log BF = -0.41$ $\eta_p^2 < 0.001$

1161

1162 *Table 3-1 The effects of cueing on proportions and pupil size.*

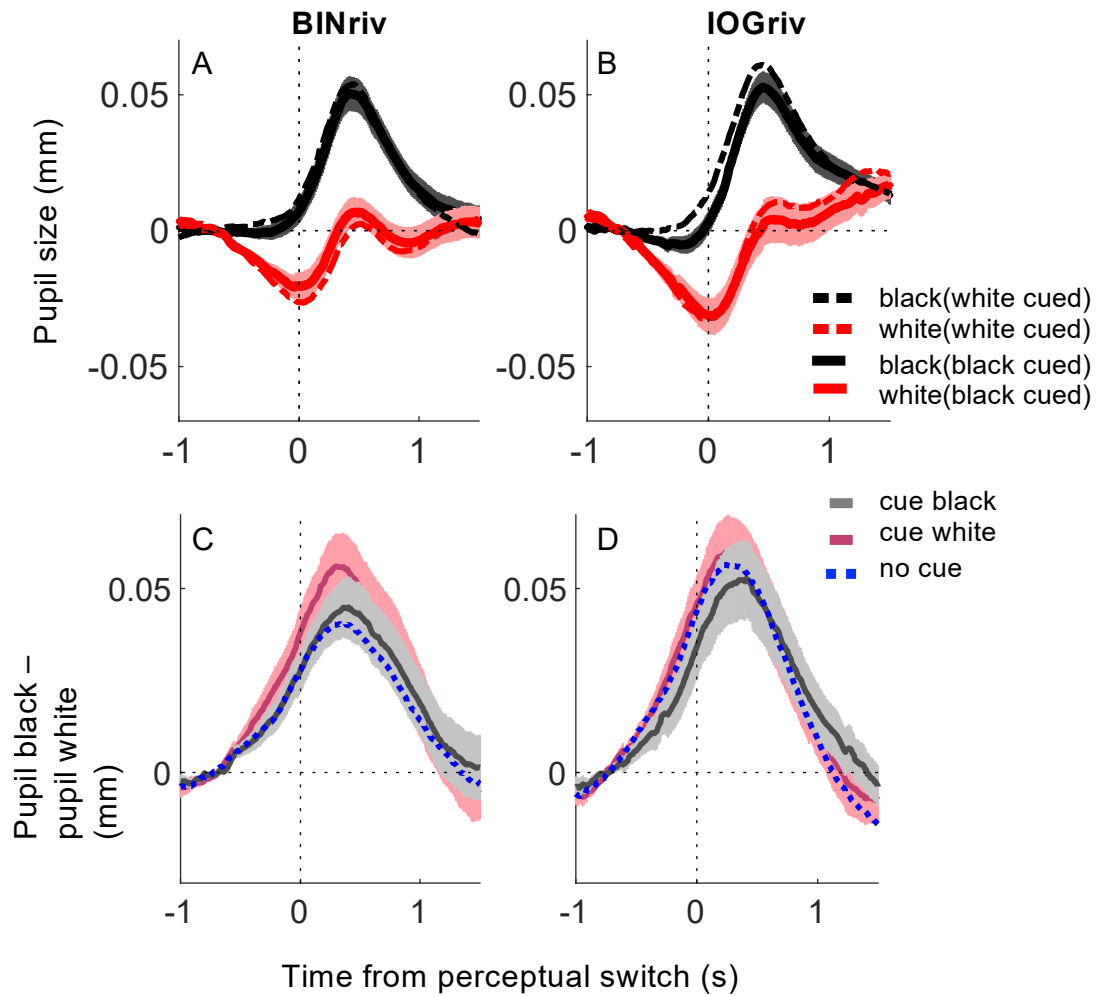
1163 *Three-way ANOVA for attention cueing results, with factors: dominant percept (white/black*

1164 *disk), cueing (white/black cued), rivalry type (binocular/interocular grouping rivalry). These*

1165 *results were not affected by skipping this baseline correction step or defining pupil baseline*

1166 *over a wider temporal interval (Table 7-1 in the Appendix).*

1167 Based on the assumption that attention cueing boosts perceptual dominance by enhancing
1168 the effective strength of the cued percept, we expected to find an enhancement of the pupil
1169 responses accompanying perceptual alternations. For example, we predicted that dilations
1170 concurrent with black percept dominance would be increased when cueing black. To test for
1171 this effect, Figure 3C, D plots the mean baseline-corrected pupil size over a fixed interval [
1172 0.5:1s] around the perceptual switch for each percept type and attention cueing condition
1173 (the same interval used for computing pupil size in the no-cue condition, shown by dotted
1174 lines). Red curves show pupil size during white percepts and black curves during black
1175 percepts; the two cueing conditions (white/black percept cued) are separated on the x-axis.
1176 The format is the same as that used to expose the effects of attention on the proportions of
1177 dominant percepts in Figure 3 A,B. According to our hypothesis, attention should have
1178 affected mean pupil size, displacing the continuous curves away from the dashed lines that
1179 report the no-cueing results. However, no such systematic displacement was observed. This
1180 was confirmed statistically (Table 1, rightmost column, both the main effect of cued percept
1181 and the interaction between dominant percept and cued percept are nonsignificant, with log
1182 Factors < -0.5). Figure 4 shows the full pupil time courses across cueing conditions, using the
1183 same format as in Figure 1, and supporting the same conclusions drawn from Figure 3 and
1184 Table 1. The curves are remarkably similar regardless of whether the white or the black
1185 percept was cued; as a result, the amplitude of the pupil modulation (computed as the
1186 difference between pupil size during black–white disk percepts) was not affected by attention
1187 cueing. These figures were computed after baseline correcting pupil traces, i.e., subtracting
1188 the average pupil diameter preceding each perceptual switch before averaging traces across
1189 switches. We verified that our pupil baseline values were not affected by attention cueing and
1190 we checked that skipping this baseline correction step or defining pupil baseline over a
1191 wider temporal interval (5:5 s, the whole interval over which we tracked pupil size for each
1192 perceptual switch) did not alter our conclusions (Table 7-1; Fig. 7-2 in the Appendix).



1193

1194

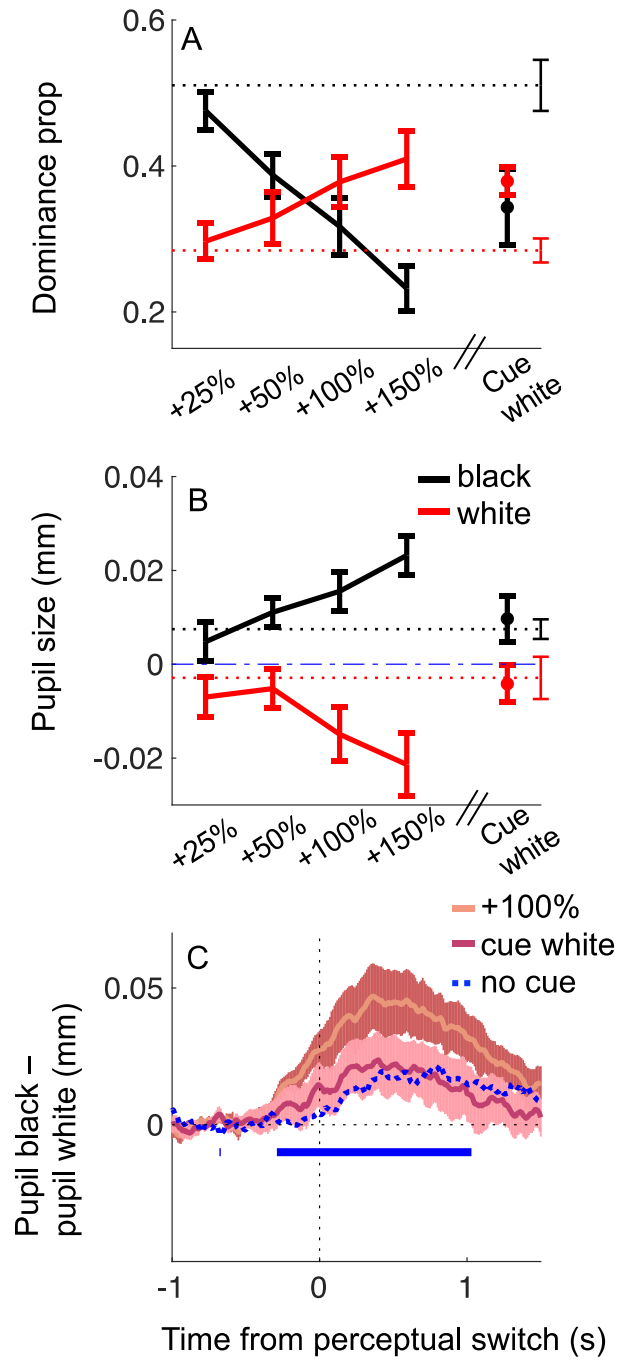
1195 *Figure 3-4 Pupil time courses are comparable across cueing conditions*

1196 *A–B: pupil size traces aligned to perceptual switches towards exclusive dominance of a white*
 1197 *disk or a black disk percept computed across phases in individual participants and then*
 1198 *averaged for each cueing condition, separately for binocular rivalry and interocular grouping*
 1199 *rivalry. C–D: time course of the difference between baseline-corrected pupil size during black*
 1200 *and white percepts, computed in individual participants and then averaged for each cueing*
 1201 *condition. The resulting traces show no effect of cueing. The same conclusions can be drawn*
 1202 *skipping the baseline correction step or defining pupil baseline over a wider temporal interval*
 1203 *around perceptual switch, as shown in Figure 7-2 in the Appendix. In all panels: shadings report*
 1204 *means ± 1 s.e. across participants.*

1205 We computed an attentional modulation index for pupil size (Eq. 4), logically similar to the
1206 attentional modulation index computed for perceptual dominance (Eq. 3). Attentional
1207 modulation indices for pupil size were distributed around zero for all participants (as shown
1208 on the ordinates of Fig. 3E, F). Even selecting the subsample of participants who showed a
1209 significant behavioural effect of attention cueing (Fig. 3E, F, red dots), the pupil attentional
1210 modulation remained non-significantly different from zero ($t(26) = 1.15$, $p = 0.25$, $\log\text{BF} = -$
1211 0.42 for binocular rivalry and $t(19) = 1.72$, $p = 0.10$, $\log\text{BF} = -0.09$ for interocular grouping
1212 rivalry). Thus, our results show disagreement between pupillometric and behavioural
1213 measures of perceptual dominance. Only perceptual alternations were affected by attention
1214 cueing, not the accompanying pupil modulations. Could this be because of the lack of
1215 sensitivity of pupillometry? We gathered several pieces of evidence against this possibility.
1216 First, not only we did not find any evidence of an effect of attention, but we also obtained
1217 evidence in support of the null hypothesis (no effect of attention) using the Bayes factor
1218 (Keyesers et al., 2020). Because the log-Bayes factor is defined as the log-likelihood ratio of the
1219 experimental and the null hypothesis, a value smaller than 0.5 indicates that the null
1220 hypothesis is three times more likely than the experimental hypothesis given the data
1221 (conversely, a log-Bayes factor larger than 0.5 implies that the experimental hypothesis is
1222 three times more likely than the null hypothesis given the data). As shown in Table 1, the effect
1223 of attention was associated with nonsignificant p-values mostly accompanied by log-Bayes
1224 factors smaller than 0.5, indicating substantial evidence (Kass & Raftery, 1995) against the
1225 hypothesis that attention cueing affects pupil size. Second, we verified that the reliability of
1226 pupil measurements was high (test-retest reliability on the pupil size difference: $r = 0.72$, $p <$
1227 0.001 , $\log\text{BF} = 4.78$ and $r = 0.81$, $p < 0.001$, $\log\text{BF} = 7.11$ for binocular rivalry and interocular
1228 grouping rivalry, respectively), comparable to the reliability of the behavioural measurements
1229 (test-retest reliability for dominance proportions: $r = 0.72$, $p < 0.001$, $\log\text{BF} = 4.84$ and $r = 0.79$,
1230 $p < 0.001$, $\log\text{BF} = 6.73$ for binocular rivalry and inter-ocular grouping rivalry, respectively).
1231 Third, we found that pupil measurements were sensitive enough to report the slight
1232 imbalance between eyes observed in our set of (nonamblyopic) participants. This was shown
1233 by splitting the same set of perceptual phases (binocular rivalry with attention cueing) in two
1234 ways: according to whether the reported percept was cued or uncued, and according to
1235 whether it matched the stimulus presented in the dominant or nondominant eye. This
1236 measure confirmed that pupil size was insensitive to attention cueing (pupil modulations were

1237 not different when the cued or un-cued stimulus was perceived, $t(37) = 1.23$, $p = 0.23$, $\log BF$
1238 $= -0.46$), but it did report eye-dominance (pupil modulations being larger in phases where
1239 percepts matched the stimulus in the dominant eye, $t(37) = 2.59$, $p = 0.01$, $\log BF = 0.51$).
1240 Fourth, we ruled out the possibility that the amplitude of pupil modulations was already
1241 saturated in the no cue condition, by measuring pupil modulations in a simulated rivalry
1242 condition. The latter was not intended as a replay-rivalry condition; it was run at the beginning
1243 of the experiment, training our participants to report perceptual alternations, and it did not
1244 reproduce the dynamics of exclusive dominance and mixed percepts observed during rivalry.
1245 However, it did allow us to estimate the pupil modulations elicited by physical alternations of
1246 the white and black disk, which measures the maximum modulation possible elicited by
1247 perceptual alternations during rivalry. We found that the latter were $\sim 40\%$ of the modulations
1248 during simulated rivalry (39.13 ± 8.15 for binocular rivalry and 43.80 ± 10.26 for interocular
1249 grouping rivalry, mean ± 1 SE across participants). This implies that there was ample space for
1250 the putative boosting effect of attention, ruling out ceiling as an explanation for the lack of
1251 such effect. Fifth, and finally, we showed with a control experiment that pupil size modulations
1252 reliably track changes in stimulus strength of a size compatible with those simulating the
1253 effects of attention cueing on perceptual dominance (Fig. 5). This was tested in a separate
1254 cohort of participants and with a different set-up, where we repeated the attentional
1255 manipulation (comparing trials where the white disk was cued vs no cue trials) and, in
1256 separate no cue trials, we manipulated the physical strength of the white disk increasing it by
1257 25%, 50%, 100%, or 150% (for technical reasons, we had to decrease the average luminance
1258 of the stimuli in the equal contrast conditions, which was about 10 times lower than in the
1259 main experiment).

1260



1261
1262

1263 *Figure 3-5 Effects of attention cueing vs. enhancing contrast*

1264 *A-B: perceptual dominance for exclusive white or black disk percepts, in the no cue condition*
 1265 *(dashed lines) or when the physical contrast of the white disk was enhanced /cued (continuous*
 1266 *lines, contrast or cueing condition indicated on the abscissa). Error bars report ± 1 s.e. across*

1267 participants. C: time course of the difference between baseline-corrected pupil size during
 1268 black and white percepts, computed in individual participants and then averaged for each
 1269 condition. The blue marks on the x-axis highlight timepoints where pairwise comparisons
 1270 between the +100% and the no cue condition traces are significant ($p < 0.05$ FDR corrected).
 1271 Shadings report mean ± 1 s.e. across participants.

1272

1273 A 2x5 repeated measures ANOVA showed that perceptual dominance was affected by the
 1274 contrast modulation (Fig. 5A), resulting in a significant interaction between dominant percept
 1275 (white/black) and contrast condition on the proportion of exclusive dominance phases (Table
 1276 2). Importantly, the same pattern was found for the pupil modulation (Fig. 5B). Increasing the
 1277 difference in the physical strength between the two stimuli (i.e., increasing the contrast of the
 1278 white disk), enhanced the pupil response, resulting in a significant interaction between the
 1279 pupil response to the dominant percept and contrast condition.

	Proportions	Pupil size
Dominant percept	$F_{(1,9)} = 4.47$ $p = 0.06$ $\log BF = 0.19$	$F_{(1,9)} = 18.40^*$ $p = 0.002$ $\log BF = 13.99$
Contrast increment	$F_{(4,9)} = 4.23^*$ $p = 0.007$ $\log BF = -0.44$	$F_{(4,9)} = 1.16$ $p = 0.34$ $\log BF = -1.30$
Dominant percept x contrast increment	$F_{(4,9)} = 39.75^*$ $p < 0.001$ $\log BF = 12.36$	$F_{(4,9)} = 14.11^*$ $p < 0.001$ $\log BF = 3.38$

1280

1281

1282 *Table 3-2 Contrast enhancement effects.*

1283 *Two-way ANOVA for contrast enhancement results, with factors: dominant percept*
 1284 *(white/black disk) and contrast increment (25, 50,100,150 %). Greenhouse – Geisser corrected*
 1285 *values.*

1286

1287 However, in line with the results of the main experiment, the effects of attention cueing on
 1288 perceptual dominance and pupil modulations were very different. While cueing the white disk
 1289 modulated perceptual dominance in favour of the white stimulus, it did not modulate the

1290 relative pupil response (Fig. 5A, B, rightmost point; Table 3), replicating our main experiment
 1291 results. These observations were further supported by directly comparing the cueing
 1292 condition with the contrast condition that better mimicked the effect of attention on
 1293 dominance proportions: the 100% contrast increase (Table 3), in line with the estimates
 1294 reported in Chong et al., 2005. Cueing the white disk and increasing its contrast by 100%,
 1295 despite producing comparable behavioural results, elicited very different pupil responses.
 1296 While the 100% contrast increase elicited significantly stronger pupil modulations than in the
 1297 equal contrast (no cue) condition, pupil modulations when the white disk was cued were
 1298 indistinguishable from those in the no cue condition (Figure 5C).

	MI Proportions	MI Pupil size
Cueing vs. no cue	$t_{(9)} = 5.66^*$ $p < 0.001$ $\log BF = 2.04$	$t_{(9)} = 0.66$ $p = 0.52$ $\log BF = -0.43$

	Proportions	Pupil size
25% contrast increment vs. cueing	$t_{(9)} = 5.46^*$ $p < 0.001$ $\log BF = 1.95$	$t_{(9)} = 0.41$ $p = 0.69$ $\log BF = -0.48$
50% contrast increment vs. cueing	$t_{(9)} = 2.43^*$ $p = 0.04$ $\log BF = 0.33$	$t_{(9)} = 0.52$ $p = 0.61$ $\log BF = -0.45$
100% contrast increment vs. cueing	$t_{(9)} = 0.77$ $p = 0.46$ $\log BF = -0.40$	$t_{(9)} = 3.29^*$ $p = 0.01$ $\log BF = 0.81$
150% contrast increment vs. cueing	$t_{(9)} = 3.83^*$ $p = 0.004$ $\log BF = 1.11$	$t_{(9)} = 4.73^*$ $p = 0.001$ $\log BF = 1.58$

1299

1300 *Table 3-3 The effects of cueing on proportions and pupil size in the control experiment.*

1301 *Modulation indices from the control experiment: comparison of attention cueing vs. no cue*
 1302 *(first row) and attention cueing vs. contrast enhancement by 25, 50, 100 and 150%.*

1303

1304 As a confirmatory analysis, we also checked the cross-correlation between the rate of pupil
 1305 size change and perceptual reports (see Materials and Methods). The peak cross-correlation

1306 was significantly larger than zero in no-cue conditions ($t(37) = 5.41$, $p < .001$, $\log BF = 3.70$),
1307 further confirming that pupil modulations reliably tracked perceptual alternations; and it was
1308 higher when the white stimulus contrast was doubled (control experiment +100% contrast,
1309 $t(9) = 2.32$, $p = .04$, $\log BF = .28$), indicating that it is indicative of stimulus strength. However,
1310 the peak cross-correlation was indistinguishable across cueing conditions (white cued vs. no
1311 cue: $t(37) = 1.23$, $p = .22$, $\log BF = -.45$; $t(9) = 0.83$, $p = .42$, $\log BF = -.39$, in the main and the
1312 control experiment respectively), confirming that cueing did not alter the reliability of pupil
1313 modulations.

1314

1315 3.3.1 Analysis of mixed percepts

1316

1317 All the analyses presented to this point are focused on exclusive dominance phases. In this
1318 section we consider perceptual and pupillary reports for the third perceptual state that
1319 participants had the option to report: mixed percepts, defined as anything but the exclusive
1320 dominance of a white or black disk percept.

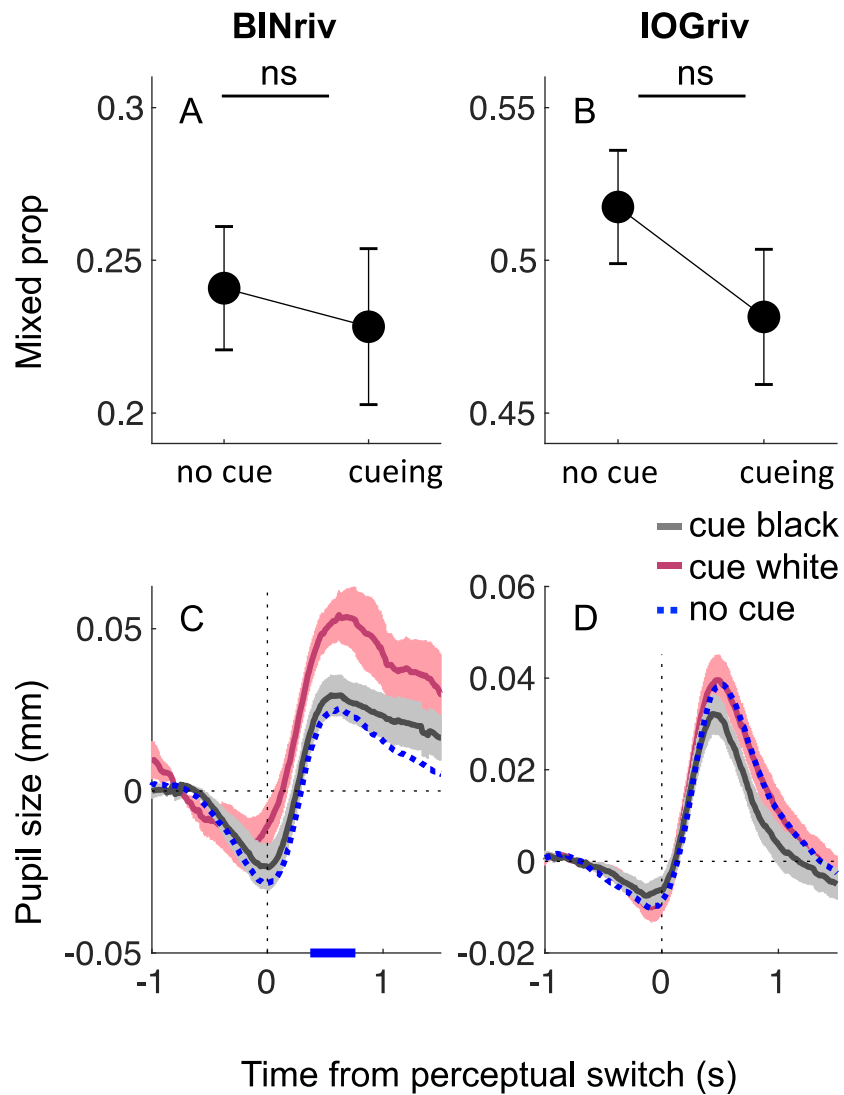
1321 Previous work (Brascamp et al., 2006; K. C. Dieter et al., 2017a) highlighted the importance of
1322 quantifying the fraction of return transitions, where mixed percepts are interposed between
1323 two periods of dominance of the same percept (e.g., black disk percept, followed by mixed
1324 percept, followed by another black disk percept). In no-cueing conditions, these return
1325 transitions represented a small fraction of all transitions (about 15%) for binocular rivalry and
1326 a greater fraction for interocular grouping rivalry (about 40%). Attention cueing dramatically
1327 affected the distribution of these transitions, as the proportion of black-mixed-black
1328 transitions increased when cueing black and white-mixed-white transitions increased when
1329 cueing white. This resulted in a significant interaction between factors “dominance percept
1330 after a return transition” and “cued percept” in a 2x2 ANOVA for both binocular rivalry ($F(1,37)$
1331 $= 20.19$, $p < .001$, $\log BF = 1.75$) and interocular grouping rivalry ($F(1,37) = 12.91$, $p < .001$,
1332 $\log BF = 2.94$). This indicates that attention cueing also affected the frequency of dominance
1333 phases, besides modulating the duration of individual dominance phases.

1334 Figure 6 quantifies the overall percentage of mixed percepts in binocular and interocular
1335 grouping rivalry. Attention cueing did not affect the proportion of mixed percepts in binocular
1336 rivalry, which averaged $.24 \pm .02$ and $.23 \pm .02$ for no cueing and cueing conditions ($t(37) = .80$,
1337 $p = .43$, $\log BF = -.63$). In interocular grouping rivalry, the difference was also non-significant

1338 but there was a trend towards reduced mixed reports in the cueing condition ($.52 \pm .02$ and
1339 $.48 \pm .02$ for no cueing and cueing respectively, $t(37) = 1.71$, $p = .10$, $\log BF = -.18$). Based on this
1340 observation, we cannot exclude the possibility that attention cueing may have promoted
1341 interocular grouping.

1342 Figure 6 C-D shows pupil traces aligned to the onset of mixed percepts, separately for no
1343 cueing and the two attention cueing conditions; note that this is conceptually equivalent to
1344 analysing data for exclusive dominance phases aligned to their offset, rather than the onset
1345 (same conventions as in Figure 4 C-D). A difference between cueing conditions is apparent for
1346 binocular rivalry, suggesting enhanced pupil dilation when the white percept was cued. No
1347 such effect is observed for interocular grouping rivalry. This difference between the two rivalry
1348 types may suggest that the cueing effect is specifically related to fusion percepts (grey disk
1349 percepts), which likely represented a minor percentage of mixed reports in interocular
1350 grouping rivalry (the largest majority being monocular half white, half black disk percepts).
1351 The relative pupil dilation may indicate that fusion events were perceived as grey disks of a
1352 darker shade during white cueing than during black cueing or no cueing. There are at least
1353 two reasons why this could happen. One possibility is that white cueing indeed enhanced the
1354 effective strength of the white stimulus, implying that the black stimulus strength had to reach
1355 a higher threshold before a white-dominance report switched to a mixed report. If this is the
1356 case, however, it is unclear why such difference in effective strength should not show in pupil
1357 traces during phases of exclusive white dominance (Figures 3 and 4). Another possibility is
1358 that cueing may have affected decision criteria so that fusion percepts reported as mixed were
1359 generally darker under white cueing (effectively prolonging exclusive white-dominance
1360 phases) than under black cueing conditions.

1361



1362

1363 *Figure 3-6 Effects of attention cueing on mixed percepts.*

1364 *A: proportion of mixed percepts in no cueing or cueing conditions (collapsed across white and*
 1365 *black cued). Error bars report ± 1 s.e. across participants*

1366 *B: pupil traces during mixed percepts in the three cueing conditions. Shaded areas show ± 1*
 1367 *s.e. across participants and blue marks on the x-axis highlight timepoints where pairwise*
 1368 *comparisons between the white and black cueing conditions are significant ($p < 0.05$ FDR*
 1369 *corrected).*

1370

1371 3.4 Discussion

1372 We used pupillometry to investigate the effects of endogenous attention on binocular rivalry
1373 and interocular grouping rivalry. We confirmed that pupil size tracks perceptual oscillations
1374 during binocular rivalry, despite constant luminance stimulation, and we extended this
1375 observation to interocular grouping rivalry. This is consistent with the large body of work
1376 suggesting that the subcortical circuit generating the pupillary light response can be
1377 modulated by perceptual signals (Binda & Gamlin, 2017; Binda & Murray, 2015a; Mathôt,
1378 2018). Our finding that similar pupillary modulations accompany interocular grouping rivalry
1379 constrains the origin of the modulatory signals to visual cortical areas (they must hold a
1380 representation of stimulus brightness) with access to binocular information (they must be able
1381 to combine information from the two eyes). We found that manipulating endogenous
1382 attention reliably affected perceptual alternations, enhancing dominance of the cued percept
1383 during binocular rivalry, in line with previous work (Chong et al., 2005; Hancock & Andrews,
1384 2007; Meng & Tong, 2004; Mitchell et al., 2004; Paffen & Alais, 2011). To our knowledge, this
1385 is the first study manipulating attention in interocular grouping rivalry. We found that
1386 attention cueing had the same or slightly smaller effects on interocular grouping rivalry as on
1387 binocular rivalry. This suggests that eye-based and pattern-based competition are similarly
1388 permeable to endogenous attention; it also suggests that different degrees of attentional
1389 control (as observed, for example, comparing Necker cube vs binocular rivalry; (Meng & Tong,
1390 2004b)) may be related to differences in stimulus complexity rather than to the involvement
1391 of different levels (monocular vs binocular) of cortical processing. Many have suggested that
1392 attention cueing acts by enhancing the perceptual strength of the cued signals (Carrasco,
1393 2011). This is in line with evidence that focusing attention at a spatial location or feature
1394 enhances its representation in early visual cortex, as measured with EEG (F. Di Russo, 2003;
1395 Hillyard & Anllo-Vento, 1998; S. P. Kelly et al., 2008; Khoe et al., 2008; Mishra & Hillyard, 2009;
1396 J. Wang et al., 2007), fMRI (Boynton, 2009; T. Liu et al., 2005; Pestilli et al., 2011; Saenz et al.,
1397 2002), or indexed by enhanced pupillary response to light stimuli at the attended location
1398 (Binda & Murray, 2015). Transferring this knowledge to the context of rivalry, we expected
1399 that cueing attention to one of the rivalling percepts would enhance its effective strength and
1400 thereby increase its dominance. Using pupillometry, we intended to indirectly index this
1401 phenomenon. We established that the magnitude of pupil-size modulations accompanying

1402 rivalry is sensitive to effective stimulus strength as set by ocular dominance (control analysis
1403 of binocular rivalry data from the main experiment) or physical contrast changes (control
1404 experiment). On this basis, we predicted that attention cueing would have a similar effect as
1405 physical contrast enhancement, namely an amplification of pupil modulations. However, we
1406 obtained evidence against this prediction, as pupil responses during periods of exclusive
1407 dominance were reliably unaffected by attention cueing.

1408 The simplest way to explain this negative finding is putting it down to insufficient sensitivity
1409 of the pupillometric measurements. However, our reliability analysis, Bayesian statistics and
1410 results from a control analysis and a control experiment all coherently speak against this
1411 possibility. We therefore speculate on a few logical alternatives.

1412 During binocular rivalry, most of the time is spent in exclusive dominance, where competition
1413 between rivalling stimuli is resolved, leaving only one visible stimulus and no distracter. In
1414 these conditions, attention may be automatically driven to the dominant stimulus (Li et al.,
1415 2017), leaving little space for endogenous re-directing of attention. Although this is consistent
1416 with attention affecting early visual processing in markedly different ways at the onset of
1417 rivalry vs. for non-rivaling stimuli (Khoe et al., 2008; Mishra & Hillyard, 2009), the model by Li
1418 et al., 2017 does not explicitly account for the small but reliable effects of attention cueing on
1419 perceptual alternations during rivalry. To account for these, one possibility is assuming that
1420 attention cueing primarily affects rivalry when the competition between stimuli is unresolved,
1421 namely in the brief times marking transitions between exclusive dominance phases, when the
1422 depth of suppression decreases (Alais et al., 2010). This idea has been suggested previously
1423 and supported by the observation that exogenous cues are mostly effective when presented
1424 near the end of individual dominance periods (K. C. Dieter et al., 2015). In this scenario, we
1425 could reconcile our behavioural and pupillometry results by assuming that attention enhances
1426 the strength of cued percepts only in short intervals near perceptual switches, not during the
1427 entire dominance phases. This could be consistent with our observation that the only effects
1428 of cueing over pupil traces were observed in a brief interval during mixed percepts.

1429 An alternative possibility is that attention cueing affects rivalry dynamics by acting on a
1430 stimulus representation that is not represented in pupil dynamics. Available evidence is
1431 consistent with pupil size integrating a cortical representation of stimulus brightness (e.g., one
1432 that oscillates, tracking rivalry dynamics), but we lack direct knowledge on the level at which
1433 such visual representation is generated and fed into the pupil control circuit (Binda & Gamlin,

1434 2017). On the other hand, evidence indicates that rivalrous perception is orchestrated by the
1435 interplay of fronto-parietal and occipital regions, which participate in different degrees
1436 depending on the details of the stimulus and task (Logothetis et al., 1996; Sterzer et al., 2009;
1437 Sterzer & Kleinschmidt, 2007). It is possible, then, that attention affects competition after the
1438 stage where visual representations are fed to pupil control – whether this needs to be a
1439 decisional stage or still a sensory representation cannot be determined based on the available
1440 research.

1441 This is not the first case where we find that the pupillary responses are independent of
1442 physical luminance and yet inconsistent with perceptual judgments (Pomè, Binda, et al., 2020;
1443 Tortelli et al., 2021a, 2021b; Turi et al., 2018). These inconsistencies were generally explained
1444 by calling decisional factors into the picture, as these may bias or add variability to perceptual
1445 reports while leaving pupil size unaffected (Tortelli et al., 2021b). That contextual factors other
1446 than physical luminance affect pupil size and perception similarly but independently – if it
1447 proves recurrent and reliable across paradigms – might call for an updated model of pupil
1448 control. It might suggest that separate processing pathways support perception and pupil
1449 control, in analogy (or perhaps in overlap) with the separate pathways supporting vision for
1450 perception and vision for action (Goodale & Milner, 1992).

1451 In conclusion, we find that pupil size oscillates in phase with perceptual oscillations during
1452 binocular and interocular grouping rivalry, implying cortical control. Despite this, and despite
1453 the reliable effects of attention cueing on behavioural reports, pupil size during periods of
1454 exclusive dominance does not show any modulation with attention. This introduces new
1455 constraints for models of attention in rivalry and pupil control: either attention cueing affects
1456 perception without enhancing the dominant percept, or we hold multiple representations of
1457 the dominant percept that independently regulate behavioural reports and pupil size and are
1458 differentially affected by attention cueing.

1459

1460

1461

1462

1463 4 Chapter 4 – Pupil size as an index of ocular dominance plasticity

1464

1465 4.1 Introduction

1466

1467 When incompatible images are simultaneously presented to the eyes, perception alternates
1468 between the two, even though the visual input remains constant. This phenomenon is known
1469 as 'binocular rivalry' and has a long tradition as an experimental model for investigating the
1470 neural mechanisms of conscious perception (LEVELT, 1966; Bartels & Logothetis, 2010; Blake
1471 & Logothetis, 2002).

1472 Perceptual dominance in binocular rivalry is a reliable index of ocular dominance
1473 (Acquafredda et al., 2023). At any given moment, the reported perceptual dominance during
1474 binocular rivalry mirrors the fluctuating contribution of each eye to conscious visual
1475 perception. While ocular dominance is typically established during the critical period (Hensch
1476 and Quinlan, 2018; Hubel & Wiesel, 1965), recent studies have shown that a form of
1477 homeostatic plasticity of ocular dominance is retained throughout adulthood (see Castaldi et
1478 al., 2020). The first study to describe this phenomenon was published by Lunghi and
1479 colleagues in 2011 and showed that patching one eye for two hours transiently restores ocular
1480 dominance plasticity in the adult brain (Lunghi et al., 2011); following deprivation, the
1481 deprived eye dominates rivalrous perception for twice as long as the nondeprived eye,
1482 indicating a strong shift of ocular dominance in favour of the deprived eye. The boost of the
1483 deprived eye was associated with an enhancement of the perceived contrast, as assessed
1484 through a contrast discrimination task (Lunghi et al., 2011). This counterintuitive effect has
1485 been related to a compensatory homeostatic response of the visual system to the temporary
1486 reduction in monocular visual input, mediated by mechanisms of contrast gain control (Binda
1487 et al., 2017; Binda & Lunghi, 2017; Lunghi, Berchicci, et al., 2015; Lunghi, Emir, et al., 2015;
1488 Lunghi et al., 2011, 2013, 2019; Lunghi & Sale, 2015; Steinwurz et al., 2020; Zhou et al., 2013,
1489 2014) This hypothesis is supported by electrophysiological and imaging techniques that
1490 showed how, following short-term monocular deprivation, visual evoked responses were
1491 enhanced in the deprived eye and reduced in the non-deprived eye (Lunghi, Berchicci, et al.,
1492 2015b)

1493 However, it is interesting to note that these physiological indices of the boost of the deprived
1494 eye are not directly related to the behavioural effect, because they were acquired in

1495 conditions that are very different from those used in behavioural testing. Visual evoked
1496 responses (EEG or fMRI) were recorded by presenting stimuli passively, in absence of any
1497 perceptual report; in addition, stimuli for EEG and fMRI measurements were delivered
1498 monocularly, i.e., separately to each eye (Binda et al., 2018; Lunghi, Berchicci, et al., 2015b).
1499 All this contrasts with the conditions of the behavioural experiments, where participants were
1500 continuously engaged in reporting their perception, which tracked the competitive
1501 interactions between the stimuli presented to the two eyes. In the present work, we aimed at
1502 tracking the effective strength of monocular signals during the behavioural assessment of the
1503 effect (based on binocular rivalry), using an objective physiological index: pupil size.

1504

1505 The perceptual alternations that occur during binocular rivalry can be accompanied by
1506 changes in pupil size, which are triggered by oscillations in the perceived brightness of the
1507 competing stimuli (Acquafredda et al., 2022; Einhäuser et al., 2008; Fahle et al., 2011; LOWE
1508 & OGLE, 1966; Naber et al., 2011) et al., 2022). Because the dominant percept influences the
1509 direction of pupil size changes, the oscillations in pupil size during binocular rivalry provide a
1510 continuous and objective physiological measure of the effective stimulus strength of the two
1511 eyes. Increased effective strength should lead to more significant fluctuations in pupil size (as
1512 directly tested through contrast manipulations in Acquafredda et al., 2022). It follows that, if
1513 monocular deprivation modulated the effective strength of the monocular stimuli, enhancing
1514 the deprived eye and suppressing the fellow eye, this should impact the size of pupil
1515 oscillations. This should make for a combined experimental paradigm, integrating perceptual
1516 reports during binocular rivalry with pupillometry, to provide simultaneous behavioural and
1517 physiological measures of ocular dominance plasticity. Given the potential implications of
1518 short-term monocular deprivation for the treatment of amblyopia in adults ((Lunghi et al.,
1519 2019); for reviews, see: (Baroncelli & Lunghi, 2021; Castaldi et al., 2020) evaluating the
1520 effectiveness of this combined experimental approach holds significant methodological and
1521 translational relevance.

1522

1523 4.2 Methods

1524

1525 4.2.1 Subjects

1526

1527 We recruited 10 participants (6 females, mean age 26.9 ± 0.77 years). These had normal or
1528 corrected-to-normal vision and normal color vision, no known history of amblyopia, eye
1529 surgery, or other active eye diseases (such as keratoconus) and balanced ocular dominance
1530 (we included all participants with a ratio of mean phase durations of the dominant over the
1531 nondominant eye smaller than 0.2 log units). Sample size was based on our previous study
1532 (Acquafredda et al., 2022), where we showed with the same set-up and the same stimuli, a
1533 detectable effect of contrast on pupil size across 10 participants.

1534

1535 4.2.2 Apparatus, stimuli and procedures

1536

1537 Experiments took place in a dark and quiet room. Visual stimuli were developed in Matlab
1538 (MATLAB r2010a, The MathWorks Inc., Natick, MA) using PsychoPhysics Toolbox routines
1539 (Brainard, 1997) housed in a Mac Pro 4.1, and displayed on a 52.5 cm-wide LCD screen, driven
1540 at a resolution of 1920 x 1080 pixels. The display was seen through a four-mirror stereoscope
1541 which enabled dichoptic viewing of two display areas of 12 x 8 deg each; a chin rest was used
1542 to stabilize head position at 57 cm from the display. In each display area, a central red fixation
1543 point (0.15 deg in diameter) surrounded by a square frame (3.5 x 3.5 deg) was shown against
1544 a uniform grey background (luminance: 12.3 cd/m²). The mirrors were carefully adjusted at
1545 the beginning of each session to ensure accurate alignment of the dichoptically presented
1546 squares. Participants were asked to keep their gaze on the fixation point shown at screen
1547 center and to refrain from blinking while the stimuli were on. Dichoptic presentations
1548 consisted of two disks, 3° in diameter, one white (maximum screen luminance 28.9 cd/m²,
1549 Michaelson contrast: 0.31) and one black (minimum screen luminance 1.7 cd/m², Michaelson
1550 contrast: 0.8). Perception alternated between exclusive dominance of the white and the black
1551 disk, or mixed percepts (either piecemeal or fusion). To discourage fusion, the disks were
1552 overlaid with thin orthogonal grey lines (45° clockwise or counterclockwise, 1 pixel wide,
1553 corresponding to 0.033 deg, and 0.5 deg apart, with the same luminance as the background).
1554 Participants were tested in two sessions, performed on two separate days. In each
1555 experimental session, binocular rivalry was measured in one block (comprising four 3-
1556 minute-long trials) before monocular patching and one immediately after (Figure 1-A). On
1557 each trial, a different combination of disk colour and line orientation was presented to each
1558 eye; combinations were varied pseudo-randomly across trials. The first trial was discarded

1559 from both sessions, because of the poor signal-to-noise ratio of the pupil responses in the
 1560 post-deprivation session, so we included in the analysis three trials per block per participant
 1561 (repeated in two sessions, so six trials in total). During the trial, participants continuously
 1562 reported perception by keeping one of three keys pressed: right or left arrows to report
 1563 dominance of the stimulus with clockwise or counterclockwise tilted lines, or the down-arrow
 1564 key any time dominance of either stimulus was incomplete (we considered piecemeal and
 1565 fusion events as “mixed”). Dominance phase distributions were adequately captured by a
 1566 typical gamma distribution (LEVELT, 1966b), with shape α and scale β parameters: $\alpha = 2.98$; β
 1567 $= 0.26$ (Equation 1; Figure 1-C). The goodness-of-fit (coefficient of determination R^2) was 0.95.

1568

$$1569 \quad f(x|\alpha, \beta) = \frac{1}{\beta^\alpha \Gamma(\alpha)} x^{\alpha-1} e^{-\frac{x}{\beta}} \quad \text{for } x, \alpha, \beta > 0$$

1570

1571 *Equation 4-1*

1572 Where Γ is the gamma function and x the number of dominance phases.

1573

1574 4.2.3 Monocular deprivation

1575

1576 Monocular deprivation was achieved by patching the dominant eye, defined as the eye with
 1577 longer mean phase duration in binocular rivalry, for 2 hours.

1578 As in previous studies (Binda et al., 2017; Binda & Lunghi, 2017; Lunghi et al., 2011, 2013;
 1579 Steinwurz et al., 2020) we used a translucent plastic material that allowed light to reach the
 1580 retina (attenuation 15%), but no pattern information, as assessed by the Fourier transform of
 1581 a natural world image seen through the eye patch. During the 2 hours of monocular
 1582 deprivation, participants were free to read, work at the computer, or walk around the
 1583 laboratory (but not to eat or sleep).

1584 To quantify the plasticity effect elicited by monocular deprivation, we defined a deprivation
 1585 index (DI) as the ratio between the deprived and non-deprived eye mean phase durations,
 1586 before(pre) and after(post) deprivation:

1587

$$1588 \quad DI = \frac{\frac{DepPost}{NDepPost}}{\frac{DepPre}{NDepPre}}$$

1589

1590 *Equation 4-2*

1591 Note that Equation 2 can be rewritten using log-transformed mean phase durations,
1592 becoming a linear combination.

1593

$$1594 \quad \lg DI = (\lg_{DepPost} - \lg_{NDepPost}) - (\lg_{DepPre} - \lg_{NDepPre})$$

1595

1596 *Equation 4-3*

1597 A deprivation index > 1 (or logDI > 0) implies a shift of ocular dominance in favour of the
1598 deprived eye (the expected effect).

1599

1600 4.2.4 Eye tracking data acquisition and analysis

1601

1602 During rivalry, we monitored pupil diameter and two-dimensional eye position with an
1603 infrared camera (EyeLink 1000 system, SR Research, Canada) mounted below the monitor
1604 screen and behind the stereoscope. EyeLink data were streamed to the main computer
1605 through the EyeLink toolbox for Matlab (Cornelissen et al., 2002) and thereby synchronized
1606 with participant's keypresses. Pupil diameter measurements were transformed from pixels to
1607 millimeters using an artificial 4 mm pupil positioned at the approximate location of the
1608 subject's eye.

1609 Data were analysed as in Acquafredda et al., 2022. Pupil and gaze tracking data consisted of
1610 180 x 1000 (180 seconds at 1000 Hz) time points. These included signal losses, eyeblinks and
1611 other artifacts, which we cleaned out by means of the following steps (all implemented with
1612 in-house Matlab software):

1613 - Identification and removal of gross artifacts: removal of time-points with unrealistically small
1614 pupil size (<0.2 mm, corresponding to blinks or other signal losses).

1615 - Identification and removal of finer artifacts: identification of samples where pupil size varied
1616 at unrealistically high speeds (larger than 10 mm per second) and removal of the possible
1617 resulting isolated data points.

1618 - Removal of any linear trend by fitting a linear function to pupil data from each 180 s-long
1619 trial.

1620 After this cleaning procedure was applied, we verified fixation stability by measuring the
1621 dispersion of eye position samples around the mean of each trial as the bivariate confidence
1622 ellipse area (BCEA), defined as:

1623

$$1624 \quad BCEA = 2 * k * \sigma_H * \sigma_V * (1 - \rho)^{0.5}$$

1625

1626 *Equation 4-4*

1627

1628 Where k is the confidence limit for the ellipse, σ_H and σ_V are the standard deviation of eye
1629 positions in the horizontal and vertical meridian respectively, ρ is the product-moment
1630 correlation of these two position components and $k=1.14$, implying that the ellipse included
1631 68% ($1-e^{-k}$) of the distribution.

1632

1633 Cleaned pupil data and continuous recordings of perceptual reports were down-sampled to
1634 100 Hz, by taking the median of the retained time-points in non-overlapping time windows. If
1635 no retained sample was present in a window, that window was set to “NaN” (MATLAB code
1636 for “not a number”). Down-sampled pupil traces were finally parsed into epochs locked to
1637 each perceptual switch (when the subject changed perceptual report) and labelled according
1638 to the color of the dominant stimulus after the switch. Pupil time courses were averaged
1639 across epochs for each participant; further averaging across participants yields traces in Figure
1640 1-B. In order to minimize the impact of pupil size changes unrelated to the perceptual
1641 switches, we also analyzed data after subtracting a baseline from each epoch, measured in
1642 the [-1 -0.5] s interval preceeding the switch – again, adopting the same conventions as in
1643 Acquafredda et al. (2022). To compare pupil size across dominance phases and conditions (pre
1644 vs. post deprivation), we extracted an index of pupil size in each epoch by averaging its value
1645 in the [-0.5 1] s interval around the switch. Note that shifting the intervals for pupil baseline,
1646 or skipping the baseline correction step, affected the size of pupil modulations but it did not
1647 change our conclusion on the effects of monocular deprivation.

1648

1649 4.2.5 Statistical approach

1650

1651 Significance was evaluated using both p-values and log-transformed JZS Bayes Factors
1652 computed with the default scale factor of 0.707 (Wagenmakers et al., 2012). The Bayes Factor
1653 is the ratio of the likelihood of the two models H_1/H_0 , where H_1 is the experimental
1654 hypothesis (effect present) and H_0 is the null hypothesis (effect absent). By convention, a base
1655 10 logarithm of the Bayes Factor ($\log BF$) > 0.5 is considered substantial evidence in favor of

1656 H1, and $\log BF < -0.5$ substantial evidence in favor of H0. Bayesian ANOVAs were run in JASP,
1657 and the corresponding Bayes Factors represent the change from prior to posterior inclusion
1658 odds ($BF_{inclusion}$) computed across matched models.

1659

1660 4.3 Results

1661

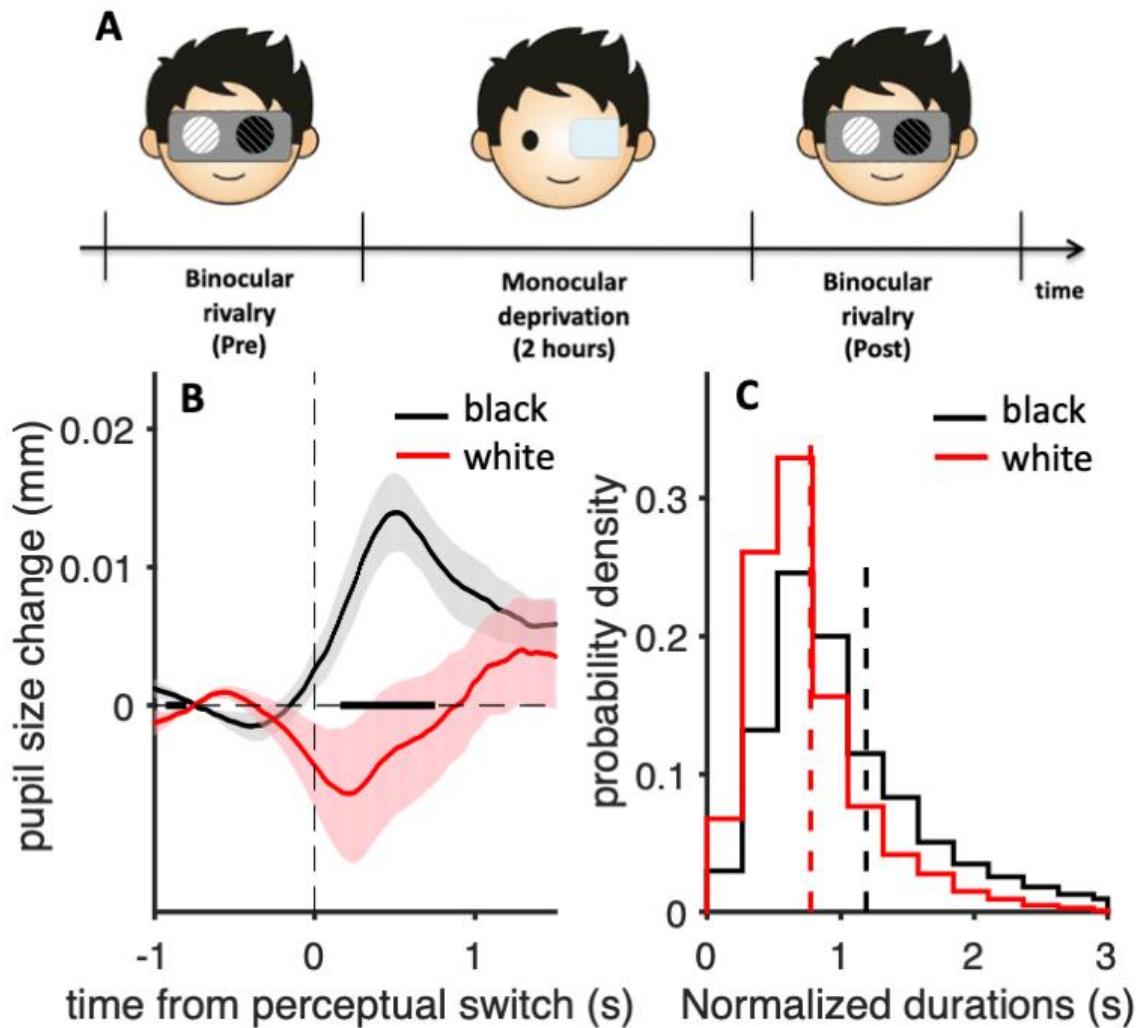
1662 In 10 adult observers, we measured perceptual alternations and pupil oscillations during
1663 binocular rivalry before and after monocular deprivation. Our primary aim was to establish
1664 whether the increase in perceptual dominance of the stimulus shown to the dominant eye
1665 induced by monocular deprivation, would yield a measurable effect on its pupil response.

1666

1667 The analysis of behavioural reports before monocular deprivation showed a clear
1668 predominance of black percept over to the white one, consistent with its higher Michelson
1669 contrast (in turn implied by the identical Weber contrast of the white and black disks). The
1670 average phase durations across subjects were 2.00 ± 0.33 seconds (mean \pm standard error of
1671 the mean) for the black percept and 1.26 ± 0.16 seconds for the white one. Dominance
1672 proportion, computed as the time during which one percept dominated over the total trial
1673 time, was 0.47 ± 0.03 for the black percept and 0.25 ± 0.03 for the white one.

1674

1675 These perceptual alternations were reliably tracked by pupil size. Despite constant
1676 stimulation, participants' pupils were relatively dilated when they reported seeing black,
1677 compared to when they reported seeing white (Figure 1-B).



1678

1679

1680 *Figure 4-1 Experimental procedure and indices of perceptual alternations before monocular*
 1681 *deprivation.*

1682 *A: Time course of the experiment, where binocular rivalry dynamics were measured before*

1683 *and after deprivation. Short-term monocular deprivation was achieved by applying a*

1684 *translucent patch over the dominant eye for 2 hours. B: Baseline subtracted pupil size traces*

1685 *aligned to perceptual switches toward exclusive dominance of a white disk or a black disk*

1686 *percept and averaged across phases. Shadings report mean \pm SE across participants and the*

1687 *black mark on the x-axis highlights time points where the pupil difference is significantly*

1688 *different from zero (one-tailed paired t-test, $p < 0.05$ FDR corrected). C: Probability density*

1689 *function of the normalised phase durations for each stimulus (black and white), measured*

1690 *before deprivation and pooled across conditions and participants. The function conforms to*

1691 *the typical gamma distribution.*

1692

1693 Having established the perceptual and pupil size oscillations before monocular deprivation
1694 (“pre” condition), we proceeded to assess the impact of monocular deprivation upon the two
1695 measures (“post” vs. “pre” conditions).

1696

1697 Following patch removal, we tested four blocks of binocular rivalry (3 minutes each). Across
1698 blocks, we alternated the eye to which the black and white disks and the associated oriented
1699 lines were delivered – as customarily done to minimize the impact of adaptation and
1700 astigmatism. Each participant took part in two monocular deprivation sessions with swapped
1701 color-eye assignments. Results were analysed after pooling data from blocks where the white
1702 disk was delivered to the deprived eye and blocks where the black disk was delivered to the
1703 deprived eye. The effect of deprivation was tested using a one-way ANOVA with factor time
1704 at three levels: “pre” deprivation, “post: white” and “post: black” meaning post-deprivation
1705 blocks with the white or black disk delivered to the deprived eye.

1706 Behavioral results were consistent with previous studies, in that monocular deprivation
1707 shifted ocular dominance in favour of the deprived eye, irrespectively of the color-eye
1708 assignment. The ANOVA revealed a significant effect of patching on perceptual dominance
1709 (Figure 2A; $F= 15.77$, $p < .001$), and post-hoc tests showed that it is due to an increase of the
1710 black-white perceptual dominance when the black stimulus was shown to the deprived eye
1711 ($|t(9)| = 2.81$, $p_{holm} = 0.02$) and a decrease when the white stimulus was given to the
1712 deprived eye ($|t(9)| = 2.80$, $p_{holm} = 0.02$; t-test between the two levels: $|t(9)| = 5.61$, $p <$
1713 $.001$).

1714

1715 Based on the assumption that monocular deprivation boosts perceptual dominance by
1716 enhancing the effective strength of the percept shown to the deprived eye, we anticipated
1717 that the pupil oscillations accompanying perceptual alternations would be amplified. We
1718 predicted that constrictions concurrent with white percept dominance would be increased
1719 when the white stimulus was delivered to the deprived eye, and that dilations elicited by the
1720 black percept would be increased when the black stimulus was delivered to the deprived eye.
1721 This would result in larger differences in pupil size during black vs. white percepts after
1722 deprivation, as compared to before deprivation. We tested for this effect by looking at the

1723 average pupil-size difference in the usual [-.5 1] s interval relative to perceptual switches and
1724 analysing it with the same ANOVA used for perceptual reports.

1725 This revealed a significant effect of patching on the pupil modulation ($F = 4.99$, $p = 0.02$). In
1726 addition, post-hoc tests showed that this effect was selective due to an increase in pupil
1727 modulations when the white stimulus was shown to the deprived eye ($|t(9)| = 2.94$, $p_{holm} =$
1728 0.03), while the “post – blackdep” condition was not significantly different from the “pre”
1729 condition ($|t(9)| = 0.45$, $p_{holm} = 0.65$; t-test between the two “post” conditions: $|t(9)| =$
1730 2.48 , $p = 0.05$).

1731 We verified that the deprivation effects could not be explained by differences in eye-
1732 movements patterns by averaging the BCEA values across trials and comparing them
1733 across conditions ($F = 1.24$, $p = 0.31$).

1734

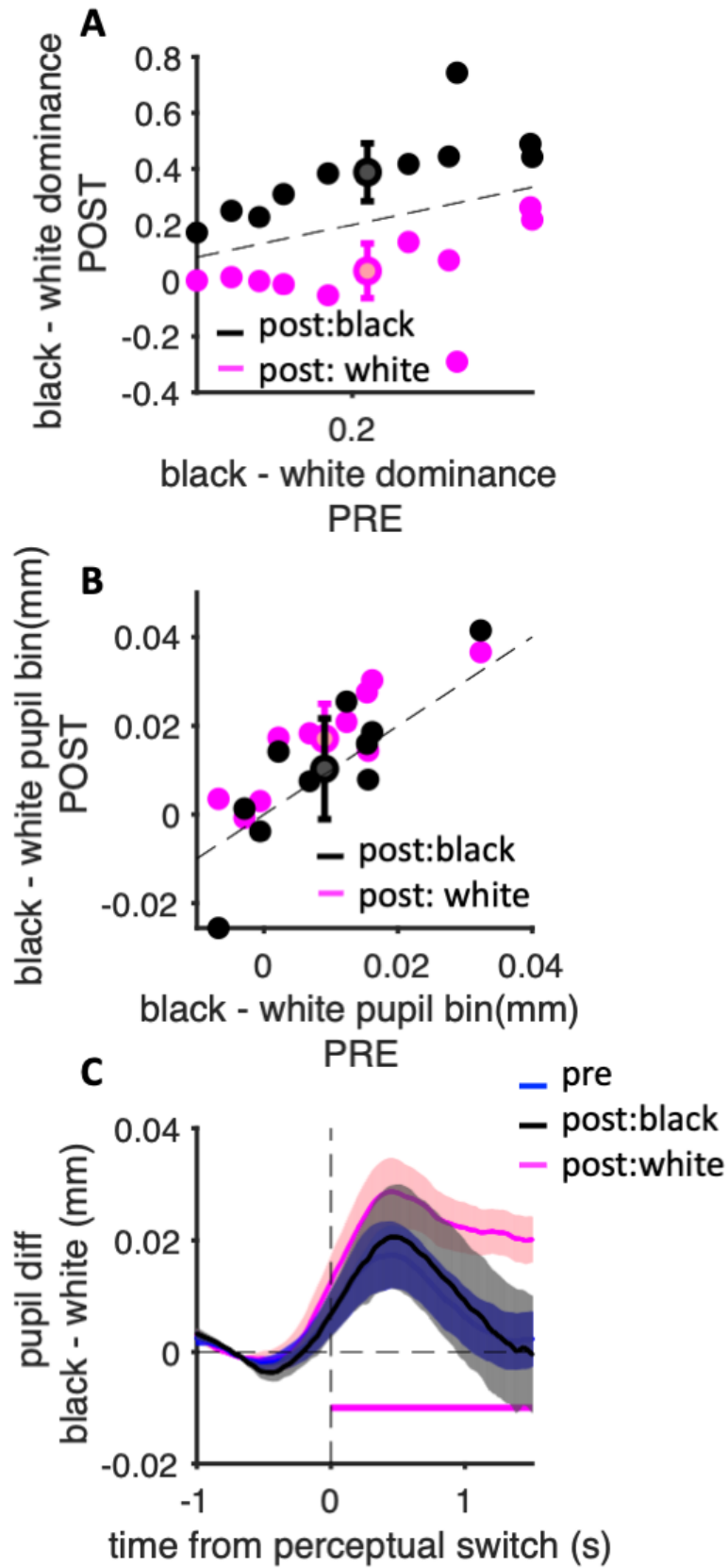
1735 We also analyzed mixed percept phases, where participants reported fusion-derived
1736 (or piecemeal) percepts as dominating perception. We found no effect of monocular
1737 patching, neither on their proportion ($F = 0.92$, $p = 0.41$) nor on the evoked pupil
1738 response ($F = 0.10$, $p = 0.90$).

1739

1740

1741

1742



1743

1744

1745 *Figure 4-2 Monocular deprivation effects on perceptual dominance and pupil modulations.*

1746 *A: Difference between white and black dominance proportions measured before (x-axis) and*
1747 *after (y-axis) monocular deprivation. Single dots report individual values when the white*
1748 *(magenta dots) or the black stimulus stimulus (black dots) was shown to the deprived eye,*
1749 *after monocular deprivation. Error bars indicate mean \pm S.E. across participants.*

1750 *B: Difference between baseline-corrected pupil size (in time bin $-.5:1$ s around perceptual*
1751 *switch) in black and white dominance phases measured before (x-axis) and after (y-axis)*
1752 *monocular deprivation. Single dots report individual values when the white (magenta dots) or*
1753 *the black stimulus stimulus (black dots) was shown to the deprived eye, after monocular*
1754 *deprivation. Error bars indicate mean \pm S.E. across participants.*

1755 *C: Time course of the difference between baseline-corrected pupil size during black and white*
1756 *percepts computed before (blue trace) and after monocular deprivation (black trace for*
1757 *blackdep condition, magenta trace for whitedep condition). Shadings report mean \pm SE across*
1758 *participants; marks on the x-axis highlight time points where the pupil difference after*
1759 *deprivation (magenta for “post-whitedep” and black for “post-blackdep”) is significantly*
1760 *different from the “pre” condition (paired t-tests, $p < 0.05$ FDR corrected).*

1761

1762

1763

1764 4.4 Discussion

1765

1766 In this study, we investigated the effects of short-term monocular deprivation on the pupil
1767 response evoked by rivalling visual stimuli.

1768 We successfully replicated the effects of short-term monocular deprivation on perceptual
1769 dominance during binocular rivalry, which consisted of a clear bias in favour of the eye that
1770 had been deprived of visual input (Lunghi et al., 2011, 2013).

1771 We also confirmed that pupil size tracks perceptual oscillations during binocular rivalry,
1772 despite constant stimulation, consistently with a large body of work suggesting that the
1773 subcortical circuit generating the pupillary light response is modulated by perceptual signals
1774 (Binda & Gamlin, 2017; Binda & Murray, 2015a; Mathôt, 2018). In line with our predictions,
1775 we found that these pupil size changes during rivalry were modulated by monocular
1776 deprivation, and increased after patch removal. This effect is in line with the hypothesis that
1777 monocular deprivation boosts the effective strength of the deprived eye.

1778 Surprisingly, the effect on pupil modulations differed depending on which stimulus, white or
1779 black, was delivered to the deprived eye. When the white stimulus was shown to the deprived
1780 eye, it elicited significantly larger pupil modulations, whereas the effect was non-significant
1781 when the black stimulus was delivered to the deprived eye.

1782 This asymmetry in our results may be explained by considering that black stimuli generally
1783 drive a much weaker pupillary response than bright stimuli, implying weaker modulations
1784 thereof (e.g., Binda & Murray, 2015).

1785 It is interesting to compare these results with those in Acquafredda et al., 2022, where we
1786 used the same technique to measure the effects of attention during rivalry. Voluntary
1787 attention to one of the rivalry stimuli and short-term deprivation of one eye produced similar
1788 effects on perceptual reports – a modulation of about 10-20% dominance. However, the
1789 effects on pupil oscillations differed. Only monocular deprivation, not voluntary attention,
1790 modulated pupil responses. This suggests that these two factors affect rivalry at very different
1791 levels; as suggested in Acquafredda et al., 2022), attention could alter rivalry dynamics by
1792 acting at a higher level than monocular deprivation; it could affect perceptual decisions, rather
1793 than sensory representations. Of course, this suggestion requires further experimental tests.
1794 Our findings attest to the sensitivity of the pupillometric technique for tracking perceptual
1795 modulations; they also suggest that similar perceptual effects can be accompanied by very
1796 different modulations on effective strength, likely implicating distinct neural underpinnings.
1797 There is increasing evidence on the relevance of pupillometry in investigating a variety of
1798 neural phenomena, including neuroplasticity (Binda & Lunghi, 2017; Viglione et al., 2023). For
1799 the first time, we were able to integrate the pupillometric technique into one of the standard
1800 tests for revealing short-term monocular deprivation effects – binocular rivalry. Our results
1801 indicate that enhanced pupil modulations serve as an objective, automatic and unconscious
1802 index of the increased dominance of the deprived eye following patch removal.

1803

1804

1805

1806

1807 5 Chapter 5 - Short-term monocular deprivation in adult humans
1808 alters functional brain connectivity measured with ultra-high field
1809 Magnetic Resonance Imaging
1810

1811 5.1 Introduction
1812

1813 Monocular deprivation is the classical paradigm to investigate ocular dominance plasticity.
1814 During development, closing one eye for a prolonged period of time leads to amblyopia, a
1815 permanent loss of the deprived eye representation in the visual cortex, producing a shift of
1816 ocular dominance in favour of the non-deprived eye (HENSCH & QUINLAN, 2018; Hubel &
1817 Wiesel, 1965; Wiesel & Hubel, 1963). In adult humans, a shorter period of monocular patch
1818 (only two hours) leads to a paradoxical shift of ocular dominance: temporary and opposite to
1819 that produced during development, consisting of a transient boost of the deprived eye (Bai et
1820 al., 2017; Binda & Lunghi, 2017; Castaldi et al., 2020; Chadnova et al., 2017; Lunghi, Berchicci,
1821 et al., 2015b; Lunghi, Emir, et al., 2015; Lunghi et al., 2011, 2013, 2019; Lunghi & Sale, 2015;
1822 Lyu et al., 2020; Min et al., 2018; Schwenk et al., 2020; M. Wang et al., 2020; J. Zhou et al.,
1823 2013, 2014, 2015). This phenomenon was interpreted as a form of homeostatic plasticity
1824 (Turrigiano, 2012). The effects of short-term monocular deprivation have been extensively
1825 studied with electrophysiological and imaging techniques, which have consistently shown a
1826 change in the ocular drive of cortical visual evoked responses in favour of the deprived eye
1827 (Binda et al., 2018; Lunghi, Berchicci, et al., 2015b). Crucially, these effects were found not
1828 only in the visual cortex, but also in a key nucleus of the visual thalamus: the ventral Pulvinar
1829 (Kurzawski et al., 2022). The same study failed to find any effect of deprivation in the lateral
1830 geniculate nucleus (LGN) (Kurzawski et al., 2022). This suggests that the primary visual cortex
1831 (V1) modulation is not inherited from LGN, since the former was reliably observed in a dataset
1832 where the latter was absent.

1833 this observation also opens the possibility that the pulvinar plays an important role in
1834 mediating the effect of monocular deprivation.

1835 The pulvinar is the largest nucleus in the primate thalamus and it is anatomically and
1836 functionally heterogeneous (Bridge et al., 2016). Functional connectivity analyses have
1837 revealed two distinct subregions, namely the ventral (vPulv) and dorsal (dPulv) regions (Arcaro
1838 et al., 2015, 2018). While dPulv exhibits stronger connections with the parietal and frontal
1839 cortex, the vPulv region is primarily connected with the occipital cortex, particularly with areas

1840 along the ventral pathway. This finding aligns with similar results observed in other primates
1841 (Kaas & Lyon, 2007).

1842 Unlike the first-order thalamic relay nuclei, including the LGN, which receive their driving input
1843 from subcortical sources and project to layer 4 of the corresponding unimodal cortical area,
1844 most of the pulvinar neurons receive driving input from layer 5 of the cerebral cortex and
1845 project to layer 4 of a higher cortical area. These connections give rise to a cortico-thalamo-
1846 cortical route for both feedforward and feedback corticocortical communication (Arcaro et al.,
1847 2018; Benarroch, 2015; Sherman, 2005; Shipp, 2003).

1848 It is thanks to its recurrent connectivity with the cortex that this thalamic nucleus is receiving
1849 more and more attention for its involvement in a variety of brain functions, including attention
1850 (Kaas & Lyon, 2007; Purushothaman et al., 2012; Saalman et al., 2012; Sherman & Guillery,
1851 2002; Shipp, 2003; H. Zhou et al., 2016), sensory-motor integration in the context of eye
1852 movements (Miura & Scanziani, 2022) and modulation of bottom-up and top-down cortical
1853 pathways (Bridge et al., 2016; Galuske et al., 2019; Jaramillo et al., 2019; Kanai et al., 2015; Z.
1854 Liu et al., 2012).

1855 Recently, Ziminski and colleagues (Ziminski et al., 2023) have also shown its involvement in
1856 plasticity mechanisms, demonstrating that learning-dependent changes in thalamocortical
1857 connectivity, gate sensory processing through GABAergic inhibition in the visual cortex. The
1858 idea that experience-dependent changes in the adult brain can be modulated by top-down
1859 gating mechanisms has been also proposed in (Steinwurz et al., 2023), which shows that de-
1860 synchronization of visual information and voluntary actions is sufficient to trigger ocular
1861 dominance plasticity, suggesting that homeostatic plasticity is gated by circuits integrating
1862 visual inputs and actions outcomes.

1863 Here, we hypothesise that the effects of monocular deprivation might extend beyond
1864 modulations of visual evoked responses to a (temporary) reorganization of thalamo-cortical
1865 circuits.

1866 To test this hypothesis, we investigate the effects of short-term monocular deprivation on the
1867 resting state functional connectivity of two thalamic nuclei: the ventral Pulvinar and the LGN.

1868
1869
1870
1871
1872

1873 5.2 Materials and Methods

1874

1875 5.2.1 Participants and ethics statement

1876

1877 Experimental procedures are in line with the declaration of Helsinki and were approved by
1878 the regional ethics committee [Comitato Etico Pediatrico Regionale—Azienda Ospedaliero-
1879 Universitaria Meyer—Firenze (FI)] and by the Italian Ministry of Health, under the protocol
1880 ‘Plasticità e multimodalità delle prime aree visive: studio in risonanza magnetica a campo
1881 ultra alto (7T)’ version #1 dated 11/11/2015. Written informed consent was obtained from
1882 each participant, which included consent to process and preserve the data and publish them
1883 in anonymous form. Twenty-five healthy volunteers with normal or corrected-to-normal
1884 visual acuity were examined (13 females including one author, mean age \pm S.E.M.= 26.6 \pm
1885 3.7). We analyzed data from two fMRI sessions, acquired before and after 2 hours of
1886 monocular deprivation.

1887 5.2.2 Short-term monocular deprivation

1888

1889 Monocular deprivation was achieved by patching the dominant eye for 2 hours. The
1890 operational definition of dominant eye applied to the eye showing the longer phase durations
1891 during the baseline binocular rivalry measurements. Like in previous studies (Lunghi et al.,
1892 2011, 2013), we used a translucent eye-patch made of plastic material allowing light to reach
1893 the retina (attenuation 0.07 logUnits, at least 3 times smaller than the threshold for
1894 discriminating a full-field luminance decrement (Knau, 2000) and more than ten times smaller
1895 than the minimum photopic luminance decrement required for shifting the spatial (Van Nes
1896 & Bouman, 1967) or temporal contrast sensitivity function (D. H. Kelly, 1961). The patch
1897 prevents pattern vision, as assessed by the Fourier transform of a natural world image seen
1898 through the eye-patch. During the 2 hours of monocular deprivation, participants were free
1899 to walk, read and use a computer.

1900 5.2.3 Binocular rivalry

1901

1902 Binocular rivalry was measured in two short sessions (each comprising two runs of 3 min
1903 each), immediately before each fMRI session to estimate the transient ocular dominance shift
1904 (pre- vs. post deprivation). Stimuli were presented on a 15-inch LCD monitor, placed at a 57
1905 cm distance, and were viewed through anaglyph red-blue goggles (right lens blue, left lens
1906 red). Stimuli were composed of two oblique orthogonal red and blue gratings (orientation:

1907 ±45°, size: 3°, spatial frequency: 2 cpd, contrast 50%), surrounded by a white smoothed circle,
1908 presented on a black uniform background in central vision. Peak luminance of the red grating
1909 was reduced to match the peak luminance of the blue one using photometric measures.
1910 During stimulus presentation, participants were asked to respond with the computer
1911 keyboard and report which grating (red or blue or a mixture of the two) they perceived as
1912 dominant by continuous keypresses.
1913 We defined ocular dominance as the proportion of dominance time spent seeing through
1914 either eye.

1915

$$1916 \quad ODI = \frac{Time_{DE} - Time_{NDE}}{Time_{DE} + Time_{NDE}}$$

1917

1918

1919 *Equation 5-1*

1920

1921 Where DE stands for Dominant Eye and NDE stands for Non-dominant Eye. From this, we
1922 derived an index of ocular dominance shift by taking the difference between ocular
1923 dominance indices acquired before and after the 2h monocular deprivation.

1924 The ocular dominance shift following monocular deprivation (mean ± S.E.M: 0.18 ± 0.02) was
1925 significant across participants (one sample t-test: |t(24)| = 7.36, p < 0.001, lgBF = 5.06),
1926 validating the efficacy of monocular deprivation paradigm in triggering ocular dominance
1927 plasticity in our dataset.

1928

1929 5.2.4 MR system and sequences

1930

1931 Scanning was performed on a Discovery MR950 7 T whole body MRI system (GE Healthcare,
1932 Milwaukee, WI, USA) equipped with a 2-channel transmit driven in quadrature mode, a 32-
1933 channel receive coil (Nova Medical, Wilmington, MA, USA) and a high-performance gradient
1934 system (50 mT/m maximum amplitude and 200 mT/m/ms slew rate).

1935 Anatomical images were acquired at 1 mm isotropic resolution using a T1-weighted
1936 magnetization-prepared fast Fast Spoiled Gradient Echo (FSPGR) with the following
1937 parameters: TR = 6 ms, TE = 2.2 ms. FA = 12 deg, rBW = 50 kHz, TI = 450 ms, ASSET = 2. Two
1938 different sets of functional images were acquired. One with spatial resolution 1.5 mm and
1939 slice thickness 1.4 mm with slice spacing = 0.1 mm, TR = 3 s, TE = 23 ms, rBW = 250 kHz,
1940 ASSET = 2, phase encoding direction AP-PA. The other with spatial resolution 1.5 mm and slice

1941 thickness 1.4 mm with slice spacing = 0.1 mm, TR = 1 s, TE = 23 ms, rBW = 250 kHz, ASSET = 2,
1942 phase encoding direction AP-PA. For the first four participants, these scans were acquired at
1943 a TR of 0.8 s. For each EPI sequence, we acquired an additional volume with the reversed
1944 phase encoding direction (Posterior-to-Anterior), used for distortion correction.

1945 We acquired each set of functional images (the acquisitions at TR = 3s first, followed by
1946 acquisitions at TR = 1s) in a resting state condition, before and after monocular deprivation.
1947 During the acquisitions, that lasted respectively 8 and 4 minutes, subjects were in the dark,
1948 instructed to keep their eyes closed and not to fall asleep.

1949 1950 5.2.5 fMRI preprocessing

1951
1952 Analyses were performed mainly with Freesurfer v6.0.0, with some contributions of the
1953 SPM12 and BrainVoyager 20.6 and FSL version 5.0.10 (Jenkinson et al., 2012) packages.
1954 Anatomical images were corrected for intensity bias using SPM12 (Friston et al., 2007) and
1955 processed by a standard procedure for segmentation implemented in Freesurfer (recon-
1956 all: Fischl et al., 2002). Functional images were corrected for subject movements (Goebel et
1957 al., 2006) and undistorted using EPI images with reversed phase encoding direction (Brain
1958 Voyager COPE plug-in (Jezzard & Balaban, 1995)). We then exported the preprocessed images
1959 from BrainVoyager to NiFTi format.

1960 Each individual participants' first functional acquisition (acquired right after the anatomical
1961 images), was aligned to the corresponding T1 images using ANTs, by means of an affine
1962 registration matrix and a warp field (AVANTS et al., 2008; Avants et al., 2011) For all subsequent
1963 functional acquisitions, a rigid transformation matrix was computed to align them to the first
1964 acquisition. All transformation matrices were applied to align each individual participants'
1965 preprocessed BOLD data (which had been slice-time, motion, and distortion corrected)
1966 through the antsRegistrationSyN.sh routine (Tustison & Avants, 2013), so that all functional
1967 acquisitions were aligned to the T1 anatomical image and to the reference functional image.
1968 Functional images were then projected to the cortical surface of each hemisphere. Each
1969 hemisphere was then aligned to a left/right symmetric template hemisphere (fsaverage_sym
1970 Greve et al., 2013) and data were smoothed with an isotropic Gaussian kernel (FWHM= 5
1971 mm).

1972

1973 5.2.6 ROI definition

1974

1975 Thalamic ROIs (vPulv, LGN and dPulv) were defined in the MNI space based on the recently
1976 published NSD dataset, for which they were defined based on a combination of functional
1977 data (retinotopic mapping experiments) constrained with anatomical features (Arcaro et al.,
1978 2015). Each subject's T1 image was aligned to the MNI template available in (Collins et al.,
1979 1995; Mazziotta et al., 2001), and the resulting transformation matrices were applied to the
1980 thalamic ROIs to align them to each subject's anatomy through ANTs functions. BOLD time
1981 series were averaged across voxels within each ROI, resulting in one time series per each
1982 participant, ROI, and condition.

1983

1984 Cortical ROIs were defined based on the cortical parcellation atlas by Glasser et al. (Glasser et
1985 al., 2016). Area MT+ was obtained by combination of areas MT and MST. BOLD time series
1986 were averaged across vertices within each ROI, resulting in one time series per each
1987 participant, ROI, and condition.

1988

1989 5.2.7 Analysis performed on data acquired at TR = 3s

1990

1991 5.2.7.1 *Functional connectivity analysis*

1992

1993 After slice-time, motion correction and alignment, additional steps were performed on the
1994 resting state data: band-pass temporal filtering retaining frequencies in the 0.01– 0.1 Hz band;
1995 removal by regression of several sources of variance (Arcaro et al., 2018) : (1) the six motion-
1996 parameter estimates and their temporal derivatives, (2) the signal from ventricular and white
1997 matter regions (derived for each subject from the recon-all segmentation procedure after
1998 subtracting the thalamic rois of interest), (3) physiological parameters (respiration and cardiac
1999 pulsation preprocessed with the PhysIO Toolbox (Kasper et al., 2017)). To minimize the effects
2000 due to the filtering procedure, the initial 10 TRs and the last 10 TRs were removed from each
2001 scan.

2002 We generated super-subjects functional connectivity maps for each condition by
2003 concatenating for each vertex, the z-scored individual participant's BOLD signals and then
2004 computing the Pearson's correlation between each voxel and the super-subjects thalamic ROIs
2005 (derived from concatenating the average individual time courses).

2006 Next, we compared the cortical connectivity patterns in the two conditions by computing
2007 vertex-wise differences in Person's r values (post- pre deprivation), resulting in maps of
2008 functional connectivity differences.

2009 To evaluate the effect across subjects for the individual cortical ROIs, we complemented these
2010 analyses with a within-subjects analysis. We computed the Pearson's correlation between the
2011 averaged time courses of the thalamic seeds and the cortical ROIs for each condition for each
2012 subject and assessed the statistical significance by paired t-tests.

2013

2014 5.2.7.2 Statistical analysis

2015

2016 To evaluate the statistical significance of the functional connectivity maps, we transformed
2017 the individual Pearson's correlation values into t values with the following formula (Cohen et
2018 al., 2003):

2019

$$t = \frac{r}{\sqrt{\frac{1-r^2}{n-2}}}$$

2020

2021 Equation 5-2

2022 Where r is the Pearson's correlation value and n is the degrees of freedom (n = number of
2023 time points * number of subjects). The p-value is calculated as the corresponding two-sided
2024 p-value for the t-distribution with n-1 degrees of freedom.

2025 For the maps of functional connectivity differences, in a first step the correlation
2026 coefficients r for pre and post deprivation conditions were transformed using
2027 Fisher z transformation:

2028

$$z = \frac{1}{2} \ln \frac{1+r}{1-r}$$

2029 Equation 5-3

2030 Then the relative standard error was computed as following:

2031

$$SE_{post-pre} = \sqrt{\frac{1}{n_{pre}-3} + \frac{1}{n_{post}-3}}$$

2032 Equation 5-4

2033 And used to compute the z-score of the functional connectivity differences (Witz et al., 1990):

2034

$$Z_{diff} = \frac{Z_{post} - Z_{pre}}{SE_{post-pre}}$$

2035 Equation 5-5

2036 The associated p-value was calculated as the corresponding two-sided p-value for the z-
2037 distribution. Using an alpha of 0.05, p-values were assessed for significance following False
2038 Discovery Rate (FDR) correction (Benjamini & Hochberg, 1995) and used to mask the
2039 connectivity maps.

2040 Moreover, a cluster threshold was applied to all connectivity maps using the FreeSurfer
2041 function `mri_surfcluster`. The cluster threshold area was set to 200 mm², which was designed
2042 to exclude small clusters but include MT, the smallest area of interest.

2043

2044 5.2.8 Analysis performed on data acquired at TR = 1s

2045

2046 After slice-time, motion correction and alignment, similar steps were performed: high-pass
2047 temporal filtering retaining frequencies higher than 0.01 Hz; removal by regression of several
2048 sources of variance: (1) the six motion- parameter estimates and their temporal derivatives,
2049 (2) physiological parameters (respiration and cardiac pulsation preprocessed with the PhysIO
2050 Toolbox (Kasper et al., 2017)).

2051 On this set of functional images, we measured the effective connectivity between two
2052 thalamic ROIs (vPulv and LGN) and the primary visual cortex (V1). We extracted the mean time
2053 course across voxels for each of the three ROIs (defined as described above) and performed:
2054 (1) dynamic causal modeling, using the rDCM toolbox (Frässle et al., 2017, 2018), available as
2055 part of the TAPAS software collection (Frässle et al., 2021) and (2) a cross-correlation analysis
2056 using the `xcorr` built-in MATLAB function.

2057

2058 The DCM routine provides an estimated connectivity pattern described with parameter
2059 estimates for each connection. To compare the effective connectivity before and after
2060 deprivation, we applied a 3x2 ANOVA to the connectivity parameters, with factors: nodes
2061 (LGN-V1 vs. vPulv-V1 vs. LGN-vPulv), condition (pre vs. post deprivation) and directionality
2062 (feedforward vs. feedback). A further 2x2 ANOVA was run separately for each seed together
2063 with post-hoc t-tests.

2064 Moreover, paired t-tests were applied to cross-correlation values to assess any changes
2065 following monocular deprivation at different lags.

2066

2067 5.2.9 Diffusion tensor imaging preprocessing and analysis

2068

2069 Diffusion data was first formatted according to BIDS standard (Gorgolewski et al., 2016) and

2070 further preprocessed with QSIprep (Cieslak et al., 2021). Preprocessing involved distortion
2071 correction, denoising using MP-PCA, motion correction and registration to the anatomical
2072 template. Tensor fitting and reconstruction of the whole brain tractogram were performed
2073 with pyAFQ. Tractogram was generated with 1500000 seeds using a CSD model and was
2074 limited by a white matter mask. We segmented three bundles. LGN to V1, vPulv to V1 and
2075 one summary bundle – the Optic radiations. To delineate LGN and vPulv bundles, we used
2076 the same ROIs as in the functional analysis. To map optic radiations, we use predefined ROIs
2077 available in pyAFQ. After successfully labelling tracts that belong to each bundle the outlier
2078 tracts were removed. A single tract was considered an outlier if it was 4 SD away from the
2079 mean length of the bundle or 3 SD away from the mean location of the bundle. Fractional
2080 Anisotropy (FA) tract profiles of clean bundles were generated after resampling the tract
2081 length to 100 points.

2082 For each participant, we estimated the tract profiles of FA values before and after monocular
2083 deprivation and compared them with paired t-tests. Using an alpha of 0.05, p-values were
2084 assessed for significance following Bonferroni-Holm correction for multiple comparisons
2085 (Holm, S. (1979)).

2086

2087 5.3 Results

2088

2089 In 25 adult participants, we measured the resting state brain functional connectivity in two
2090 conditions, before and after 2 hours of monocular eye patching (Figure 1A).

2091 Pooling data across participants, we computed seed-based functional connectivity maps for
2092 two thalamic seeds: ventral Pulvinar and LGN (shown in the MNI space in Figure 1B).

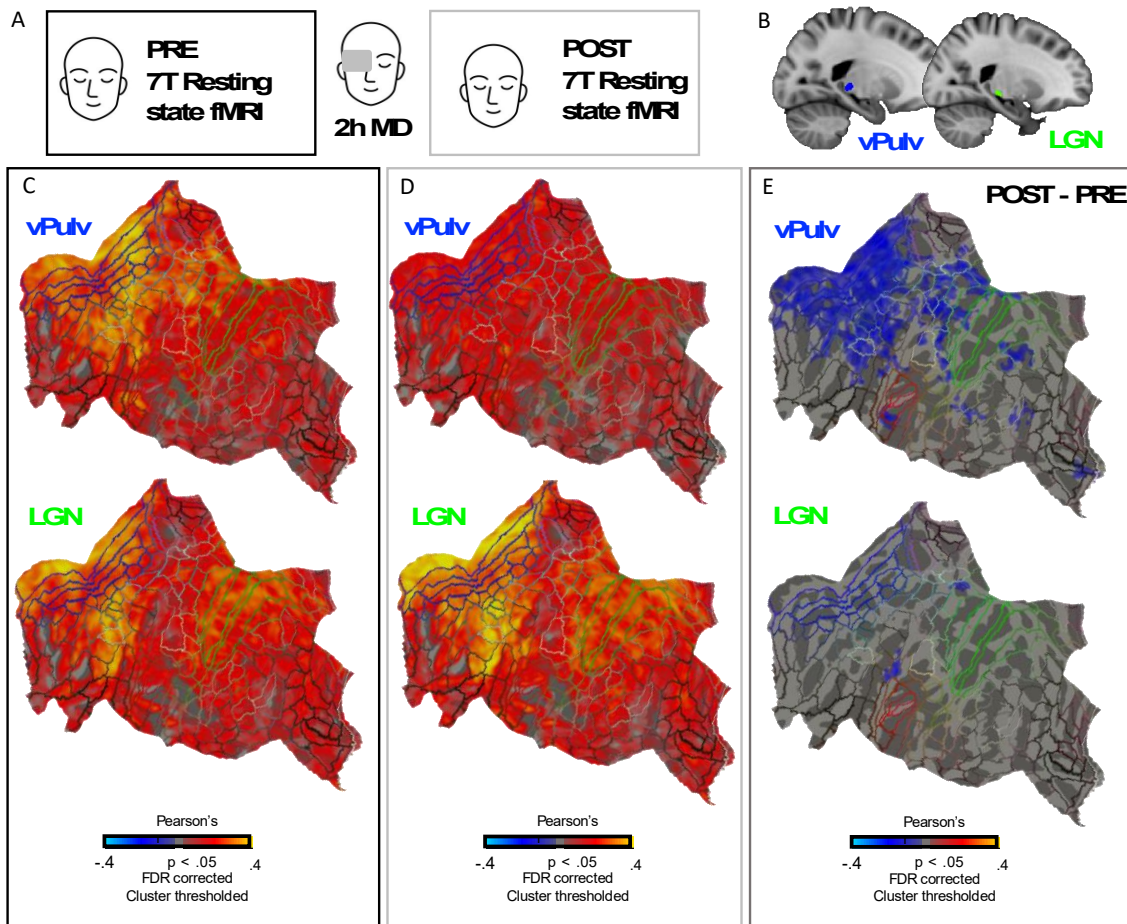
2093 The functional connectivity maps show Pearson's correlation indices for each vertex, following
2094 FDR correction and cluster threshold (see Methods).

2095 Before monocular deprivation, the functional connectivity maps of the two thalamic regions
2096 were similar, as both vPulv and LGN were strongly functionally connected to the visual cortex,
2097 as shown in Figure 1C.

2098 After two hours of monocular deprivation however, the functional connectivity of the ventral
2099 Pulvinar with the visual cortex decreased (i.e. the magnitude of Pearson's correlations
2100 decreased – Figure 1 - D). The LGN connectivity pattern, on the other hand, did not change.

2101 Pearson's correlation differences are shown in the rightmost part of Figure 1 (E) which shows
 2102 the extent of the decrease, that includes most part of the visual cortex.

2103
 2104
 2105



2106
 2107
 2108

2109 *Figure 5-1 vPulv and LGN functional connectivity patterns*

2110 *A – Experimental design. Resting state functional images were acquired before and after two*
 2111 *hours of monocular deprivation. Participants were instructed to keep their eyes closed for the*
 2112 *entire duration of the acquisitions. B – Sagittal view of the thalamic ROIs mapped on the 1*
 2113 *mm³ MNI template. C-D Super-subjects correlation maps computed before (C) and after (D)*
 2114 *monocular deprivation for the two thalamic seeds: vPulv and LGN. E- Maps of super-subjects*
 2115 *correlation differences (post–pre deprivation) for vPulv and LGN.*

2116 *All maps are thresholded by False Discovery Rate (FDR) corrected p values (alpha = 0.05) and*
 2117 *cluster size (threshold = 200 mm²).*

2118

2119 These observations were replicated with a within-subjects approach. For each participant, we
2120 correlated the average time courses of the cortical areas of interest with the average time
2121 course of each thalamic seed. Figure 2 shows the individual correlation values of vPulv (A) and
2122 LGN (B) with the primary visual cortex, before and after monocular deprivation.

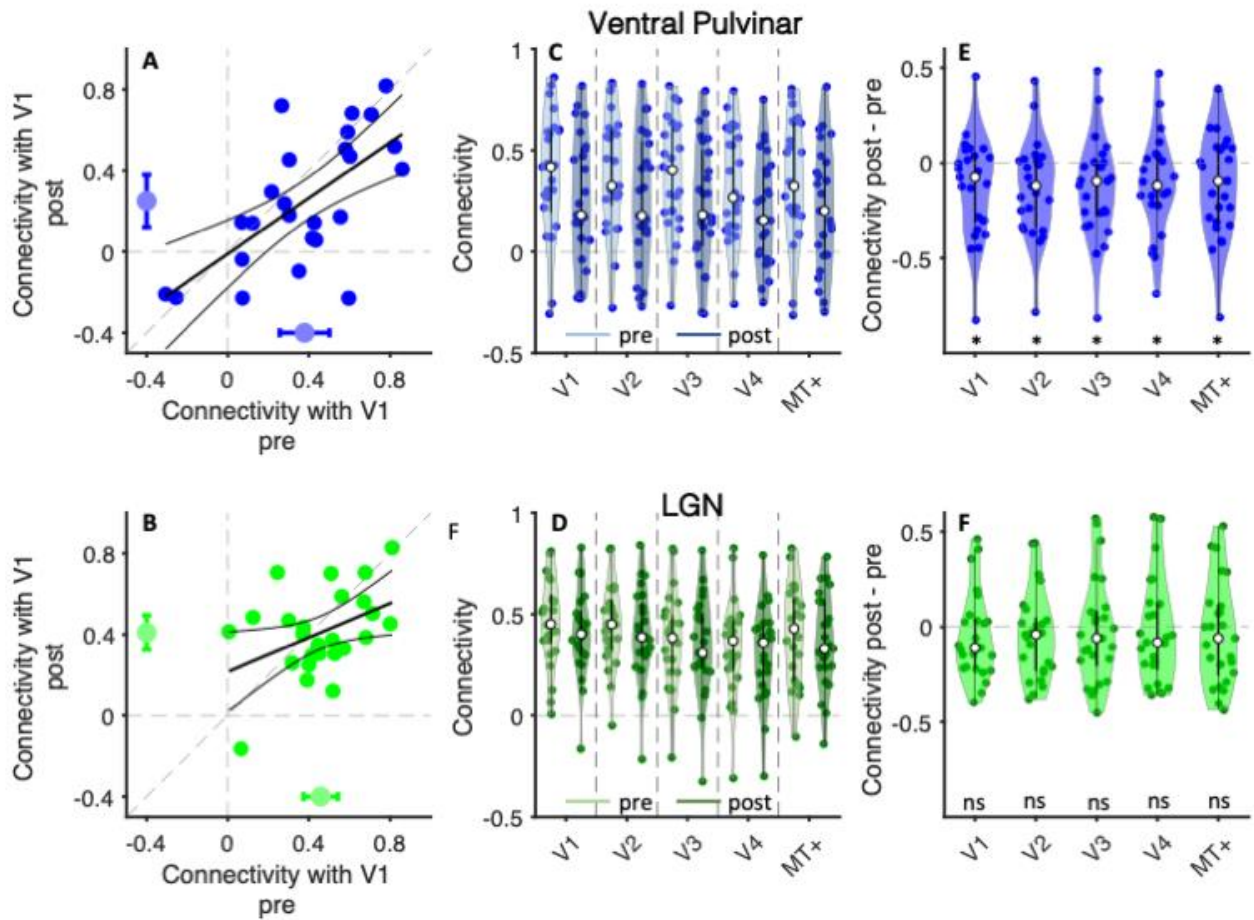
2123 Both thalamic regions were positively and significantly correlated with V1 both before (vPulv:
2124 $|t(24)|=6.19$, $p<0.001$, $\lg\text{BF}$: 3.94; LGN: $|t(24)|=10.87$, $p<.001$, $\lg\text{BF}$: 8.02), and after
2125 monocular deprivation (vPulv: $|t(24)|=3.87$, $p<.001$, $\lg\text{BF}$: 1.65; LGN: $|t(24)|=9.70$, $p<.001$,
2126 $\lg\text{BF}$: 7.10). The correlation values in the two conditions were also significantly correlated
2127 across subjects, suggesting a good reliability for both vPulv and LGN functional connectivity
2128 measures (vPulv: $r = 0.65$, $p <.001$, $\lg\text{BF} = 1.87$; LGN: $r = 0.42$, $p=0.04$, $\lg\text{BF} = 0.13$).

2129 After monocular deprivation however, only the correlation of V1 with the vPulv decreased
2130 ($|t(24)|=2.47$, $p=0.02$, $\lg\text{BF}$: 0.41), leaving the correlation with LGN unaffected ($|t(24)|=1.08$,
2131 $p=0.29$, $\lg\text{BF} = -0.45$).

2132 After investigating V1 connectivity with vPulv and LGN, we quantified the effect of monocular
2133 deprivation on neighbouring visual regions, namely V2, V3, V4 and area MT+. Similarly to V1,
2134 all these areas showed a significant and positive correlation with vPulv and LGN in both
2135 conditions (one sample t-tests: all $|t| > 5$, all $p_{\text{FDRcorrected}} < .001$) and decreased connectivity
2136 with the ventral Pulvinar (one sample t-tests: all $|t| > 2$, all $p_{\text{FDRcorrected}} < .05$), but not with
2137 LGN (all $|t| < 1$, all $p_{\text{FDRcorrected}} > .05$).

2138 We also investigated the functional connectivity of these cortical visual regions with the
2139 primary visual cortex and the dorsal Pulvinar. We found no effect of monocular deprivation
2140 across subjects (see Appendix).

2141



2142
 2143
 2144
 2145
 2146
 2147
 2148
 2149
 2150
 2151
 2152
 2153
 2154
 2155
 2156
 2157
 2158

Figure 5-2 vPulv and LGN functional connectivity with the visual cortex.

A–B: Individual correlation values of vPulv (A) and LGN (B) with the primary visual cortex (V1). The x-axis reports values before monocular deprivation, the y-axis reports values after monocular deprivation. Error bars show mean \pm 1 S.E.M. across subjects. The continuous black lines show the best-fitting line and its 95% confidence intervals.

C–D: Violin plots report, for each cortical region (shown on the x-axis), the Pearson’s correlation with vPulv and LGN before and after monocular deprivation. E–F: Violin plots report for each cortical region (shown on the x-axis) the correlation values difference (post – pre), with vPulv (E) and LGN (F). From C to H, thick black error bars indicate the ends of the first and third quartiles, and thin black bars indicate 95% confidence intervals. The white circle indicates the median across subjects. Single points indicate individual values. In-text values correspond to FDR corrected p -values for one sample t -tests against zero (* $p_{FDR} < .05$; ** $p_{FDR} < .01$; *** $p_{FDR} < .001$, $^{ns}p_{FDR} > .05$).

2159

2160 Notably, functional connectivity changes induced by monocular deprivation occurred in
2161 absence of any variations in signal-to-noise ratio or amplitude spectra in either of the seed
2162 regions (see Table 7-2 and Figure 7-4 in the Appendix).

2163

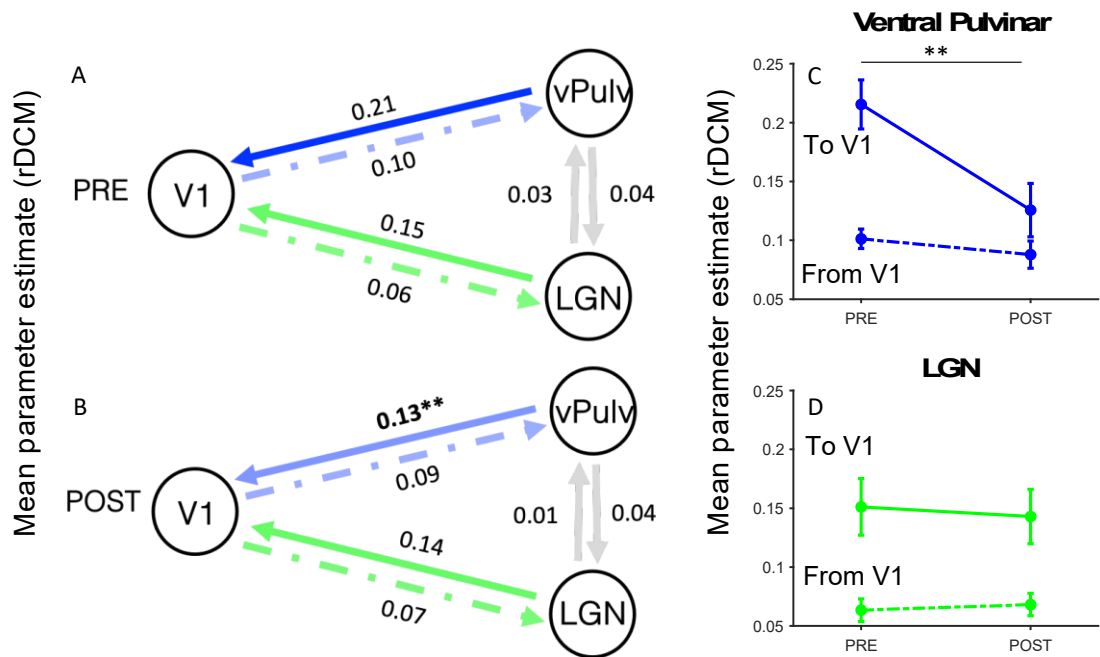
2164 These results were replicated and expanded on another dataset, acquired right after, at a
2165 higher temporal frequency (TR = 1 second). We applied the rDCM (regression dynamic causal
2166 modelling, see methods) to examine the bidirectional connections among our nodes, namely
2167 V1, vPulv and LGN. We then compared the parameter estimates for each connection with
2168 ANOVAs.

2169 Figure 3 A-B shows the parameter estimates for each connection (i.e. the relative weight of
2170 each connection in the network) for the two conditions, averaged across participants.

2171 A 3x2 ANOVA with factors: nodes (LGN-V1 vs. vPulv-V1 vs. LGN-vPulv), condition (pre vs. post
2172 deprivation) and directionality (feedforward vs. feedback), showed a significant interaction
2173 between all factors ($F(1,24) = 4.62, p = 0.04$). A further 2x2 ANOVA was run separately for LGN
2174 and vPulv. Direct LGN-vPulv negligible connections, shown in grey in Figure 3 A-B, were not
2175 investigated further. The two 2x2 ANOVAs showed that, while for LGN there was only a main
2176 effect of directionality ($F(1,24) = 17.10, p < 0.001$) and no interaction with the conditions
2177 ($F(1,24) = 0.27, p = 0.61$), for vPulv there was a significant interaction between directionality
2178 and condition ($F(1,24) = 11.48, p < 0.01$).

2179 A post-hoc analysis revealed that, as reported in Figure 3C-D, monocular deprivation affected
2180 selectively the vPulv-V1 connection (paired t-test pre vs. post: $|t(24)| = 3.8, p < .001, \lgBF =$
2181 1.60), leaving the reciprocal unaffected (paired t-test pre vs. post: $|t(24)| = 1.71, p = 0.1, \lgBF$
2182 $= -0.12$).

2183



2184

2185

2186 *Figure 5-3 vPulv and LGN effective connectivity with V1 assessed with Dynamic Causal*
 2187 *Modeling*

2188 *A-B: Scheme of nodes and connections considered in our network. In-text values are group-*
 2189 *average parameter estimates obtained from rDCM, indicating the contributions of each*
 2190 *connection, pre (A) and post(B) deprivation. C-D: Parameter estimates obtained from rDCM*
 2191 *averaged across subjects for the two conditions (pre and post-monocular deprivation). The*
 2192 *continuous lines report the connections leaving the vPulv (C) and LGN (D) to reach the primary*
 2193 *visual cortex. Dashed lines report the opposite directionality (from V1 to thalamus). Error bars*
 2194 *show mean \pm 1 S.E.M. across subjects. Asterisks report significance for the 2x2 interaction;*
 2195 *(* $p < .05$; ** $p < .01$; *** $p < .001$).*

2196

2197 These observations on effective connectivity were complemented by a cross-correlation
 2198 analysis (Figure 4). We computed the cross-correlation between the average V1 time courses
 2199 and each thalamic ROI, and evaluated the effect of monocular deprivation at different lags:

2200 At negative lags (from -3 to -1), where correlation values measure the similarity between the
 2201 thalamic time course and shifted (delayed) copy of the V1 time course, thus the strength of
 2202 the thalamus --> V1 directionality.

2203 At positive lags (from 1 to 3), where the thalamic time course is correlated with an anticipated
2204 copy of the V1 time course, thus correlation values measure the strength of the V1 à thalamus
2205 directionality.

2206

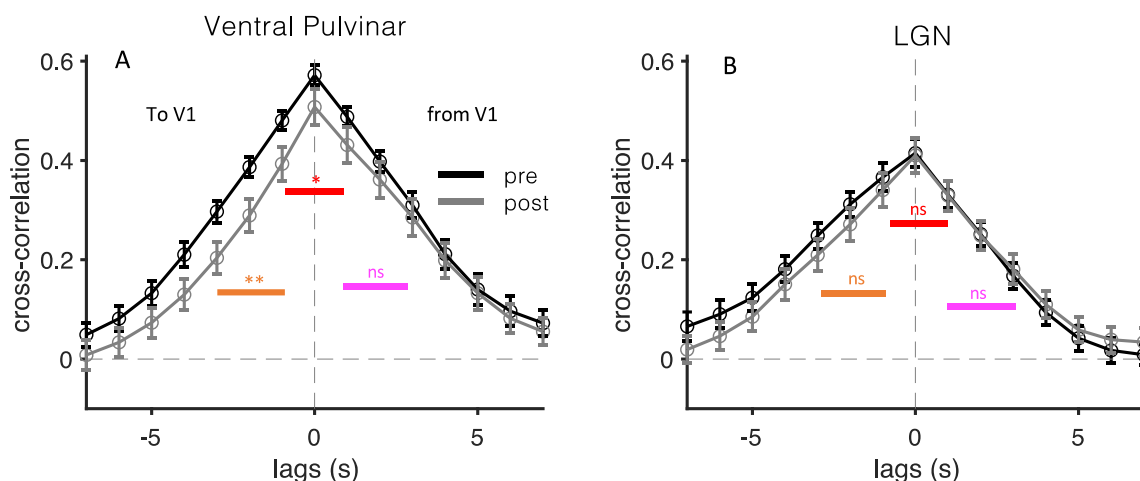
2207 We also investigated the zero-lag range (lags from -1 to +1), which corresponds to Pearson's
2208 correlation between two time courses, with no shift between the two. By doing so, we aimed
2209 at verifying the replicability of our main findings (at TR=3seconds) on a dataset with different
2210 temporal characteristics.

2211

2212 These analyses show that the average cross-correlation around zero between V1 and vPulv
2213 decreased after monocular deprivation ($|t(24)| = 2.22$, $p < .05$, $\lgBF = 0.22$), replicating our
2214 main findings.

2215 A significant effect of deprivation for vPulv was found at negative lags ($|t(24)| = 3.11$, $p < .01$,
2216 $\lgBF = 0.95$), replicating the rDCM results: a decrease of connectivity in the vPulv à V1
2217 direction.

2218 No significant effect was found for positive lags ($|t(24)| = 1.14$, $p = .27$, $\lgBF = -0.42$), nor for
2219 LGN cross-correlation values (at 0: $|t(24)| = 1.26$, $p = .22$, $\lgBF = -0.37$; negative lags: $|t(24)| =$
2220 0.10 , $p = .91$, $\lgBF = -0.67$; positive lags: $|t(24)| = 0.43$, $p = .67$, $\lgBF = -0.63$)



2221

2222

2223 *Figure 5-4 vPulv and LGN effective connectivity with V1 assessed with a cross-correlation*
2224 *analysis*

2225 *A-B: Normalized cross-correlation values between vPulv (a) or LGN (b) and V1, as a function*
2226 *of temporal lags, measured before (black symbols) and after monocular deprivation (grey*
2227 *symbols). Error bars show mean \pm 1 S.E.M. across subjects. At negative lags, correlation values*
2228 *quantify the connectivity in the thalamus \rightarrow V1 directionality. At positive lags, correlation*
2229 *values quantify the connectivity in the V1 \rightarrow thalamus directionality. Asterisks and bars report*
2230 *significance of one sample t-tests performed across subjects against zero. The red ones report*
2231 *significance for the average of the three time points around zero (lags from -1 to +1); orange*
2232 *symbols report significance for the average of the three time points before zero (lags from -3*
2233 *to -1); magenta symbols report significance for the average of the three time points after zero*
2234 *(lags from 1 to +3); (* $p < .05$; ** $p < .01$; *** $p < .001$).*

2235

2236 Finally, we checked whether monocular deprivation had any effect on the anatomical
2237 connections giving rise to the optic radiation, the bundle of projection fibres that link the
2238 thalamus with the visual cortex (Moini & Piran, 2020). For each participant, we estimated the
2239 Fractional Anisotropy tract profiles, before and after monocular deprivation, for the LGN-V1
2240 tract and the vPulv – V1 tract. As shown in Figure 5 for the two tracts, the group averages
2241 computed for the two conditions fully overlap. Paired t-tests excluded any effect of
2242 monocular deprivation on the optic radiation fibres in our dataset (all $p_{\text{FDRcorrected}} > .05$).

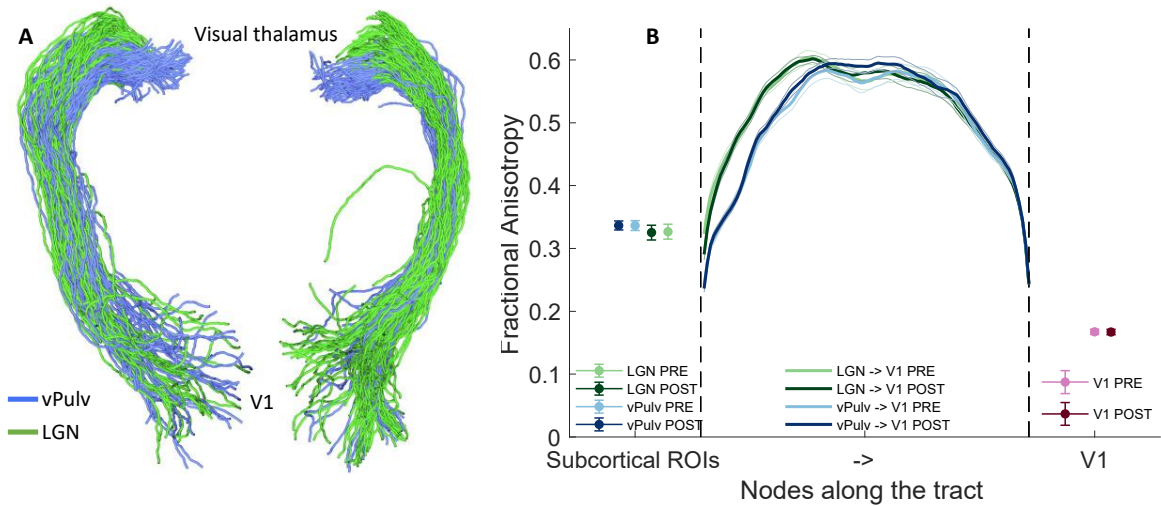
2243 We further investigate the diffusivity properties of our regions of interest to check for any
2244 changes in structural integrity following monocular deprivation. We did not find any pre-post
2245 deprivation differences in any of them (paired t-tests: vPulv: $|t(24)| = 0.04$, $p = 0.97$, $\lg\text{BF} = -$
2246 0.67 ; LGN: $|t(24)| = 0.25$, $p = 0.81$, $\lg\text{BF} = -0.66$; V1: $|t(24)| = 0.28$, $p = 0.78$, $\lg\text{BF} = -0.66$).

2247

2248

2249

2250



2251
2252
2253
2254

Figure 5-5 Mean optic radiation profiles

2255 *A: Cleaned bundles of LGN - V1 (green) and vPulv - V1 (blue) for a representative subject*
 2256 *generated with DSI-STUDIO. B: Fractional anisotropy values as a function of nodes along the*
 2257 *thalamus – V1 tract, measured before and after monocular deprivation, reported with the*
 2258 *brighter and darker plots respectively. Thick continuous lines show mean values, shaded areas*
 2259 *report mean ± 1 S.E.M. across subjects. Error bars show mean fractional anisotropy values for*
 2260 *the three ROIs of interest ± 1 S.E.M. across subjects. Using an alpha of 0.05, p-values were*
 2261 *assessed for significance following Bonferroni-Holm correction for multiple comparisons.*

2262
2263

5.4 Discussion

2265

2266 Our research investigated the impact of monocular deprivation on the communication
 2267 between the visual cortex and the visual thalamus. What we discovered was that only two
 2268 hours of monocular deprivation led to a significant decrease in functional connectivity
 2269 between the visual cortex (V1 and extra striatal areas) and the ventral Pulvinal. The functional
 2270 connectivity patterns of LGN and dPulv were unaffected, consistently with the results from
 2271 Kurzawski et al., 2022 on visual evoked responses.

2272 These findings were replicated and further expanded on a second dataset, acquired at a
 2273 higher temporal resolution, which allowed us to specifically examine how monocular
 2274 deprivation affected each direction of the reciprocal thalamo-cortical connections.

2275 Our results indicate that the decline in functional connectivity selectively affected the
 2276 connections originating from the ventral Pulvinal and heading towards the primary visual

2277 cortex. The effects of monocular deprivation exclusively involved functional connectivity,
2278 without any accompanying anatomical reconfiguration. These negative results were in line
2279 with our expectations, given that our manipulation was very brief. However, we predict that
2280 after repeated monocular deprivation sessions (see Lunghi et al., 2019), the reported visual
2281 acuity improvement (Lunghi et al., 2019) might be supported by functional changes as well as
2282 anatomical reconfigurations. We are currently testing this hypothesis on a population of
2283 amblyopic patients, replicating Lunghi et al., paradigm (short-term inverse occlusion,
2284 combined with moderate physical exercise).

2285

2286 A recent study by Kurzwaski and colleagues (Kurzwaski et al., 2022) showed that the effects of
2287 monocular deprivation on the ocular drive of visual evoked responses extended from the
2288 visual cortex to the ventral Pulvinar, but not to LGN. This led them to suggest that monocular
2289 deprivation effects do not stem from modulations at the level of monocular cells that are
2290 inherited by the primary visual cortex, but instead, they might be modulated by the cortical
2291 connections with the ventral Pulvinar.

2292 We support this hypothesis and further speculate that the role of the ventral Pulvinar in
2293 mediating this short-term plasticity phenomenon might be related to predictive coding
2294 mechanisms.

2295 Predictive coding is a theoretical framework proposing that the brain processes sensory
2296 information by making predictions about incoming sensory inputs. It would use prior
2297 knowledge to build hierarchical internal predictions, which are compared with incoming
2298 information to continuously adapt these internal models and minimize prediction errors
2299 (Clark, 2013; Friston, 2005, 2010; George & Hawkins, 2009; Hohwy Jakob, 2013; Huang & Rao,
2300 2011; Mumford, 1992; Rao & Ballard, 1999), predictive coding suggests that the brain
2301 constantly generates and compare predictions on how the world should look like, based on
2302 prior experiences, with incoming visual information.

2303 Recent work has proposed the Pulvinar (and its ventral portion in the context of visual
2304 processing) as the perfect candidate for gating bottom-up information and its integration with
2305 high-level predictions. Through modulation of cortical oscillatory activity and modulation of
2306 prediction error units in the superficial layers via diffuse projections, the Pulvinar would
2307 regulate the integration between ascending prediction errors and descending expectations
2308 (Bridge et al., 2016; Galuske et al., 2019; Jaramillo et al., 2019; Z. Liu et al., 2012).

2309 In light of our results, we hypothesise that depriving one eye of visual input, as in monocular
2310 deprivation, would lead to a mismatch between the brain's predictions based on the
2311 participant's interactions with the environment and the actual sensory input. The deprived
2312 eye's inability to transmit visual changes produced by the participant's actions could result in
2313 an increased discrepancy between what the brain predicts (based on priors, actions, and input
2314 from the open eye) and what it perceives.

2315 To reduce prediction errors and improve the accuracy of perception, the brain may undergo a
2316 reconfiguration of cortical circuits. This reconfiguration could involve adjusting the relative
2317 contributions of bottom-up sensory evidence (actual sensory input) and top-down predictions
2318 (what the brain expects to see). Crucially, this reconfiguration would involve the thalamo-
2319 cortical reciprocal connections, hence the effect of monocular deprivation on the vPulv -> V1
2320 connectivity.

2321 This idea is supported by a recent study conducted by Steinwurz and colleagues (Steinwurz
2322 et al., 2023) showing that de-synchronization of visual information and voluntary actions
2323 (achieved by introducing a visual delay in one eye while participants actively performed a
2324 visuomotor task) triggers ocular dominance plasticity, comparably to monocular contrast
2325 deprivation.

2326 The contribution of sensory-motion integration circuits to monocular deprivation effects is
2327 also coherent with our results on V1 functional connectivity. Although this aspect might need
2328 further investigation, we found that, following deprivation, V1 connectivity decreases
2329 selectively with intraparietal areas, which are thought to be involved in the transformation of
2330 sensory information into motor output (reaching, grasping, eye movements, processing of
2331 multimodal motion (for a review see Konen & Kastner, 2008). We speculate that this
2332 dissociation between V1 and intraparietal areas might be a result of the reconfiguration of the
2333 thalamo-cortical circuits mediating cortico-cortical communications.

2334

2335 Altogether, these findings align with the growing body of evidence indicating that the Pulvinar
2336 is not merely a passive relay nucleus but plays a role in a variety of mechanisms regulating
2337 information transmission to the cortex and between cortical areas (Purushothaman et al.,
2338 2012; Saalman et al., 2012; Sherman & Guillery, 2002; Shipp, 2003; H. Zhou et al., 2016).
2339 These include mediating learning-dependent changes in sensory processing through
2340 GABAergic inhibition in the visual cortex (Ziminski et al., 2023).

2341 In conclusion, the present study shows that the effects of monocular deprivation in adult
2342 humans are not limited to a gain change of visual evoked responses, but also involve a global
2343 system reconfiguration, with the ventral Pulvinar as a focal point. These results are in line
2344 with previous studies showing its involvement in sensory-motor integration and learning, and
2345 overall point towards a new model for experience-dependent changes in the visual system,
2346 which include short-term adjustments in the way the brain processes sensory information
2347 and integrates them with prior expectations.

2348
2349
2350
2351
2352
2353
2354
2355
2356
2357
2358
2359
2360
2361
2362
2363
2364
2365
2366
2367
2368
2369
2370
2371
2372
2373
2374
2375
2376
2377
2378
2379
2380
2381
2382
2383
2384

2385

2386 6 Chapter 6 – General discussion

2387

2388 My thesis aimed to assess contextual effects on visual perception, with a focus on binocular
2389 vision. After exploring the potentialities of binocular rivalry as a tool for studying experience-
2390 dependent changes on perceptual dominance (Chapter 2), I focused on two experimental
2391 manipulations: endogenous cueing of attention (Chapter 3), and short-term monocular
2392 deprivation (Chapter 4 and 5).

2393 Across the projects presented here, I exploited binocular rivalry as the main behavioural
2394 paradigm.

2395 In accordance with an extensive body of prior research, we showed that rivalry is a versatile
2396 experimental tool, which provides a controlled but dynamic context for studying the
2397 mechanisms that govern our visual perception. The multi-level competition that underlies this
2398 phenomenon allows for investigating both perceptual phenomena related to the stimulus, like
2399 attention, and to the eye-of-origin, like ocular dominance. In Chapter 2, we contributed
2400 substantial evidence for the reliability of binocular rivalry, based on a conspicuous amount of
2401 data collected in four different setups and with three different sets of stimuli. A thorough
2402 statistical approach allowed us to indicate that not all parameters that can be extracted from
2403 binocular rivalry have the same stability. Ocular dominance was found to be a trait-like
2404 characteristic stable over time; this confirms that binocular rivalry is a valid tool to follow
2405 short-term changes of sensory eye-dominance. Switch rate and mixed percepts, however,
2406 were sensitive to state-related changes; for example, day-by-day fluctuations in the speed of
2407 rivalry alternations could not be explained by the internal noise of the measure. This suggests
2408 that internal states can drive systematic changes in the dynamics of perception. This raises the
2409 question: Are these changes in perception itself, or are they related to participants' decision-
2410 making processes?

2411 The work presented in Chapter 3 is broadly related to this question. We focused our efforts
2412 on attention, a modulatory factor of binocular rivalry dynamics (Chong et al., 2005; K. C. Dieter
2413 et al., 2016; Hancock & Andrews, 2007; Meng & Tong, 2004a; Mitchell et al., 2004; Paffen et
2414 al., 2006; van Ee et al., 2005). We investigated the effects of endogenous cueing on rivalry
2415 dynamics, as indexed by both perceptual reports and the associated pupil responses. We

2416 expected that more attended stimuli would generate stronger pupil responses, as observed in
2417 non-rivalry-based paradigms. Quite surprisingly, our results showed that attention biased the
2418 perceptual dominance of the cued stimulus without boosting the associated pupil response.
2419 These results suggest two possible answers to our experimental question.

2420 One possibility is that attention, the state-dependent variable of interest, does affect the
2421 strength of the representation of the cued stimulus, but it does so only when both stimuli are
2422 comparable in strength, so during fusion-derived perceptual phases. This outcome can be
2423 predicted by the attentional model of binocular rivalry (Li et al., 2017). In this model, the two
2424 rival stimuli continuously compete for attentional resources and attention is modelled as
2425 multiplicative gain. At any given moment, the stimulus associated with stronger sensory
2426 responses attracts a larger share of attention. This model predicts that, during dominance
2427 phases (i.e., when competition between rivaling stimuli is resolved in favour of one or the
2428 other stimulus/eye), attention is automatically driven to the dominant stimulus, leaving little
2429 space for endogenous re-directing of attention. However, during periods of unresolved
2430 competition (i.e., mixed percepts, when the two stimuli are equally represented in
2431 perception), endogenous attention might act by selecting the cued stimulus and increasing its
2432 perceptual strength (K. C. Dieter et al., 2015). This interpretation could be consistent with our
2433 observation of a mild pupil modulation during phases of mixed perception. Selective attention
2434 is often described as the ability to focus on and prioritize relevant information while filtering
2435 out irrelevant information (Plebanek & Sloutsky, 2019). In this description of the mechanisms
2436 of attention, the competition among inputs seems to be crucial. Supporting the idea proposed
2437 by (K. C. Dieter et al., 2015), we hypothesise that attention is effective in producing changes
2438 in the stimulus appearance only when this competition is not completely resolved. This
2439 observation also raises interesting questions on the contribution of a suppressed stimulus, the
2440 inhibition of which is amplified by bottom-up exogenous attention, to perception, and
2441 whether awareness of the competing stimuli is necessary for selective attention (Mack et al.,
2442 2002; Norman et al., 2015).

2443 Another possibility is that attention does not act on the effective strength at all, but rather
2444 biases decision towards the cued stimulus. This would suggest that internal states, like
2445 endogenous attention, can favour one stimulus in perception without altering its appearance.
2446 In this picture, when reality is stable (retinal stimulation does not change in binocular rivalry)
2447 and low-level perception is mediated by the sensory responses evoked by the visual input, the

2448 brain would comply to the goal (attending one stimulus), by changing the internal decision
2449 thresholds, causing the same perceptual outcome to be labelled differently based on
2450 attentional demands. According to this hypothesis, perceptual reports and pupil size
2451 measurements can be dissociated and provide two reliable measures of two different neural
2452 representations that correspond to the same physical input but are differentially affected by
2453 attention. Perceptual reports would be guided by a visual representation that is further
2454 shaped by decision criteria; pupil responses would more directly track the effective content of
2455 perception.

2456

2457 In Chapter 4 we report, with the use of the same combined paradigm, the perceptual outcome
2458 of sensory deprivation: monocular contrast deprivation. This paradigm has been extensively
2459 employed to investigate short-term ocular dominance plasticity, described as a form of
2460 homeostatic plasticity (Turrigiano, 2012). In line with previous studies, we found that following
2461 monocular deprivation, the deprived eye dominance was boosted (Binda et al., 2018; Lunghi,
2462 Berchicci, et al., 2015a; Lunghi et al., 2013; J. Zhou et al., 2013, 2014). Unlike the attentional
2463 effect, this perceptual boost was accompanied by a measurable change in the relative pupil
2464 responses, which we used as an index of effective stimulus strength. Our findings suggest that
2465 this manipulation of sensory history was effective in triggering a change in the content of
2466 perception, making the deprived eye stronger in the competition for awareness, thus
2467 increasing the perceived strength of the stimulus shown to it.

2468 What are the mechanisms underlying this perceptual change? Previous studies proposed an
2469 up-regulation of the contrast gain-control mechanisms, boosting the neuronal responses to
2470 compensate for the reduced incoming signal in the deprived eye (Castaldi et al., 2020). An
2471 alternative proposal is that increased inhibition of the non-deprived could be responsible for
2472 the effect (Gong et al., 2023; Lyu et al., 2020). Our work, presented in Chapter 5, suggests that
2473 contrast-gain control may not be the only or the main mechanism supporting the perceptual
2474 consequences of short-term monocular deprivation. In a series of fMRI experiments, we
2475 moved away from measuring contrast-gain and from visually evoked responses, and simply
2476 looked at brain activity in resting state conditions. We found that this was strongly and
2477 systematically affected by the 2h-long monocular deprivation. Specifically, functional
2478 connectivity between the visual cortex and the visual thalamus was affected; even more
2479 specifically, the modulation was selective for one thalamic sub-nucleus (ventral pulvinar) and

2480 spared the others (including the LGN). Our interpretation of this result is inspired by the
2481 “predictive coding” literature, whereby the pulvinar has been implicated in relaying signals
2482 related to “a priori” information and predictions to the visual cortex, where they are combined
2483 with incoming sensory information (Kaas & Lyon, 2007; Purushothaman et al., 2012; Saalman
2484 et al., 2012; Sherman & Guillery, 2002; Shipp, 2003; H. Zhou et al., 2016) and modulate
2485 learning-dependent changes (Ziminski et al., 2023). We suggest that the temporary
2486 disconnection between the pulvinar and the visual cortex following monocular deprivation
2487 reflects the mismatch between incoming sensory input and top-down predictions. We
2488 propose that this reconfiguration could allow for adjusting the relative contributions of
2489 bottom-up sensory evidence (sensory input) and top-down predictions (what the brain
2490 expects to see). This hypothesis represents a radical shift compared to the standard
2491 “homeostatic plasticity” model and clearly, it will require further experimental and theoretical
2492 efforts to be validated.

2493

2494 6.1 Conclusions and future direction

2495

2496 The ability to adapt to varying task requirements and changes in the external environment is
2497 a distinctive feature of our brain. Understanding this flexibility is not only crucial from a
2498 theoretical perspective. It also holds strong applicative potential in the context of pathological
2499 conditions, where re-opening windows of plasticity could foster functional recovery. For
2500 example, the treatment of adult amblyopic patients could be directly impacted by a firmer
2501 understanding of homeostatic plasticity. I am currently hoping to extend my investigations in
2502 this direction, testing the possibility that the transient functional reorganization observed
2503 after monocular deprivation could evolve into enduring neuroplastic changes, which could
2504 lead towards the amelioration of visual function in adult amblyopic individuals.

2505

2506

2507

2508

2509

2510

2511

2512

2513

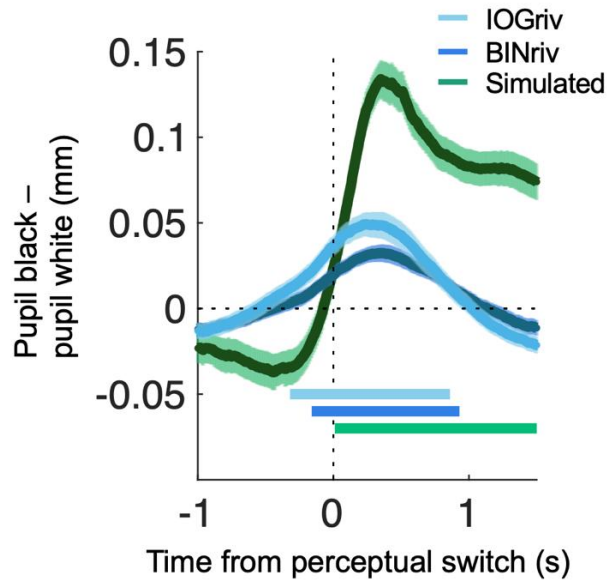
2514

2515

2516 7 Appendix

2517

2518 7.1 Extended data from Chapter 3



2519

2520 *Figure 7-1 Pupil size modulations in rivalry and simulation conditions.*

2521

2522

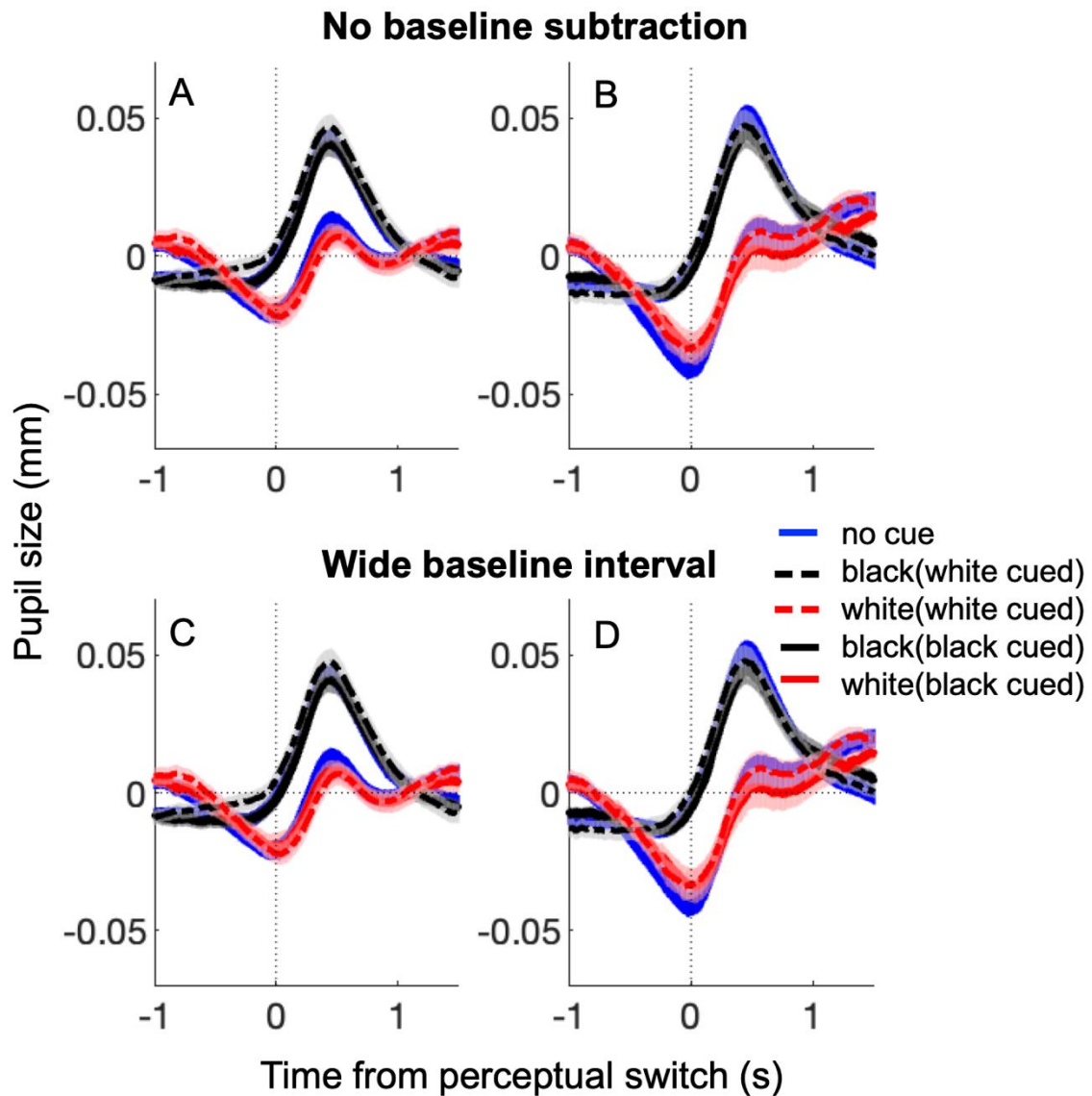
2523 *Time course of the difference between pupil size during black and white percepts, computed*
2524 *in individual participants and then averaged for binocular rivalry (dark blue curve), interocular*
2525 *grouping rivalry (light blue curve) and simulation (green curve). In all panels: shadings report*
2526 *mean ± 1 s.e. across participants and the marks on the x-axis highlight timepoints where each*
2527 *trace is significantly different from 0 (one-tailed t-test, $p < 0.05$ FDR corrected).*

2528

2529 Pupil modulations during binocular and interocular grouping rivalry averaged respectively
2530 $39.14 \pm 8.15\%$ (mean ± 1 s.e. across participants) and $43.80 \pm 10.26\%$ of the pupil size
2531 modulations observed during simulated rivalry, as previously reported by Binda and
2532 colleagues (Binda et al., 2013a) in a different spatial-attention task.

2533 Moreover, they consistently started before the perceptual switch, and this was more
2534 pronounced in the rivalry conditions than in the simulated rivalry (significant pupil difference
2535 started 160 ms before the switch in binocular and 320 ms in interocular grouping rivalry,

2536 compared with almost no latency for simulated rivalry). This finding, in line with (Fahle et al.,
2537 2011; Naber et al., 2011) may reflect the graded nature of rivalry transitions, which may delay
2538 change detection in rivalry compared with the sharp transitions used in the simulated rivalry
2539 condition.
2540



2541
2542
2543

2544 *Figure 7-2 Pupil modulations track perceptual alternations comparably across cueing*
2545 *conditions irrespectively of whether and how pupil traces are baseline corrected.*

2546 *Pupil size traces aligned to perceptual switches towards exclusive dominance of a white disk*
2547 *or a black disk percept and averaged across phases, separately for binocular rivalry (A) and*
2548 *interocular grouping rivalry (B) and separately for the two cueing conditions: cueing the white*
2549 *percept (dashed lines) or the black percept (continuous lines). Shading report ± 1 s.e. across*
2550 *participants.*

2551 *These traces are computed without subtracting any baseline correction (A-B) and after*
2552 *subtracting a baseline computed as average pupil size in the [-5:5] s interval around perceptual*
2553 *switch (C-D). Note how the resulting traces are virtually indistinguishable: in both cases, pupil*
2554 *size still allows to discriminate white and black percepts (red and black curves are clearly*
2555 *separated) but shows no effect of cueing (dashed and continuous lines are virtually*
2556 *superimposed, together with the blue traces).*

2557

2558 Coherently, we found that cueing did not affect pre-switch pupil baseline used for the main
2559 Figures, which was computed in the [-1:-.5] s interval from the perceptual switch (main effect
2560 of cued percept: $F_{(1,37)} = 1.51$, $p = 0.23$, $\log BF = -0.60$; dominant percept x cued percept
2561 interaction: $F_{(1,37)} = 0.14$, $p = 0.71$, $\log BF = -0.74$).

2562

2563

	No bsl sub	Bsl sub [-5 5]
dominant percept	$F_{(1,37)} = 40.09^*$ $p < 0.001$ $\log BF = 22.35$	$F_{(1,37)} = 38.61^*$ $p < 0.001$ $\log BF = 21.73$
rivalry type	$F_{(1,37)} = 2.17$ $p = 0.15$ $\log BF = -0.52$	$F_{(1,37)} = 2.12$ $p = 0.15$ $\log BF = -0.54$
cued percept	$F_{(1,37)} = 2.58$ $p = 0.12$ $\log BF = -0.61$	$F_{(1,37)} = 2.72$ $p = 0.11$ $\log BF = -0.57$
dominant percept x rivalry type	$F_{(1,37)} = 1.10$ $p = 0.30$ $\log BF = -0.52$	$F_{(1,37)} = 0.99$ $p = 0.32$ $\log BF = -0.52$
dominant percept x cued percept	$F_{(1,37)} = 1.00$ $p = 0.32$ $\log BF = -0.50$	$F_{(1,37)} = 0.98$ $p = 0.33$ $\log BF = -0.63$
rivalry type x cued percept	$F_{(1,37)} = 0.04$ $p = 0.85$ $\log BF = -0.77$	$F_{(1,37)} = 0.05$ $p = 0.82$ $\log BF = -0.79$
dominant percept x rivalry type x cued percept	$F_{(1,37)} = 1.67$ $p = 0.20$ $\log BF = -0.51$	$F_{(1,37)} = 1.77$ $p = 0.19$ $\log BF = -0.49$

2564

2565

2566 *Table 7-1 Three-way ANOVA for attention cueing results*

2567 *Three-way ANOVA for attention cueing results, with factors: dominant percept (white/black*
2568 *disk), cueing (white/black cued), rivalry type (binocular/interocular grouping rivalry).*

2569 *We confirmed our results on cueing with a three-way ANOVA entered with the average pupil*
2570 *size in the interval [-.5:1] s (the same interval used for Table 1 in the main text) but now*
2571 *skipping the baseline correction step (first column) or subtracting a baseline computed as the*
2572 *average pupil size in the [-5:5] s interval around perceptual switch (second column). In both*
2573 *cases, we confirm the main effect of dominant percept type and the absence of any reliable*
2574 *effect of attention cueing, suggesting that our results are not limited to the specific window*
2575 *we used to compute the baseline pupil size.*

2576
2577
2578

7.2 Extended data from Chapter 5

ROI	Pre	Post	Paired t-test pre vs. post
vPulv	44.70 ± 0.77	44.00 ± 0.77	t(24) = 1.20 p = 0.25 lgBF = -0.41
LGN	42.97 ± 0.64	42.94 ± 0.42	t(24) = 0.08 p = 0.94 lgBF = -0.67
dPulv	41.61± 1.67	39.80 ± 1.98	t(24) = 0.64 p = 0.53 lgBF = -0.60
V1	121.54± 9.03	120.60± 8.54	t(24) = 0.09 p =0.93 lgBF = -0.67

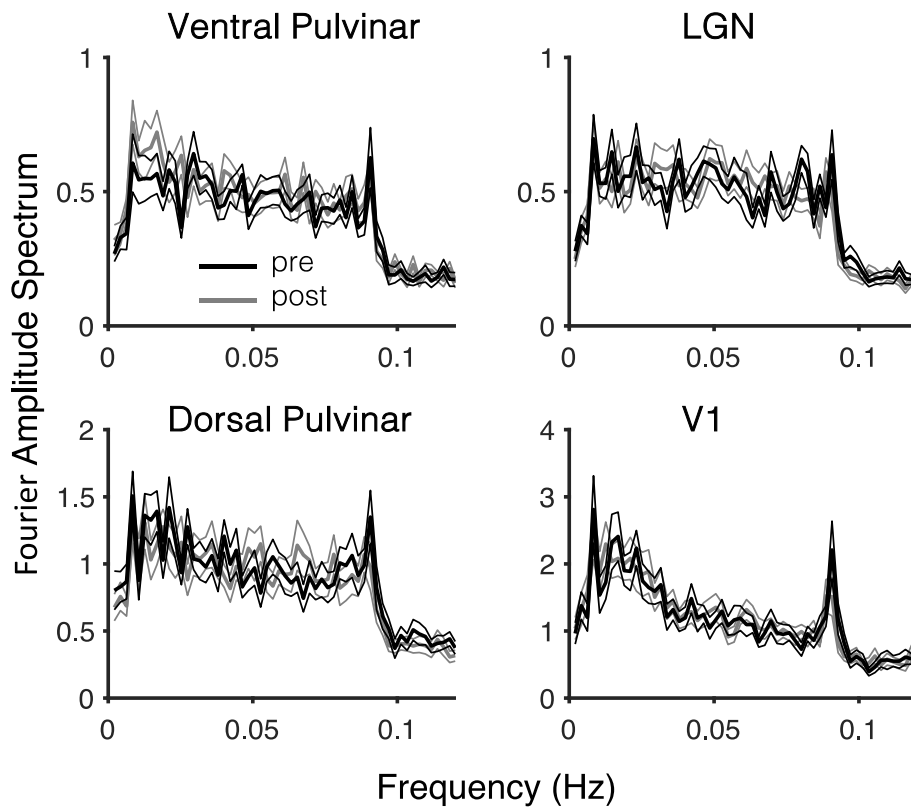
2579
2580
2581

2582 *Table 7-2 Signal-to-noise ratios for the seed regions of interest*

2583 *Signal-to-noise ratio (SNR) of the BOLD activities in the four seed regions of interest. For each*
2584 *condition, SNRs were computed as the voxel-wise ratio between the average activity across*
2585 *time and its standard deviation, then averaged across voxels and across subjects. Reported*
2586 *values are mean ±S.E.M.*

2587 *Paired t-tests, reported in the leftmost column, show that the SNR for each region did not*
2588 *change after monocular deprivation.*

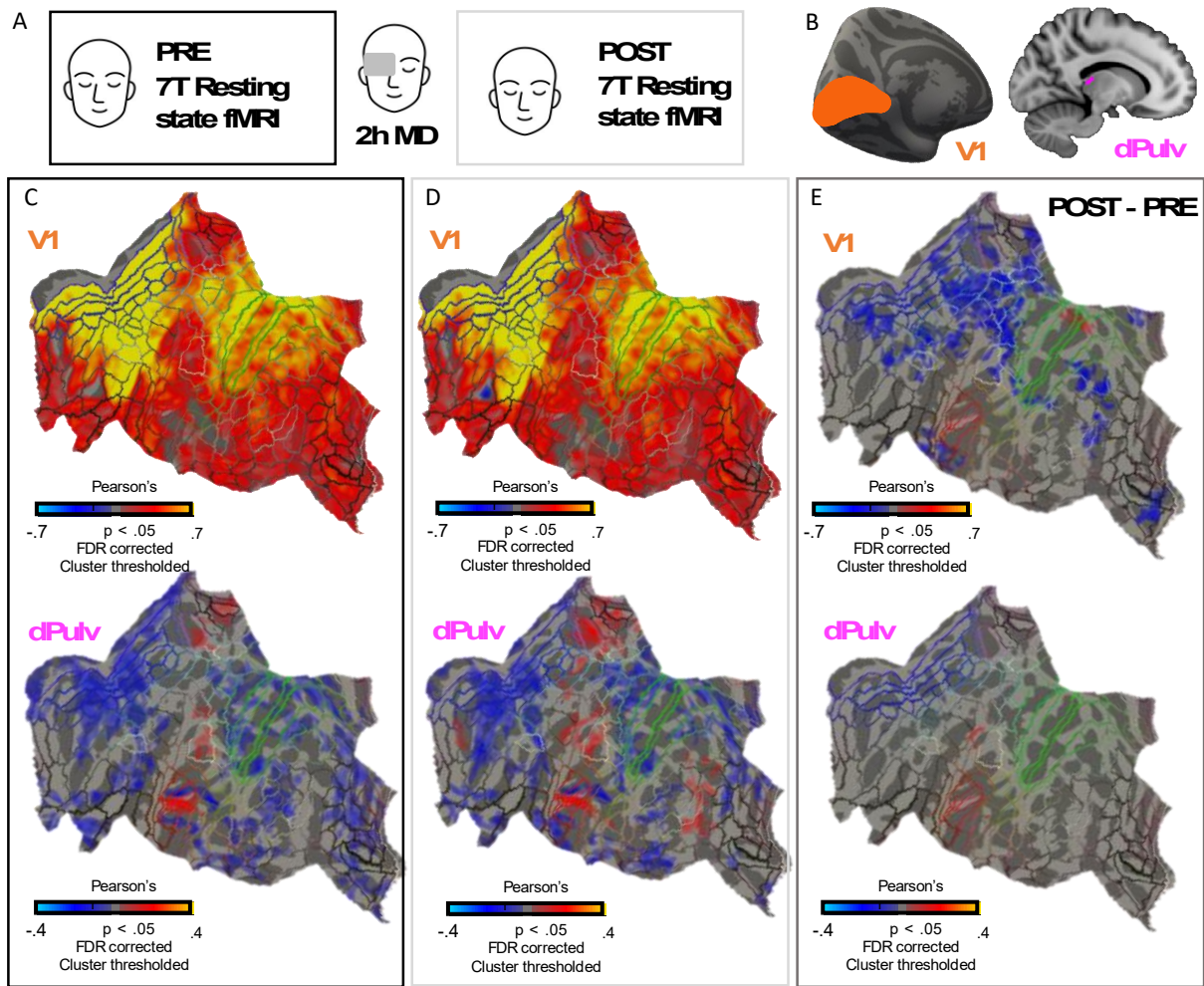
2589



2590
 2591
 2592
 2593
 2594
 2595
 2596
 2597
 2598

Figure 7-3 Fourier amplitude spectra for the seed regions of interest

*Group-average Fourier amplitude spectra for the four seed regions of interest before (black plot) and after (grey plot) monocular deprivation. Reported values are mean \pm S.E.M. Paired *t*-tests showed no changes after monocular deprivation at any temporal frequency (all $p_{FDRcorrected} > 0.05$).*

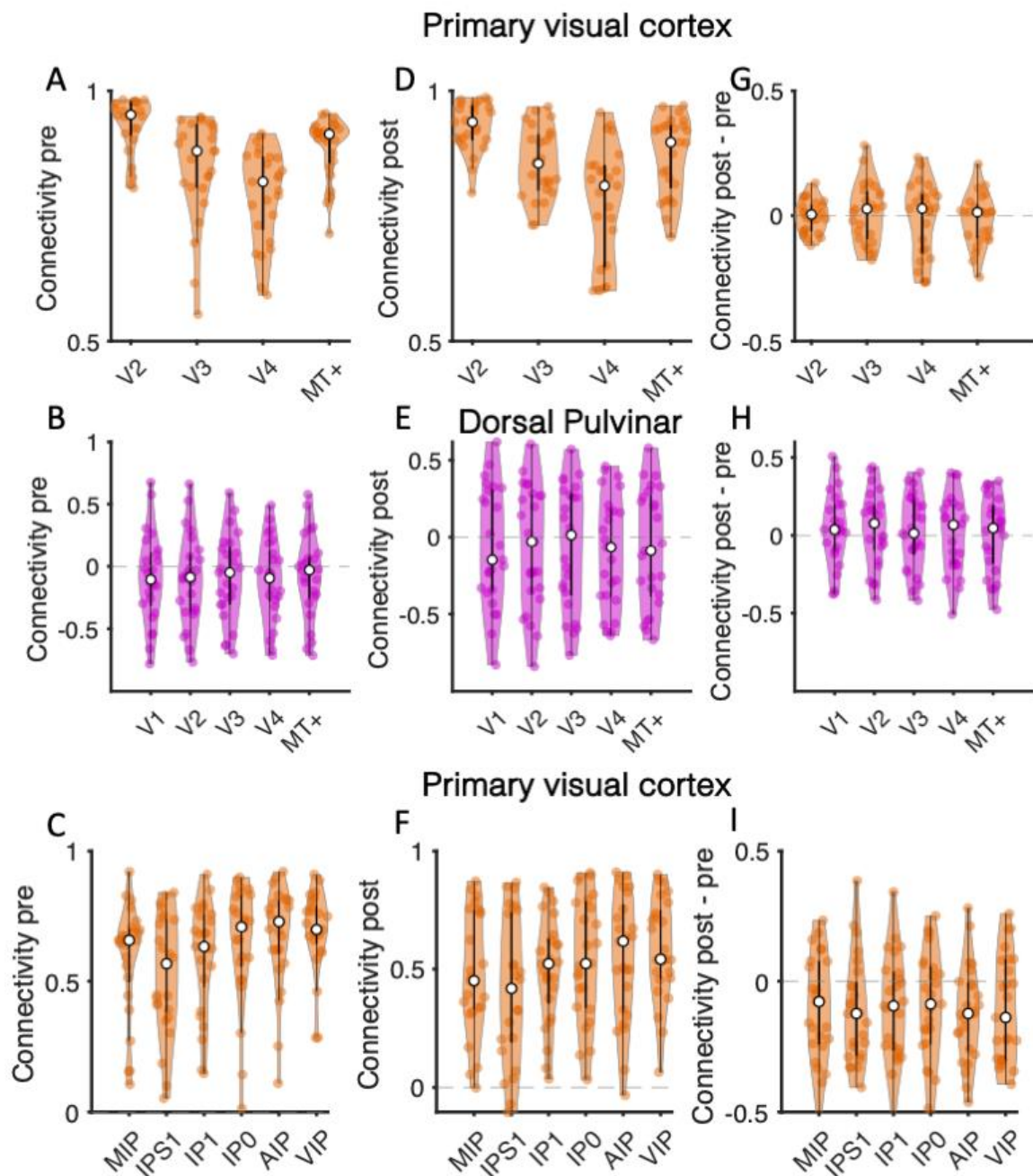


2599
2600

2601 *Figure 7-4 V1 and dPulv functional connectivity patterns*

2602 *A – Experimental design. Resting state functional images were acquired before and after two*
 2603 *hours of monocular deprivation. Participants were instructed to keep their eyes closed for the*
 2604 *entire duration of the acquisitions. B – Sagittal view of the V1 ROI mapped on the*
 2605 *fsaverage_sym surface template and dPulv mapped on the 1 mm³ MNI template. C-D Super-*
 2606 *subjects correlation maps computed before (C) and after (D) monocular deprivation for the*
 2607 *two seeds: V1 and dPulv. E- Maps of super-subjects correlation differences (post–pre*
 2608 *deprivation) for V1 and dPulv. All maps are thresholded by False Discovery Rate (FDR)*
 2609 *corrected p values (alpha = 0.05) and cluster size (threshold = 200 mm²).*

2610



2611

2612

2613 *Figure 7-5 V1 and dPulv functional connectivity with visual and intraparietal regions*

2614 *A-F: Correlation between the cortical regions of interest (on the x-axis) and V1 (A,C,D,F) or*

2615 *dPulv (B,E) before and after monocular deprivation. G-I: Differences in correlation values (post*

2616 *– pre deprivation) between the cortical regions of interest (on the x-axis) and V1 (G,I) or dPulv*

2617 *(H). From A to I, thick black error bars indicate the ends of the first and third quartiles, thin*

2618 *black bars indicate 95% confidence intervals. The white circle indicates the median across*

2619 *subjects. Single points indicate individual values.*

2620
2621
2622
2623
2624
2625
2626
2627
2628
2629
2630
2631
2632
2633
2634
2635
2636
2637
2638
2639
2640
2641
2642
2643
2644
2645
2646
2647
2648
2649
2650
2651
2652
2653
2654
2655
2656
2657
2658
2659

Figures 7-4 and 7-5 show the effects of monocular deprivation on two supplementary seed regions, the primary visual cortex and the dorsal pulvinar.

These correlation maps show no effect of monocular deprivation on the functional connectivity pattern of the dPulv, which remained uncorrelated with the visual cortex (Figure 7-4), as confirmed by the within-subjects analysis (Figure 7-5; one sample t-tests: all $|t(24)| > 1$, all $p_{FDRcorrected} > .05$).

V1 functional connectivity showed a different outcome. The super-subjects maps show a decrease in functional connectivity between V1 and the intra-parietal cortex (Figure 7-4). We confirmed this observation by performing one-sample t-tests across subjects on the post-pre differences, that showed a significant connectivity decrease with the Intraparietal Areas (Figure 7-5 bottom panel: all $|t(24)| > 2.5$, all $p_{FDRcorrected} < .05$). No effect of monocular patching was found on the connectivity between V1 and extra striatal areas (Figure 7-5; one sample t-tests on post-pre differences: all $|t(24)| > 0.4$, all $p_{FDRcorrected} > .05$).

2660 8 Bibliography

2661

2662 Acquafredda, M., Binda, P., & Lunghi, C. (2022). Attention Cueing in Rivalry: Insights from
2663 Pupillometry. *Eneuro*, 9(3), ENEURO.0497-21.2022.
2664 <https://doi.org/10.1523/ENEURO.0497-21.2022>

2665 Acquafredda, M., Sari, İ. D., Steinwurz, C., Lunghi, C., & Binda, P. (2023). Measuring the
2666 reliability of binocular rivalry. *Journal of Vision*, 23(10), 5.
2667 <https://doi.org/10.1167/jov.23.10.5>

2668 Alais, D., & Blake, R. (2015). *Binocular rivalry and perceptual ambiguity*.

2669 Alais D., Blake, R., & PH.D, R. B. (2005). *Binocular Rivalry*.

2670 Alais, D., Cass, J., O’Shea, R. P., & Blake, R. (2010). Visual sensitivity underlying changes in
2671 visual consciousness. *Current Biology*, 20(15), 1362–1367.
2672 <https://doi.org/10.1016/j.cub.2010.06.015>

2673 Alais, D., O’Shea, R. P., Mesana-Alais, C., & Wilson, I. G. (2000). On Binocular Alternation.
2674 *Perception*, 29(12), 1437–1445. <https://doi.org/10.1068/p3017>

2675 Alais, D., van Boxtel, J. J., Parker, A., & van Ee, R. (2010). Attending to auditory signals slows
2676 visual alternations in binocular rivalry. *Vision Research*, 50(10), 929–935.
2677 <https://doi.org/10.1016/j.visres.2010.03.010>

2678 Alpers, G. W., Adolph, D., & Pauli, P. (2011). Emotional scenes and facial expressions elicit
2679 different psychophysiological responses. *International Journal of Psychophysiology*,
2680 80(3), 173–181. <https://doi.org/10.1016/j.ijpsycho.2011.01.010>

2681 Altman, D. G., & Bland, J. M. (1983). Measurement in Medicine: The Analysis of Method
2682 Comparison Studies. *The Statistician*, 32(3), 307. <https://doi.org/10.2307/2987937>

2683 Animal, S., Steinwurz, C., Dardano, A., Sancho-Bornez, V., Del Prato, S., Morrone, M. C.,
2684 Daniele, G., & Binda, P. (2023). Effect of fasting on short-term visual plasticity in adult
2685 humans. *European Journal of Neuroscience*, 57(1), 148–162.
2686 <https://doi.org/10.1111/ejn.15873>

2687 Arcaro, M. J., Pinsk, M. A., Chen, J., & Kastner, S. (2018). Organizing principles of pulvino-
2688 cortical functional coupling in humans. *Nature Communications*, 9(1).
2689 <https://doi.org/10.1038/s41467-018-07725-6>

2690 Arcaro, M. J., Pinsk, M. A., & Kastner, S. (2015). The anatomical and functional organization of
2691 the human visual pulvinar. *Journal of Neuroscience*, 35(27), 9848–9871.
2692 <https://doi.org/10.1523/JNEUROSCI.1575-14.2015>

2693 Avants, B. B., Tustison, N. J., Song, G., Cook, P. A., Klein, A., & Gee, J. C. (2011). A reproducible
2694 evaluation of ANTs similarity metric performance in brain image registration.
2695 *NeuroImage*, 54(3), 2033–2044. <https://doi.org/10.1016/j.neuroimage.2010.09.025>

2696 AVANTS, B., EPSTEIN, C., GROSSMAN, M., & GEE, J. (2008). Symmetric diffeomorphic image
2697 registration with cross-correlation: Evaluating automated labeling of elderly and
2698 neurodegenerative brain. *Medical Image Analysis*, 12(1), 26–41.
2699 <https://doi.org/10.1016/j.media.2007.06.004>

2700 Bai, J., Dong, X., He, S., & Bao, M. (2017a). Monocular deprivation of Fourier phase information
2701 boosts the deprived eye’s dominance during interocular competition but not interocular
2702 phase combination. *Neuroscience*, 352, 122–130.
2703 <https://doi.org/10.1016/j.neuroscience.2017.03.053>

2704 Bai, J., Dong, X., He, S., & Bao, M. (2017b). Monocular deprivation of Fourier phase
2705 information boosts the deprived eye’s dominance during interocular competition but not

2706 interocular phase combination. *Neuroscience*, 352, 122–130.
2707 <https://doi.org/10.1016/j.neuroscience.2017.03.053>

2708 Baker, D. H. (2010). Visual Consciousness: The Binocular Rivalry Explosion. *Current Biology*,
2709 20(15), R644–R646. <https://doi.org/10.1016/j.cub.2010.06.010>

2710 Bao, M., Dong, B., Liu, L., Engel, S. A., & Jiang, Y. (2018). The Best of Both Worlds: Adaptation
2711 During Natural Tasks Produces Long-Lasting Plasticity in Perceptual Ocular Dominance.
2712 *Psychological Science*, 29(1), 14–33. <https://doi.org/10.1177/0956797617728126>

2713 Baroncelli, L., & Lunghi, C. (2021). Neuroplasticity of the visual cortex: in sickness and in
2714 health. *Experimental Neurology*, 335, 113515.
2715 <https://doi.org/10.1016/j.expneurol.2020.113515>

2716 Bartels, A., & Logothetis, N. K. (2010). Binocular rivalry: A time dependence of eye and
2717 stimulus contributions. *Journal of Vision*, 10(12), 3–3. <https://doi.org/10.1167/10.12.3>

2718 Benarroch, E. E. (2015). Pulvinar: Associative role in cortical function and clinical correlations.
2719 In *Neurology* (Vol. 84, Issue 7, pp. 738–747). Lippincott Williams and Wilkins.
2720 <https://doi.org/10.1212/WNL.0000000000001276>

2721 Benjamini, Y., & Hochberg, Y. (1995). Controlling the False Discovery Rate: A Practical and
2722 Powerful Approach to Multiple Testing. *Journal of the Royal Statistical Society: Series B*
2723 *(Methodological)*, 57(1), 289–300. <https://doi.org/10.1111/j.2517-6161.1995.tb02031.x>

2724 Binda, P., & Gamlin, P. D. (2017). Renewed Attention on the Pupil Light Reflex. *Trends in*
2725 *Neurosciences*, 40(8), 455–457. <https://doi.org/10.1016/j.tins.2017.06.007>

2726 Binda, P., Kurzawski, J., Lunghi, C., Biagi, L., Tosetti, M., & Morrone, M. C. (2017). Short-term
2727 monocular deprivation enhances 7T BOLD responses and reduces neural selectivity in V1.
2728 *Journal of Vision*, 17(10), 577. <https://doi.org/10.1167/17.10.577>

2729 Binda, P., Kurzawski, J. W., Lunghi, C., Biagi, L., Tosetti, M., & Morrone, M. C. (2018). Response
2730 to short-term deprivation of the human adult visual cortex measured with 7T BOLD. *ELife*,
2731 7. <https://doi.org/10.7554/eLife.40014>

2732 Binda, P., & Lunghi, C. (2017). Short-Term Monocular Deprivation Enhances Physiological
2733 Pupillary Oscillations. *Neural Plasticity*, 2017, 1–10.
2734 <https://doi.org/10.1155/2017/6724631>

2735 Binda, P., & Murray, S. O. (2015a). Keeping a large-pupilled eye on high-level visual processing.
2736 *Trends in Cognitive Sciences*, 19(1), 1–3. <https://doi.org/10.1016/j.tics.2014.11.002>

2737 Binda, P., & Murray, S. O. (2015b). Spatial attention increases the pupillary response to light
2738 changes. *Journal of Vision*, 15(2), 1–1. <https://doi.org/10.1167/15.2.1>

2739 Binda, P., Pereverzeva, M., & Murray, S. O. (2013a). Attention to Bright Surfaces Enhances the
2740 Pupillary Light Reflex. *The Journal of Neuroscience*, 33(5), 2199–2204.
2741 <https://doi.org/10.1523/JNEUROSCI.3440-12.2013>

2742 Binda, P., Pereverzeva, M., & Murray, S. O. (2013b). Pupil constrictions to photographs of the
2743 sun. *Journal of Vision*, 13(6), 8–8. <https://doi.org/10.1167/13.6.8>

2744 Binda, P., Pereverzeva, M., & Murray, S. O. (2014). Pupil size reflects the focus of feature-based
2745 attention. *Journal of Neurophysiology*, 112(12), 3046–3052.
2746 <https://doi.org/10.1152/jn.00502.2014>

2747 Blake, R. (1989). A neural theory of binocular rivalry. *Psychological Review*, 96(1), 145–167.
2748 <https://doi.org/10.1037/0033-295X.96.1.145>

2749 Blake, R., & Logothetis, N. K. (2002). Visual competition. *Nature Reviews Neuroscience*, 3(1),
2750 13–21. <https://doi.org/10.1038/nrn701>

2751 Blake, R., Westendorf, D. H., & Overton, R. (1980). What is Suppressed during Binocular
2752 Rivalry? *Perception*, 9(2), 223–231. <https://doi.org/10.1068/p090223>

2753 Bombeke, K., Duthoo, W., Mueller, S. C., Hopf, J.-M., & Boehler, C. N. (2016). Pupil size directly
2754 modulates the feedforward response in human primary visual cortex independently of
2755 attention. *NeuroImage*, *127*, 67–73. <https://doi.org/10.1016/j.neuroimage.2015.11.072>
2756 Boynton, G. M. (2009). A framework for describing the effects of attention on visual responses.
2757 *Vision Research*, *49*(10), 1129–1143. <https://doi.org/10.1016/j.visres.2008.11.001>
2758 Brainard, D. H. (1997). The Psychophysics Toolbox. *Spatial Vision*, *10*(4), 433–436.
2759 <https://doi.org/10.1163/156856897X00357>
2760 Brascamp, J. W., Becker, M. W., & Hambrick, D. Z. (2018). Revisiting individual differences in
2761 the time course of binocular rivalry. *Journal of Vision*, *18*(7), 3.
2762 <https://doi.org/10.1167/18.7.3>
2763 Brascamp, J. W., & Blake, R. (2012). Inattention Abolishes Binocular Rivalry: Perceptual
2764 Evidence. *Psychological Science*, *23*(10), 1159–1167.
2765 <https://doi.org/10.1177/0956797612440100>
2766 Brascamp, J. W., de Hollander, G., Wertheimer, M. D., DePew, A. N., & Knapen, T. (2021).
2767 Separable pupillary signatures of perception and action during perceptual multistability.
2768 *ELife*, *10*. <https://doi.org/10.7554/eLife.66161>
2769 Brascamp, J. W., Klink, P. C., & Levelt, W. J. M. (2015). The “laws” of binocular rivalry: 50 years
2770 of Levelt’s propositions. In *Vision Research* (Vol. 109, Issue Part A, pp. 20–37). Elsevier
2771 Ltd. <https://doi.org/10.1016/j.visres.2015.02.019>
2772 Brascamp, J. W., van Ee, R., Noest, A. J., Jacobs, R. H. A. H., & van den Berg, A. V. (2006). The
2773 time course of binocular rivalry reveals a fundamental role of noise. *Journal of Vision*,
2774 *6*(11), 8–8. <https://doi.org/10.1167/6.11.8>
2775 Bridge, H., Leopold, D. A., & Bourne, J. A. (2016a). Adaptive Pulvinar Circuitry Supports Visual
2776 Cognition. *Trends in Cognitive Sciences*, *20*(2), 146–157.
2777 <https://doi.org/10.1016/j.tics.2015.10.003>
2778 Bridge, H., Leopold, D. A., & Bourne, J. A. (2016b). Adaptive Pulvinar Circuitry Supports Visual
2779 Cognition. In *Trends in Cognitive Sciences* (Vol. 20, Issue 2, pp. 146–157). Elsevier Ltd.
2780 <https://doi.org/10.1016/j.tics.2015.10.003>
2781 Carrasco, M. (2011). Visual attention: The past 25 years. *Vision Research*, *51*(13), 1484–1525.
2782 <https://doi.org/10.1016/j.visres.2011.04.012>
2783 Carrasco, M., & Barbot, A. (2019). Spatial attention alters visual appearance. *Current Opinion*
2784 *in Psychology*, *29*, 56–64. <https://doi.org/10.1016/j.copsyc.2018.10.010>
2785 Carter, O. L., & Pettigrew, J. D. (2003). A Common Oscillator for Perceptual Rivalries?
2786 *Perception*, *32*(3), 295–305. <https://doi.org/10.1068/p3472>
2787 Castaldi, E., Lunghi, C., & Morrone, M. C. (2020). Neuroplasticity in adult human visual cortex.
2788 *Neuroscience & Biobehavioral Reviews*, *112*, 542–552.
2789 <https://doi.org/10.1016/j.neubiorev.2020.02.028>
2790 Chadnova, E., Reynaud, A., Clavagnier, S., & Hess, R. F. (2017). Short-term monocular occlusion
2791 produces changes in ocular dominance by a reciprocal modulation of interocular
2792 inhibition. *Scientific Reports*, *7*(1), 41747. <https://doi.org/10.1038/srep41747>
2793 Chong, S. C., Tadin, D., & Blake, R. (2005a). Endogenous attention prolongs dominance
2794 durations in binocular rivalry. *Journal of Vision*, *5*(11), 6. <https://doi.org/10.1167/5.11.6>
2795 Chong, S. C., Tadin, D., & Blake, R. (2005b). Endogenous attention prolongs dominance
2796 durations in binocular rivalry. *Journal of Vision*, *5*(11), 1004–1012.
2797 <https://doi.org/10.1167/5.11.6>
2798 Cieslak, M., Cook, P. A., He, X., Yeh, F.-C., Dhollander, T., Adebimpe, A., Aguirre, G. K., Bassett,
2799 D. S., Betzel, R. F., Bourque, J., Cabral, L. M., Davatzikos, C., Detre, J. A., Earl, E., Elliott, M.

2800 A., Fadnavis, S., Fair, D. A., Foran, W., Fotiadis, P., ... Satterthwaite, T. D. (2021). QSIPrep:
2801 an integrative platform for preprocessing and reconstructing diffusion MRI data. *Nature*
2802 *Methods*, 18(7), 775–778. <https://doi.org/10.1038/s41592-021-01185-5>

2803 Clark, A. (2013). Whatever next? Predictive brains, situated agents, and the future of cognitive
2804 science. *Behavioral and Brain Sciences*, 36(3), 181–204.
2805 <https://doi.org/10.1017/S0140525X12000477>

2806 COBB, W. A., MORTON, H. B., & ETTLINGER, G. (1967). Cerebral Potentials evoked by Pattern
2807 Reversal and their Suppression in Visual Rivalry. *Nature*, 216(5120), 1123–1125.
2808 <https://doi.org/10.1038/2161123b0>

2809 Cohen, J., Cohen, P., West, S. G., & Aiken, L. S. (2003). *Applied multiple regression/correlation*
2810 *analysis for the behavioral sciences (3rd ed.)*. Mahwah, NJ: Lawrence Erlbaum.

2811 Collins, D. L., Holmes, C. J., Peters, T. M., & Evans, A. C. (1995). Automatic 3-D model-based
2812 neuroanatomical segmentation. *Human Brain Mapping*, 3(3), 190–208.
2813 <https://doi.org/10.1002/hbm.460030304>

2814 Cornelissen, F. W., Peters, E. M., & Palmer, J. (2002). The Eyelink Toolbox: Eye tracking with
2815 MATLAB and the Psychophysics Toolbox. *Behavior Research Methods, Instruments, &*
2816 *Computers*, 34(4), 613–617. <https://doi.org/10.3758/BF03195489>

2817 de Gee, J. W., Tsetsos, K., Schwabe, L., Urai, A. E., McCormick, D., McGinley, M. J., & Donner,
2818 T. H. (2020). Pupil-linked phasic arousal predicts a reduction of choice bias across species
2819 and decision domains. *ELife*, 9. <https://doi.org/10.7554/eLife.54014>

2820 Di Russo, F. (2003). Source Analysis of Event-related Cortical Activity during Visuo-spatial
2821 Attention. *Cerebral Cortex*, 13(5), 486–499. <https://doi.org/10.1093/cercor/13.5.486>

2822 Di Russo, F., Martínez, A., Sereno, M. I., Pitzalis, S., & Hillyard, S. A. (2002). Cortical sources of
2823 the early components of the visual evoked potential. *Human Brain Mapping*, 15(2), 95–
2824 111. <https://doi.org/10.1002/hbm.10010>

2825 Dieter, K. C., Brascamp, J., Tadin, D., & Blake, R. (2016). Does visual attention drive the
2826 dynamics of bistable perception? *Attention, Perception, & Psychophysics*, 78(7), 1861–
2827 1873. <https://doi.org/10.3758/s13414-016-1143-2>

2828 Dieter, K. C., Melnick, M. D., & Tadin, D. (2015). When can attention influence binocular
2829 rivalry? *Attention, Perception, and Psychophysics*, 77(6), 1908–1918.
2830 <https://doi.org/10.3758/s13414-015-0905-6>

2831 Dieter, K. C., Sy, J., & Blake, R. (2017a). Persistent Biases in Binocular Rivalry Dynamics within
2832 the Visual Field. *Vision*, 1(3), 18. <https://doi.org/10.3390/vision1030018>

2833 Dieter, K. C., Sy, J. L., & Blake, R. (2017b). Individual differences in sensory eye dominance
2834 reflected in the dynamics of binocular rivalry. *Vision Research*, 141, 40–50.
2835 <https://doi.org/10.1016/j.visres.2016.09.014>

2836 Ding, Y., Naber, M., Gayet, S., Van der Stigchel, S., & Paffen, C. L. E. (2018). Assessing the
2837 generalizability of eye dominance across binocular rivalry, onset rivalry, and continuous
2838 flash suppression. *Journal of Vision*, 18(6), 6. <https://doi.org/10.1167/18.6.6>

2839 Dunn, S., & Jones, M. (2020). Binocular rivalry dynamics associated with high levels of self-
2840 reported autistic traits suggest an imbalance of cortical excitation and inhibition.
2841 *Behavioural Brain Research*, 388, 112603. <https://doi.org/10.1016/j.bbr.2020.112603>

2842 DURAND, A. C. (1910). A METHOD OF DETERMINING OCULAR DOMINANCE. *JAMA: The*
2843 *Journal of the American Medical Association*, 55(5), 369.
2844 <https://doi.org/10.1001/jama.1910.04330050007004>

2845 Ebitz, R. B., & Moore, T. (2017). Selective Modulation of the Pupil Light Reflex by
2846 Microstimulation of Prefrontal Cortex. *The Journal of Neuroscience*, 37(19), 5008–5018.
2847 <https://doi.org/10.1523/JNEUROSCI.2433-16.2017>

2848 Ebitz, R. B., Pearson, J. M., & Platt, M. L. (2014). Pupil size and social vigilance in rhesus
2849 macaques. *Frontiers in Neuroscience*, 8. <https://doi.org/10.3389/fnins.2014.00100>

2850 Einhäuser, W., Stout, J., Koch, C., & Carter, O. (2008). Pupil dilation reflects perceptual selection
2851 and predicts subsequent stability in perceptual rivalry. *Proceedings of the National
2852 Academy of Sciences*, 105(5), 1704–1709. <https://doi.org/10.1073/pnas.0707727105>

2853 Fahle, M. W., Stemmler, T., & Spang, K. M. (2011). How Much of the ?Unconscious? is Just
2854 Pre ? Threshold? *Frontiers in Human Neuroscience*, 5.
2855 <https://doi.org/10.3389/fnhum.2011.00120>

2856 Fischl, B., Salat, D. H., Busa, E., Albert, M., Dieterich, M., Haselgrove, C., van der Kouwe, A.,
2857 Killiany, R., Kennedy, D., Klaveness, S., Montillo, A., Makris, N., Rosen, B., & Dale, A. M.
2858 (2002). Whole Brain Segmentation. *Neuron*, 33(3), 341–355.
2859 [https://doi.org/10.1016/S0896-6273\(02\)00569-X](https://doi.org/10.1016/S0896-6273(02)00569-X)

2860 Fox, R., & Check, R. (1972). Independence between binocular rivalry suppression duration and
2861 magnitude of suppression. *Journal of Experimental Psychology*, 93(2), 283–289.
2862 <https://doi.org/10.1037/h0032455>

2863 Frässle, S., Harrison, S. J., Heinzle, J., Clementz, B. A., Tamminga, C. A., Sweeney, J. A., Gershon,
2864 E. S., Keshavan, M. S., Pearlson, G. D., Powers, A., & Stephan, K. E. (2021). Regression
2865 dynamic causal modeling for resting-state fMRI. *Human Brain Mapping*, 42(7), 2159–
2866 2180. <https://doi.org/10.1002/hbm.25357>

2867 Frässle, S., Lomakina, E. I., Kasper, L., Manjaly, Z. M., Leff, A., Pruessmann, K. P., Buhmann, J.
2868 M., & Stephan, K. E. (2018). A generative model of whole-brain effective connectivity.
2869 *NeuroImage*, 179, 505–529. <https://doi.org/10.1016/j.neuroimage.2018.05.058>

2870 Frässle, S., Lomakina, E. I., Razi, A., Friston, K. J., Buhmann, J. M., & Stephan, K. E. (2017).
2871 Regression DCM for fMRI. *NeuroImage*, 155, 406–421.
2872 <https://doi.org/10.1016/j.neuroimage.2017.02.090>

2873 Friston, K. (2005). A theory of cortical responses. *Philosophical Transactions of the Royal
2874 Society B: Biological Sciences*, 360(1456), 815–836.
2875 <https://doi.org/10.1098/rstb.2005.1622>

2876 Friston, K. (2010). The free-energy principle: A unified brain theory? In *Nature Reviews
2877 Neuroscience* (Vol. 11, Issue 2, pp. 127–138). <https://doi.org/10.1038/nrn2787>

2878 Friston K.J., Ashburner J.T., Kiebel S.J., Nichols T.E., & Penny W.D. (2007). *Statistical Parametric
2879 Mapping: the Analysis of Functional Brain Images*. Elsevier/Academic Press.

2880 Gallagher, R. M., & Arnold, D. H. (2014). Interpreting the Temporal Dynamics of Perceptual
2881 Rivalries. *Perception*, 43(11), 1239–1248. <https://doi.org/10.1068/p7648>

2882 Galuske, R. A. W., Munk, M. H. J., & Singer, W. (2019). Relation between gamma oscillations
2883 and neuronal plasticity in the visual cortex. *Proceedings of the National Academy of
2884 Sciences of the United States of America*, 116(46), 23317–23325.
2885 <https://doi.org/10.1073/pnas.1901277116>

2886 George, D., & Hawkins, J. (2009). Towards a Mathematical Theory of Cortical Micro-circuits.
2887 *PLoS Computational Biology*, 5(10), e1000532.
2888 <https://doi.org/10.1371/journal.pcbi.1000532>

2889 Glasser, M. F., Coalson, T. S., Robinson, E. C., Hacker, C. D., Harwell, J., Yacoub, E., Ugurbil, K.,
2890 Andersson, J., Beckmann, C. F., Jenkinson, M., Smith, S. M., & Van Essen, D. C. (2016). A

2891 multi-modal parcellation of human cerebral cortex. *Nature*, 536(7615), 171–178.
2892 <https://doi.org/10.1038/nature18933>

2893 Goebel, R., Esposito, F., & Formisano, E. (2006). Analysis of functional image analysis contest
2894 (FIAC) data with brainvoyager QX: From single-subject to cortically aligned group general
2895 linear model analysis and self-organizing group independent component analysis.
2896 *Human Brain Mapping*, 27(5), 392–401. <https://doi.org/10.1002/hbm.20249>

2897 Gong, L., Reynaud, A., Hess, R. F., & Zhou, J. (2023). The Suppressive Basis of Ocular
2898 Dominance Changes Induced by Short-Term Monocular Deprivation in Normal and
2899 Amblyopic Adults. *Investigative Ophthalmology & Visual Science*, 64(13), 2.
2900 <https://doi.org/10.1167/iovs.64.13.2>

2901 Goodale, M. A., & Milner, A. D. (1992). Separate visual pathways for perception and action.
2902 *Trends in Neurosciences*, 15(1), 20–25. [https://doi.org/10.1016/0166-2236\(92\)90344-8](https://doi.org/10.1016/0166-2236(92)90344-8)

2903 Gorgolewski, K. J., Auer, T., Calhoun, V. D., Craddock, R. C., Das, S., Duff, E. P., Flandin, G.,
2904 Ghosh, S. S., Glatard, T., Halchenko, Y. O., Handwerker, D. A., Hanke, M., Keator, D., Li, X.,
2905 Michael, Z., Maumet, C., Nichols, B. N., Nichols, T. E., Pellman, J., ... Poldrack, R. A. (2016).
2906 The brain imaging data structure, a format for organizing and describing outputs of
2907 neuroimaging experiments. *Scientific Data*, 3(1), 160044.
2908 <https://doi.org/10.1038/sdata.2016.44>

2909 Greve, D. N., Van der Haegen, L., Cai, Q., Stufflebeam, S., Sabuncu, M. R., Fischl, B., &
2910 Brysbaert, M. (2013). A Surface-based Analysis of Language Lateralization and Cortical
2911 Asymmetry. *Journal of Cognitive Neuroscience*, 25(9), 1477–1492.
2912 https://doi.org/10.1162/jocn_a_00405

2913 Han, S., Alais, D., MacDougall, H., & Verstraten, F. A. J. (2020). Brief localised monocular
2914 deprivation in adults alters binocular rivalry predominance retinotopically and reduces
2915 spatial inhibition. *Scientific Reports*, 10(1), 18739. <https://doi.org/10.1038/s41598-020-75252-w>

2917 Hancock, S., & Andrews, T. J. (2007a). The Role of Voluntary and Involuntary Attention in
2918 Selecting Perceptual Dominance during Binocular Rivalry. *Perception*, 36(2), 288–298.
2919 <https://doi.org/10.1068/p5494>

2920 Hancock, S., & Andrews, T. J. (2007b). The role of voluntary and involuntary attention in
2921 selecting perceptual dominance during binocular rivalry. *Perception*, 36(2), 288–298.
2922 <https://doi.org/10.1068/p5494>

2923 Handa, T., Uozato, H., Higa, R., Nitta, M., Kawamorita, T., Ishikawa, H., Shoji, N., & Shimizu, K.
2924 (2006). Quantitative measurement of ocular dominance using binocular rivalry induced
2925 by retinometers. *Journal of Cataract and Refractive Surgery*, 32(5), 831–836.
2926 <https://doi.org/10.1016/j.jcrs.2006.01.082>

2927 He, H.-Y., Hodos, W., & Quinlan, E. M. (2006). Visual Deprivation Reactivates Rapid Ocular
2928 Dominance Plasticity in Adult Visual Cortex. *The Journal of Neuroscience*, 26(11), 2951–
2929 2955. <https://doi.org/10.1523/JNEUROSCI.5554-05.2006>

2930 HENSCH, T. K., & QUINLAN, E. M. (2018). Critical periods in amblyopia. *Visual Neuroscience*,
2931 35, E014. <https://doi.org/10.1017/S0952523817000219>

2932 Hillyard, S. A., & Anllo-Vento, L. (1998). Event-related brain potentials in the study of visual
2933 selective attention. *Proceedings of the National Academy of Sciences*, 95(3), 781–787.
2934 <https://doi.org/10.1073/pnas.95.3.781>

2935 Hohwy Jakob. (2013). *The Predictive Mind*. Oxford, GB: Oxford University Press UK .

2936 Huang, Y., & Rao, R. P. N. (2011). Predictive coding. *WIREs Cognitive Science*, 2(5), 580–593.
2937 <https://doi.org/10.1002/wcs.142>

- 2938 Hubel, D. H., & Wiesel, T. N. (1965). RECEPTIVE FIELDS AND FUNCTIONAL ARCHITECTURE IN
 2939 TWO NONSTRIATE VISUAL AREAS (18 AND 19) OF THE CAT. *Journal of Neurophysiology*,
 2940 28(2), 229–289. <https://doi.org/10.1152/jn.1965.28.2.229>
- 2941 HURLEY, L., DEVILBISS, D., & WATERHOUSE, B. (2004). A matter of focus: monoaminergic
 2942 modulation of stimulus coding in mammalian sensory networks. *Current Opinion in*
 2943 *Neurobiology*, 14(4), 488–495. <https://doi.org/10.1016/j.conb.2004.06.007>
- 2944 Jaramillo, J., Mejias, J. F., & Wang, X. J. (2019). Engagement of Pulvino-cortical Feedforward
 2945 and Feedback Pathways in Cognitive Computations. *Neuron*, 101(2), 321-336.e9.
 2946 <https://doi.org/10.1016/j.neuron.2018.11.023>
- 2947 Jenkinson, M., Beckmann, C. F., Behrens, T. E. J., Woolrich, M. W., & Smith, S. M. (2012). FSL.
 2948 *NeuroImage*, 62(2), 782–790. <https://doi.org/10.1016/j.neuroimage.2011.09.015>
- 2949 Jezzard, P., & Balaban, R. S. (1995). Correction for geometric distortion in echo planar images
 2950 from B 0 field variations. *Magnetic Resonance in Medicine*, 34(1), 65–73.
 2951 <https://doi.org/10.1002/mrm.1910340111>
- 2952 Jia, T., Cao, L., Ye, X., Wei, Q., Xie, W., Cai, C., Dong, Y., Xia, C., Tian, Y., & Wang, K. (2020).
 2953 Difference in binocular rivalry rate between major depressive disorder and generalized
 2954 anxiety disorder. *Behavioural Brain Research*, 391, 112704.
 2955 <https://doi.org/10.1016/j.bbr.2020.112704>
- 2956 Jia, T., Ye, X., Wei, Q., Xie, W., Cai, C., Mu, J., Dong, Y., Hu, P., Hu, X., Tian, Y., & Wang, K. (2015).
 2957 Difference in the binocular rivalry rate between depressive episodes and remission.
 2958 *Physiology & Behavior*, 151, 272–278. <https://doi.org/10.1016/j.physbeh.2015.08.007>
- 2959 Kaas, J. H., & Lyon, D. C. (2007). Pulvinar contributions to the dorsal and ventral streams of
 2960 visual processing in primates. *Brain Research Reviews*, 55(2), 285–296.
 2961 <https://doi.org/10.1016/j.brainresrev.2007.02.008>
- 2962 Kalogeraki, E., Greifzu, F., Haack, F., & Löwel, S. (2014). Voluntary Physical Exercise Promotes
 2963 Ocular Dominance Plasticity in Adult Mouse Primary Visual Cortex. *The Journal of*
 2964 *Neuroscience*, 34(46), 15476–15481. <https://doi.org/10.1523/JNEUROSCI.2678-14.2014>
- 2965 Kanai, R., Komura, Y., Shipp, S., & Friston, K. (2015). Cerebral hierarchies: Predictive
 2966 processing, precision and the pulvinar. *Philosophical Transactions of the Royal Society B:*
 2967 *Biological Sciences*, 370(1668). <https://doi.org/10.1098/rstb.2014.0169>
- 2968 Kardon, R. H. (2005). Anatomy and Physiology of the Autonomic Nervous System. In *Wash and*
 2969 *Hoyt's Clinical Neuro-Ophthalmology* (6th ed., pp. 649–714). Spencer S. Eccles Health
 2970 Sciences Library, University of Utah.
- 2971 Kasper, L., Bollmann, S., Diaconescu, A. O., Hutton, C., Heinzle, J., Iglesias, S., Hauser, T. U.,
 2972 Sebold, M., Manjaly, Z.-M., Pruessmann, K. P., & Stephan, K. E. (2017). The PhysIO Toolbox
 2973 for Modeling Physiological Noise in fMRI Data. *Journal of Neuroscience Methods*, 276,
 2974 56–72. <https://doi.org/10.1016/j.jneumeth.2016.10.019>
- 2975 Kass, R. E., & Raftery, A. E. (1995). Bayes Factors. *Journal of the American Statistical*
 2976 *Association*, 90(430), 773–795. <https://doi.org/10.1080/01621459.1995.10476572>
- 2977 Kelly, D. H. (1961). Visual Responses to Time-Dependent Stimuli* I Amplitude Sensitivity
 2978 Measurements†. *Journal of the Optical Society of America*, 51(4), 422.
 2979 <https://doi.org/10.1364/JOSA.51.000422>
- 2980 Kelly, S. P., Gomez-Ramirez, M., & Foxe, J. J. (2008). Spatial Attention Modulates Initial Afferent
 2981 Activity in Human Primary Visual Cortex. *Cerebral Cortex*, 18(11), 2629–2636.
 2982 <https://doi.org/10.1093/cercor/bhn022>

- 2983 Keyzers, C., Gazzola, V., & Wagenmakers, E.-J. (2020). Using Bayes factor hypothesis testing in
 2984 neuroscience to establish evidence of absence. *Nature Neuroscience*, *23*(7), 788–799.
 2985 <https://doi.org/10.1038/s41593-020-0660-4>
- 2986 Khoe, W., Mitchell, J. F., Reynolds, J. H., & Hillyard, S. A. (2008). ERP evidence that surface-
 2987 based attention biases interocular competition during rivalry. *Journal of Vision*, *8*(3).
 2988 <https://doi.org/10.1167/8.3.18>
- 2989 Kim, H.-W., Kim, C.-Y., & Blake, R. (2017). Monocular Perceptual Deprivation from Interocular
 2990 Suppression Temporarily Imbalances Ocular Dominance. *Current Biology*, *27*(6), 884–
 2991 889. <https://doi.org/10.1016/j.cub.2017.01.063>
- 2992 Knau, H. (2000). Thresholds for detecting slowly changing Ganzfeld luminances. *Journal of the*
 2993 *Optical Society of America A*, *17*(8), 1382. <https://doi.org/10.1364/JOSAA.17.001382>
- 2994 Konen, C. S., & Kastner, S. (2008). Two hierarchically organized neural systems for object
 2995 information in human visual cortex. *Nature Neuroscience*, *11*(2), 224–231.
 2996 <https://doi.org/10.1038/nn2036>
- 2997 Kova'cs, I. K., Papathomas, T. V., Yang, M., And', A., & Fehér, A. (1996). *When the brain changes*
 2998 *its mind: Interocular grouping during binocular rivalry (psychophysicsbinocular*
 2999 *visionchromatic rivalryvisual awareness)* (Vol. 93).
- 3000 Kurzawski, J. W., Lunghi, C., Biagi, L., Tosetti, M., Morrone, M. C., & Binda, P. (2022). Short-
 3001 term plasticity in the human visual thalamus. *ELife*, *11*.
 3002 <https://doi.org/10.7554/eLife.74565>
- 3003 Kwon, M., Legge, G. E., Fang, F., Cheong, A. M. Y., & He, S. (2009). Adaptive changes in visual
 3004 cortex following prolonged contrast reduction. *Journal of Vision*, *9*(2), 20–20.
 3005 <https://doi.org/10.1167/9.2.20>
- 3006 Laeng, B., Sirois, S., & Gredebäck, G. (2012). Pupillometry: A window to the preconscious?
 3007 *Perspectives on Psychological Science*, *7*(1), 18–27.
 3008 <https://doi.org/10.1177/1745691611427305>
- 3009 Laeng, B., & Sulutvedt, U. (2014). The Eye Pupil Adjusts to Imaginary Light. *Psychological*
 3010 *Science*, *25*(1), 188–197. <https://doi.org/10.1177/0956797613503556>
- 3011 Lansing, R. W. (1964). Electroencephalographic Correlates of Binocular Rivalry in Man. *Science*,
 3012 *146*(3649), 1325–1327. <https://doi.org/10.1126/science.146.3649.1325>
- 3013 Lederer, J. (1961). Ocular Dominance. *Clinical and Experimental Optometry*, *44*(11), 531–574.
 3014 <https://doi.org/10.1111/j.1444-0938.1961.tb06505.x>
- 3015 Lehky, S. R. (1988). An Astable Multivibrator Model of Binocular Rivalry. *Perception*, *17*(2),
 3016 215–228. <https://doi.org/10.1068/p170215>
- 3017 Lehmkuhle, S. W., & Fox, R. (1975). Effect of binocular rivalry suppression on the motion
 3018 aftereffect. *Vision Research*, *15*(7), 855–859. [https://doi.org/10.1016/0042-6989\(75\)90266-7](https://doi.org/10.1016/0042-6989(75)90266-7)
- 3020 Leopold, D. A., & Logothetis, N. K. (1999). Multistable phenomena: changing views in
 3021 perception. *Trends in Cognitive Sciences*, *3*(7), 254–264. [https://doi.org/10.1016/S1364-6613\(99\)01332-7](https://doi.org/10.1016/S1364-6613(99)01332-7)
- 3023 LEVELT, W. J. M. (1966). THE ALTERNATION PROCESS IN BINOCULAR RIVALRY. *British Journal of*
 3024 *Psychology*, *57*(3–4), 225–238. <https://doi.org/10.1111/j.2044-8295.1966.tb01023.x>
- 3025 LEVELT, W. J. M. (1967). NOTE ON THE DISTRIBUTION OF DOMINANCE TIMES IN BINOCULAR
 3026 RIVALRY. *British Journal of Psychology*, *58*(1–2), 143–145.
 3027 <https://doi.org/10.1111/j.2044-8295.1967.tb01068.x>

- 3028 Levi, D. M., & Carkeet, A. (1993). Amblyopia: a consequence of abnormal visual development.
 3029 In *Early Visual Development, Normal and Abnormal* (K. Simons, pp. 391–408). Oxford
 3030 University Press, New York, NY.
- 3031 Li, H. H., Rankin, J., Rinzal, J., Carrasco, M., & Heeger, D. J. (2017). Attention model of binocular
 3032 rivalry. *Proceedings of the National Academy of Sciences of the United States of America*,
 3033 *114*(30), E6192–E6201. <https://doi.org/10.1073/pnas.1620475114>
- 3034 Liu, T., Pestilli, F., & Carrasco, M. (2005). Transient Attention Enhances Perceptual Performance
 3035 and fMRI Response in Human Visual Cortex. *Neuron*, *45*(3), 469–477.
 3036 <https://doi.org/10.1016/j.neuron.2004.12.039>
- 3037 Liu, Z., de Zwart, J. A., Yao, B., van Gelderen, P., Kuo, L. W., & Duyn, J. H. (2012). Finding
 3038 thalamic BOLD correlates to posterior alpha EEG. *NeuroImage*, *63*(3), 1060–1069.
 3039 <https://doi.org/10.1016/j.neuroimage.2012.08.025>
- 3040 Loewenfeld. (1993). *The Pupil: Anatomy, Physiology, and Clinical Applications*. Ames: Iowa
 3041 State University Press.
- 3042 Logothetis, N. K., Leopold, D. A., & Sheinberg, D. L. (1996). What is rivalling during binocular
 3043 rivalry? *Nature*, *380*(6575), 621–624. <https://doi.org/10.1038/380621a0>
- 3044 LOWE, S. W., & OGLE, K. N. (1966). Dynamics of the Pupil During Binocular Rivalry. *Archives of*
 3045 *Ophthalmology*, *75*(3), 395–403.
 3046 <https://doi.org/10.1001/archophth.1966.00970050397017>
- 3047 Lunghi, C., Berchicci, M., Morrone, M. C., & Di Russo, F. (2015). Short-term monocular
 3048 deprivation alters early components of visual evoked potentials. *Journal of Physiology*,
 3049 *593*(19), 4361–4372. <https://doi.org/10.1113/JP270950>
- 3050 Lunghi, C., Burr, D. C., & Morrone, C. (2011). Brief periods of monocular deprivation disrupt
 3051 ocular balance in human adult visual cortex. *Current Biology*, *21*(14), R538–R539.
 3052 <https://doi.org/10.1016/j.cub.2011.06.004>
- 3053 Lunghi, C., Burr, D. C., & Morrone, M. C. (2013). Long-term effects of monocular deprivation
 3054 revealed with binocular rivalry gratings modulated in luminance and in color. *Journal of*
 3055 *Vision*, *13*(6), 1–1. <https://doi.org/10.1167/13.6.1>
- 3056 Lunghi, C., Emir, U. E., Morrone, M. C., & Bridge, H. (2015). Short-Term Monocular Deprivation
 3057 Alters GABA in the Adult Human Visual Cortex. *Current Biology*, *25*(11), 1496–1501.
 3058 <https://doi.org/10.1016/j.cub.2015.04.021>
- 3059 Lunghi, C., & Sale, A. (2015). A cycling lane for brain rewiring. *Current Biology*, *25*(23), R1122–
 3060 R1123. <https://doi.org/10.1016/j.cub.2015.10.026>
- 3061 Lunghi, C., Sframeli, A. T., Lepri, A., Lepri, M., Lisi, D., Sale, A., & Morrone, M. C. (2019). A new
 3062 counterintuitive training for adult amblyopia. *Annals of Clinical and Translational*
 3063 *Neurology*, *6*(2), 274–284. <https://doi.org/10.1002/acn3.698>
- 3064 Lyu, L., He, S., Jiang, Y., Engel, S. A., & Bao, M. (2020). Natural-scene-based Steady-state Visual
 3065 Evoked Potentials Reveal Effects of Short-term Monocular Deprivation. *Neuroscience*,
 3066 *435*, 10–21. <https://doi.org/10.1016/j.neuroscience.2020.03.039>
- 3067 Mack, A., Pappas, Z., Silverman, M., & Gay, R. (2002). What we see: Inattention and the
 3068 capture of attention by meaning. *Consciousness and Cognition*, *11*(4), 488–506.
 3069 [https://doi.org/10.1016/S1053-8100\(02\)00028-4](https://doi.org/10.1016/S1053-8100(02)00028-4)
- 3070 Marx, S., & Einhauser, W. (2015). Reward modulates perception in binocular rivalry. *Journal of*
 3071 *Vision*, *15*(1), 11–11. <https://doi.org/10.1167/15.1.11>
- 3072 Mathôt, S. (2018). Pupillometry: Psychology, Physiology, and Function. *Journal of Cognition*,
 3073 *1*(1). <https://doi.org/10.5334/joc.18>

- 3074 Mathot, S., Dalmaijer, E., Grainger, J., & Van der Stigchel, S. (2014). The pupillary light response
3075 reflects exogenous attention and inhibition of return. *Journal of Vision*, *14*(14), 7–7.
3076 <https://doi.org/10.1167/14.14.7>
- 3077 Mathôt, S., Grainger, J., & Strijkers, K. (2017). Pupillary Responses to Words That Convey a
3078 Sense of Brightness or Darkness. *Psychological Science*, *28*(8), 1116–1124.
3079 <https://doi.org/10.1177/0956797617702699>
- 3080 Mathôt, S., Melmi, J.-B., van der Linden, L., & Van der Stigchel, S. (2016). The Mind-Writing
3081 Pupil: A Human-Computer Interface Based on Decoding of Covert Attention through
3082 Pupillometry. *PLOS ONE*, *11*(2), e0148805.
3083 <https://doi.org/10.1371/journal.pone.0148805>
- 3084 Mathôt, S., van der Linden, L., Grainger, J., & Vitu, F. (2013). The Pupillary Light Response
3085 Reveals the Focus of Covert Visual Attention. *PLoS ONE*, *8*(10), e78168.
3086 <https://doi.org/10.1371/journal.pone.0078168>
- 3087 Mathôt, S., & Van der Stigchel, S. (2015). New Light on the Mind's Eye. *Current Directions in*
3088 *Psychological Science*, *24*(5), 374–378. <https://doi.org/10.1177/0963721415593725>
- 3089 Mazziotta, J., Toga, A., Evans, A., Fox, P., Lancaster, J., Zilles, K., Woods, R., Paus, T., Simpson,
3090 G., Pike, B., Holmes, C., Collins, L., Thompson, P., MacDonald, D., Iacoboni, M.,
3091 Schormann, T., Amunts, K., Palomero-Gallagher, N., Geyer, S., ... Mazoyer, B. (2001). A
3092 probabilistic atlas and reference system for the human brain: International Consortium
3093 for Brain Mapping (ICBM). *Philosophical Transactions of the Royal Society of London.*
3094 *Series B: Biological Sciences*, *356*(1412), 1293–1322.
3095 <https://doi.org/10.1098/rstb.2001.0915>
- 3096 McDougal, D. H., & Gamlin, P. D. (2014). Autonomic Control of the Eye. In *Comprehensive*
3097 *Physiology* (pp. 439–473). Wiley. <https://doi.org/10.1002/cphy.c140014>
- 3098 McDougal, D. H., & Gamlin, P. D. R. (2008). Pupillary Control Pathways. In *The Senses: A*
3099 *Comprehensive Reference* (pp. 521–536). Elsevier. [https://doi.org/10.1016/B978-](https://doi.org/10.1016/B978-012370880-9.00282-6)
3100 [012370880-9.00282-6](https://doi.org/10.1016/B978-012370880-9.00282-6)
- 3101 Meng, M., & Tong, F. (2004). Can attention selectively bias bistable perception? Differences
3102 between binocular rivalry and ambiguous figures. *Journal of Vision*, *4*(7), 2.
3103 <https://doi.org/10.1167/4.7.2>
- 3104 MILLER, S. M., GYNTHNER, B. D., HESLOP, K. R., LIU, G. B., MITCHELL, P. B., NGO, T. T., PETTIGREW,
3105 J. D., & GEFFEN, L. B. (2003). Slow binocular rivalry in bipolar disorder. *Psychological*
3106 *Medicine*, *33*(4), 683–692. <https://doi.org/10.1017/S0033291703007475>
- 3107 Miller, S. M., Hansell, N. K., Ngo, T. T., Liu, G. B., Pettigrew, J. D., Martin, N. G., & Wright, M. J.
3108 (2010). Genetic contribution to individual variation in binocular rivalry rate. *Proceedings*
3109 *of the National Academy of Sciences*, *107*(6), 2664–2668.
3110 <https://doi.org/10.1073/pnas.0912149107>
- 3111 Min, S. H., Gong, L., Baldwin, A. S., Reynaud, A., He, Z., Zhou, J., & Hess, R. F. (2021). Some
3112 psychophysical tasks measure ocular dominance plasticity more reliably than others.
3113 *Journal of Vision*, *21*(8), 20. <https://doi.org/10.1167/jov.21.8.20>
- 3114 Mishra, J., & Hillyard, S. A. (2009). Endogenous attention selection during binocular rivalry at
3115 early stages of visual processing. *Vision Research*, *49*(10), 1073–1080.
3116 <https://doi.org/10.1016/j.visres.2008.02.018>
- 3117 Mitchell, J. F., Stoner, G. R., & Reynolds, J. H. (2004). Object-based attention determines
3118 dominance in binocular rivalry. *Nature*, *429*(6990), 410–413.
3119 <https://doi.org/10.1038/nature02584>

3120 Miura, S. K., & Scanziani, M. (2022). Distinguishing externally from saccade-induced motion in
3121 visual cortex. *Nature*, *610*(7930), 135–142. <https://doi.org/10.1038/s41586-022-05196->
3122 [w](https://doi.org/10.1038/s41586-022-05196-w)

3123 Moini A., & Piran P. (2020). *Functional and Clinical Neuroanatomy*. Elsevier.
3124 <https://doi.org/10.1016/C2018-0-01786-7>

3125 Mumford, D. (1992). On the computational architecture of the neocortex. *Biological*
3126 *Cybernetics*, *66*(3), 241–251. <https://doi.org/10.1007/BF00198477>

3127 Murphy, P. R., Wilming, N., Hernandez-Bocanegra, D. C., Prat-Ortega, G., & Donner, T. H.
3128 (2021). Adaptive circuit dynamics across human cortex during evidence accumulation in
3129 changing environments. *Nature Neuroscience*, *24*(7), 987–997.
3130 <https://doi.org/10.1038/s41593-021-00839-z>

3131 Naber, M., Alvarez, G. A., & Nakayama, K. (2013). Tracking the allocation of attention using
3132 human pupillary oscillations. *Frontiers in Psychology*, *4*.
3133 <https://doi.org/10.3389/fpsyg.2013.00919>

3134 Naber, M., Frässle, S., & Einhäuser, W. (2011). Perceptual Rivalry: Reflexes Reveal the Gradual
3135 Nature of Visual Awareness. *PLoS ONE*, *6*(6), e20910.
3136 <https://doi.org/10.1371/journal.pone.0020910>

3137 Nagamine, M., Yoshino, A., Yamazaki, M., Obara, M., Sato, S., Takahashi, Y., & Nomura, S.
3138 (2007). Accelerated binocular rivalry with anxious personality. *Physiology & Behavior*,
3139 *91*(1), 161–165. <https://doi.org/10.1016/j.physbeh.2007.02.016>

3140 Ngo, T. T., Mitchell, P. B., Martin, N. G., & Miller, S. M. (2011). Psychiatric and genetic studies
3141 of binocular rivalry: an endophenotype for bipolar disorder? *Acta Neuropsychiatrica*,
3142 *23*(1), 37–42. <https://doi.org/10.1111/j.1601-5215.2010.00510.x>

3143 Nguyen, B. N., Malavita, M., Carter, O. L., & McKendrick, A. M. (2021). Neuroplasticity in older
3144 adults revealed by temporary occlusion of one eye. *Cortex*, *143*, 1–11.
3145 <https://doi.org/10.1016/j.cortex.2021.07.004>

3146 Nguyen, K. N., Watanabe, T., & Andersen, G. J. (2020). Role of endogenous and exogenous
3147 attention in task-relevant visual perceptual learning. *PLOS ONE*, *15*(8), e0237912.
3148 <https://doi.org/10.1371/journal.pone.0237912>

3149 Norman, L. J., Heywood, C. A., & Kentridge, R. W. (2015). Exogenous attention to unseen
3150 objects? *Consciousness and Cognition*, *35*, 319–329.
3151 <https://doi.org/10.1016/j.concog.2015.02.015>

3152 Olmos-Solis, K., van Loon, A. M., & Olivers, C. N. L. (2018). Pupil Dilation Reflects Task
3153 Relevance Prior to Search. *Journal of Cognition*, *1*(1). <https://doi.org/10.5334/joc.12>

3154 Ooi, T. L., & He, Z. J. (1999). Binocular Rivalry and Visual Awareness: The Role of Attention.
3155 *Perception*, *28*(5), 551–574. <https://doi.org/10.1068/p2923>

3156 Ooi, T. L., & He, Z. J. (2001). Sensory eye dominance. *Optometry (St. Louis, Mo.)*, *72*(3), 168–
3157 178.

3158 Ooi, T. L., & He, Z. J. (2020). Sensory Eye Dominance: Relationship Between Eye and Brain. *Eye*
3159 *and Brain, Volume 12*, 25–31. <https://doi.org/10.2147/EB.S176931>

3160 Ooi, T. L., Su, Y. R., Natale, D. M., & He, Z. J. (2013). A push-pull treatment for strengthening
3161 the ‘lazy eye’ in amblyopia. *Current Biology*, *23*(8), R309–R310.
3162 <https://doi.org/10.1016/j.cub.2013.03.004>

3163 Paffen, C. L. E., & Alais, D. (2011). Attentional Modulation of Binocular Rivalry. *Frontiers in*
3164 *Human Neuroscience*, *5*. <https://doi.org/10.3389/fnhum.2011.00105>

3165 Paffen, C. L. E., Alais, D., & Verstraten, F. A. J. (2006). Attention Speeds Binocular Rivalry.
3166 *Psychological Science*, *17*(9), 752–756. [https://doi.org/10.1111/j.1467-](https://doi.org/10.1111/j.1467-9280.2006.01777.x)
3167 [9280.2006.01777.x](https://doi.org/10.1111/j.1467-9280.2006.01777.x)

3168 Paffen, C. L. E., & Van der Stigchel, S. (2010). Shifting spatial attention makes you flip:
3169 Exogenous visual attention triggers perceptual alternations during binocular rivalry.
3170 *Attention, Perception, & Psychophysics*, *72*(5), 1237–1243.
3171 <https://doi.org/10.3758/APP.72.5.1237>

3172 Pestilli, F., Carrasco, M., Heeger, D. J., & Gardner, J. L. (2011). Attentional Enhancement via
3173 Selection and Pooling of Early Sensory Responses in Human Visual Cortex. *Neuron*, *72*(5),
3174 832–846. <https://doi.org/10.1016/j.neuron.2011.09.025>

3175 Pfeffer, T., Keitel, C., Kluger, D. S., Keitel, A., Russmann, A., Thut, G., Donner, T. H., & Gross, J.
3176 (2022). Coupling of pupil- and neuronal population dynamics reveals diverse influences
3177 of arousal on cortical processing. *ELife*, *11*. <https://doi.org/10.7554/eLife.71890>

3178 Plebanek, D. J., & Sloutsky, V. M. (2019). Selective attention, filtering, and the development of
3179 working memory. *Developmental Science*, *22*(1). <https://doi.org/10.1111/desc.12727>

3180 Pomè, A., Binda, P., Cicchini, G. M., & Burr, D. C. (2020). Pupillometry correlates of visual
3181 priming, and their dependency on autistic traits. *Journal of Vision*, *20*(3), 3.
3182 <https://doi.org/10.1167/jovi.20.3.3>

3183 Pomè, A., Burr, D. C., Capuozzo, A., & Binda, P. (2020). Spontaneous pupillary oscillations
3184 increase during mindfulness meditation. *Current Biology*, *30*(18), R1030–R1031.
3185 <https://doi.org/10.1016/j.cub.2020.07.064>

3186 Porta, G. della. (1593). *De refractione optices parte: Libri novem*.

3187 Purushothaman, G., Marion, R., Li, K., & Casagrande, V. A. (2012). Gating and control of
3188 primary visual cortex by pulvinar. *Nature Neuroscience*, *15*(6), 905–912.
3189 <https://doi.org/10.1038/nn.3106>

3190 Qiu, S. X., Caldwell, C. L., You, J. Y., & Mendola, J. D. (2020). Binocular rivalry from luminance
3191 and contrast. *Vision Research*, *175*, 41–50. <https://doi.org/10.1016/j.visres.2020.06.006>

3192 Ramamurthy, M., & Blaser, E. (2018). Assessing the kaleidoscope of monocular deprivation
3193 effects. *Journal of Vision*, *18*(13), 14. <https://doi.org/10.1167/18.13.14>

3194 Rangelov, D., & Mattingley, J. B. (2020). Evidence accumulation during perceptual decision-
3195 making is sensitive to the dynamics of attentional selection. *NeuroImage*, *220*, 117093.
3196 <https://doi.org/10.1016/j.neuroimage.2020.117093>

3197 Rao, R. P. N., & Ballard, D. H. (1999). Predictive coding in the visual cortex: a functional
3198 interpretation of some extra-classical receptive-field effects. *Nature Neuroscience*, *2*(1),
3199 79–87. <https://doi.org/10.1038/4580>

3200 Reimer, J., Froudarakis, E., Cadwell, C. R., Yatsenko, D., Denfield, G. H., & Tolias, A. S. (2014).
3201 Pupil Fluctuations Track Fast Switching of Cortical States during Quiet Wakefulness.
3202 *Neuron*, *84*(2), 355–362. <https://doi.org/10.1016/j.neuron.2014.09.033>

3203 Reimer, J., McGinley, M. J., Liu, Y., Rodenkirch, C., Wang, Q., McCormick, D. A., & Tolias, A. S.
3204 (2016). Pupil fluctuations track rapid changes in adrenergic and cholinergic activity in
3205 cortex. *Nature Communications*, *7*(1), 13289. <https://doi.org/10.1038/ncomms13289>

3206 Richardson, J. T. E. (2011). Eta squared and partial eta squared as measures of effect size in
3207 educational research. *Educational Research Review*, *6*(2), 135–147.
3208 <https://doi.org/10.1016/j.edurev.2010.12.001>

3209 Robertson, C. E., Kravitz, D. J., Freyberg, J., Baron-Cohen, S., & Baker, C. I. (2013). Slower Rate
3210 of Binocular Rivalry in Autism. *The Journal of Neuroscience*, *33*(43), 16983–16991.
3211 <https://doi.org/10.1523/JNEUROSCI.0448-13.2013>

3212 Russo, M. A., Santarelli, D. M., & O'Rourke, D. (2017). The physiological effects of slow
3213 breathing in the healthy human. *Breathe*, *13*(4), 298–309.
3214 <https://doi.org/10.1183/20734735.009817>

3215 Saalman, Y. B., Pinsk, M. A., Wang, L., Li, X., & Kastner, S. (2012). The pulvinar regulates
3216 information transmission between cortical areas based on attention demands. *Science*,
3217 *337*(6095), 753–756. <https://doi.org/10.1126/science.1223082>

3218 Saenz, M., Buracas, G. T., & Boynton, G. M. (2002). Global effects of feature-based attention
3219 in human visual cortex. *Nature Neuroscience*, *5*(7), 631–632.
3220 <https://doi.org/10.1038/nn876>

3221 Sale, A., Maya Vetencourt, J. F., Medini, P., Cenni, M. C., Baroncelli, L., De Pasquale, R., &
3222 Maffei, L. (2007). Environmental enrichment in adulthood promotes amblyopia recovery
3223 through a reduction of intracortical inhibition. *Nature Neuroscience*, *10*(6), 679–681.
3224 <https://doi.org/10.1038/nn1899>

3225 Sari, İ. D., & Lunghi, C. (2023). Different Forms of Plasticity Interact in Adult Humans. *Eneuro*,
3226 *10*(7), ENEURO.0204-22.2023. <https://doi.org/10.1523/ENEURO.0204-22.2023>

3227 Shannon, R. W., Patrick, C. J., Jiang, Y., Bernat, E., & He, S. (2011). Genes contribute to the
3228 switching dynamics of bistable perception. *Journal of Vision*, *11*(3), 8–8.
3229 <https://doi.org/10.1167/11.3.8>

3230 Sherman, S. M. (2005). The role of the thalamus in cortical function: not just a simple relay.
3231 *Thalamus and Related Systems*, *3*(03), 205.
3232 <https://doi.org/10.1017/S1472928807000210>

3233 Sherman, S. M., & Guillery, R. W. (2002). The role of the thalamus in the flow of information
3234 to the cortex. *Philosophical Transactions of the Royal Society B: Biological Sciences*,
3235 *357*(1428), 1695–1708. <https://doi.org/10.1098/rstb.2002.1161>

3236 Shipp, S. (2003). The functional logic of cortico–pulvinar connections. *Philosophical
3237 Transactions of the Royal Society of London. Series B: Biological Sciences*, *358*(1438),
3238 1605–1624. <https://doi.org/10.1098/rstb.2002.1213>

3239 Spiegel, A., Mentch, J., Haskins, A. J., & Robertson, C. E. (2019). Slower Binocular Rivalry in the
3240 Autistic Brain. *Current Biology*, *29*(17), 2948–2953.e3.
3241 <https://doi.org/10.1016/j.cub.2019.07.026>

3242 Spolidoro, M., Baroncelli, L., Putignano, E., Maya-Vetencourt, J. F., Viegi, A., & Maffei, L. (2011).
3243 Food restriction enhances visual cortex plasticity in adulthood. *Nature Communications*,
3244 *2*(1), 320. <https://doi.org/10.1038/ncomms1323>

3245 Steinhauer, S. R., Siegle, G. J., Condray, R., & Pless, M. (2004). Sympathetic and
3246 parasympathetic innervation of pupillary dilation during sustained processing.
3247 *International Journal of Psychophysiology*, *52*(1), 77–86.
3248 <https://doi.org/10.1016/j.ijpsycho.2003.12.005>

3249 Steinwurz, C., Animal, S., Cicchini, G. M., Morrone, M. C., & Binda, P. (2020). Using
3250 psychophysical performance to predict short-term ocular dominance plasticity in human
3251 adults. *Journal of Vision*, *20*(7), 6. <https://doi.org/10.1167/jov.20.7.6>

3252 Steinwurz, C., Morrone, M. C., Sandini, G., & Binda, P. (2023). Active vision gates ocular
3253 dominance plasticity in human adults. *Current Biology*, *33*(20), R1038–R1040.
3254 <https://doi.org/10.1016/j.cub.2023.08.062>

3255 Sterzer, P., & Kleinschmidt, A. (2007). A neural basis for inference in perceptual ambiguity.
3256 *Proceedings of the National Academy of Sciences*, *104*(1), 323–328.
3257 <https://doi.org/10.1073/pnas.0609006104>

- 3258 Sterzer, P., Kleinschmidt, A., & Rees, G. (2009). The neural bases of multistable perception.
 3259 *Trends in Cognitive Sciences*, 13(7), 310–318. <https://doi.org/10.1016/j.tics.2009.04.006>
- 3260 Tong, F. (2001). Competing Theories of Binocular Rivalry: A Possible Resolution. *Brain and*
 3261 *Mind*, 2(1), 55–83. <https://doi.org/10.1023/A:1017942718744>
- 3262 Tong, F., & Engel, S. A. (2001). Interocular rivalry revealed in the human cortical blind-spot
 3263 representation. *Nature*, 411(6834), 195–199. <https://doi.org/10.1038/35075583>
- 3264 Tong, F., Meng, M., & Blake, R. (2006). Neural bases of binocular rivalry. *Trends in Cognitive*
 3265 *Sciences*, 10(11), 502–511. <https://doi.org/10.1016/j.tics.2006.09.003>
- 3266 Tong, F., Nakayama, K., Vaughan, J. T., & Kanwisher, N. (1998). Binocular Rivalry and Visual
 3267 Awareness in Human Extrastriate Cortex. *Neuron*, 21(4), 753–759.
 3268 [https://doi.org/10.1016/S0896-6273\(00\)80592-9](https://doi.org/10.1016/S0896-6273(00)80592-9)
- 3269 Tononi, G. (1998). Consciousness and Complexity. *Science*, 282(5395), 1846–1851.
 3270 <https://doi.org/10.1126/science.282.5395.1846>
- 3271 Tortelli, C., Turi, M., Burr, D. C., & Binda, P. (2021a). Objective pupillometry shows that
 3272 perceptual styles covary with autistic-like personality traits. *ELife*, 10.
 3273 <https://doi.org/10.7554/eLife.67185>
- 3274 Tortelli, C., Turi, M., Burr, D. C., & Binda, P. (2021b). Pupillary Responses Obey Emmert’s Law
 3275 and Co-vary with Autistic Traits. *Journal of Autism and Developmental Disorders*, 51(8),
 3276 2908–2919. <https://doi.org/10.1007/s10803-020-04718-7>
- 3277 Turi, M., Burr, D. C., & Binda, P. (2018). Pupillometry reveals perceptual differences that are
 3278 tightly linked to autistic traits in typical adults. *ELife*, 7.
 3279 <https://doi.org/10.7554/eLife.32399>
- 3280 Turrigiano, G. (2012). Homeostatic Synaptic Plasticity: Local and Global Mechanisms for
 3281 Stabilizing Neuronal Function. *Cold Spring Harbor Perspectives in Biology*, 4(1), a005736–
 3282 a005736. <https://doi.org/10.1101/cshperspect.a005736>
- 3283 Tustison, N. J., & Avants, B. B. (2013). Explicit B-spline regularization in diffeomorphic image
 3284 registration. *Frontiers in Neuroinformatics*, 7. <https://doi.org/10.3389/fninf.2013.00039>
- 3285 Unsworth, N., & Robison, M. K. (2016). Pupillary correlates of lapses of sustained attention.
 3286 *Cognitive, Affective, & Behavioral Neuroscience*, 16(4), 601–615.
 3287 <https://doi.org/10.3758/s13415-016-0417-4>
- 3288 van Ee, R. (2005). Dynamics of perceptual bi-stability for stereoscopic slant rivalry and a
 3289 comparison with grating, house-face, and Necker cube rivalry. *Vision Research*, 45(1), 29–
 3290 40. <https://doi.org/10.1016/j.visres.2004.07.039>
- 3291 van Ee, R., Noest, A. J., Brascamp, J. W., & van den Berg, A. V. (2006). Attentional control over
 3292 either of the two competing percepts of ambiguous stimuli revealed by a two-parameter
 3293 analysis: Means do not make the difference. *Vision Research*, 46(19), 3129–3141.
 3294 <https://doi.org/10.1016/j.visres.2006.03.017>
- 3295 van Ee, R., van Dam, L. C. J., & Brouwer, G. J. (2005). Voluntary control and the dynamics of
 3296 perceptual bi-stability. *Vision Research*, 45(1), 41–55.
 3297 <https://doi.org/10.1016/j.visres.2004.07.030>
- 3298 Van Nes, F. L., & Bouman, M. A. (1967). Spatial Modulation Transfer in the Human Eye. *Journal*
 3299 *of the Optical Society of America*, 57(3), 401. <https://doi.org/10.1364/JOSA.57.000401>
- 3300 Vetencourt, J. F. M., Sale, A., Viegi, A., Baroncelli, L., De Pasquale, R., F. O’Leary, O., Castrén,
 3301 E., & Maffei, L. (2008). The Antidepressant Fluoxetine Restores Plasticity in the Adult
 3302 Visual Cortex. *Science*, 320(5874), 385–388. <https://doi.org/10.1126/science.1150516>

- 3303 Viglione, A., Mazziotti, R., & Pizzorusso, T. (2023). From pupil to the brain: New insights for
 3304 studying cortical plasticity through pupillometry. *Frontiers in Neural Circuits*, 17.
 3305 <https://doi.org/10.3389/fncir.2023.1151847>
- 3306 Wade, N. J., & Wenderoth, P. (1978). The influence of colour and contour rivalry on the
 3307 magnitude of the tilt after-effect. *Vision Research*, 18(7), 827–835.
 3308 [https://doi.org/10.1016/0042-6989\(78\)90123-2](https://doi.org/10.1016/0042-6989(78)90123-2)
- 3309 Wagenmakers, E.-J., Wetzels, R., Borsboom, D., van der Maas, H. L. J., & Kievit, R. A. (2012). An
 3310 Agenda for Purely Confirmatory Research. *Perspectives on Psychological Science*, 7(6),
 3311 632–638. <https://doi.org/10.1177/1745691612463078>
- 3312 Wales, R., & Fox, R. (1970). Increment detection thresholds during binocular rivalry
 3313 suppression. *Perception & Psychophysics*, 8(2), 90–94.
 3314 <https://doi.org/10.3758/BF03210180>
- 3315 Wang, C.-A., & Munoz, D. (2016). Attentional modulation of pupillary light responses by
 3316 microstimulation of the superior colliculus. *Journal of Vision*, 16(12), 936.
 3317 <https://doi.org/10.1167/16.12.936>
- 3318 Wang, C.-A., & Munoz, D. P. (2015). A circuit for pupil orienting responses: implications for
 3319 cognitive modulation of pupil size. *Current Opinion in Neurobiology*, 33, 134–140.
 3320 <https://doi.org/10.1016/j.conb.2015.03.018>
- 3321 Wang, J., Clementz, B. A., & Keil, A. (2007). The neural correlates of feature-based selective
 3322 attention when viewing spatially and temporally overlapping images. *Neuropsychologia*,
 3323 45(7), 1393–1399. <https://doi.org/10.1016/j.neuropsychologia.2006.10.019>
- 3324 Wang, M., McGraw, P., & Ledgeway, T. (2020). Short-term monocular deprivation reduces
 3325 inter-ocular suppression of the deprived eye. *Vision Research*, 173, 29–40.
 3326 <https://doi.org/10.1016/j.visres.2020.05.001>
- 3327 Wheatstone, C. (1838). XVIII. Contributions to the physiology of vision. —Part the first. On
 3328 some remarkable, and hitherto unobserved, phenomena of binocular vision.
 3329 *Philosophical Transactions of the Royal Society of London*, 128, 371–394.
 3330 <https://doi.org/10.1098/rstl.1838.0019>
- 3331 Wiesel, T. N., & Hubel, D. H. (1963). SINGLE-CELL RESPONSES IN STRIATE CORTEX OF KITTENS
 3332 DEPRIVED OF VISION IN ONE EYE. *Journal of Neurophysiology*, 26(6), 1003–1017.
 3333 <https://doi.org/10.1152/jn.1963.26.6.1003>
- 3334 Wilbertz, G., van Kemenade, B. M., Schmack, K., & Sterzer, P. (2017). fMRI-based decoding of
 3335 reward effects in binocular rivalry. *Neuroscience of Consciousness*, 2017(1).
 3336 <https://doi.org/10.1093/nc/nix013>
- 3337 Witz, K., Hinkle, D. E., Wiersma, W., & Jurs, S. G. (1990). Applied Statistics for the Behavioral
 3338 Sciences. *Journal of Educational Statistics*, 15(1), 84. <https://doi.org/10.2307/1164825>
- 3339 Xiao, G., He, K., Chen, X., Wang, L., Bai, X., Gao, L., Zhu, C., & Wang, K. (2018). Slow Binocular
 3340 Rivalry as a Potential Endophenotype of Schizophrenia. *Frontiers in Neuroscience*, 12.
 3341 <https://doi.org/10.3389/fnins.2018.00634>
- 3342 Xu, J. P., He, Z. J., & Ooi, T. L. (2010). Effectively Reducing Sensory Eye Dominance with a Push-
 3343 Pull Perceptual Learning Protocol. *Current Biology*, 20(20), 1864–1868.
 3344 <https://doi.org/10.1016/j.cub.2010.09.043>
- 3345 Xu, J. P., He, Z. J., & Ooi, T. L. (2011). A binocular perimetry study of the causes and implications
 3346 of sensory eye dominance. *Vision Research*, 51(23–24), 2386–2397.
 3347 <https://doi.org/10.1016/j.visres.2011.09.012>
- 3348 Yang, C.-T. (2017). Attention and Perceptual Decision Making. In *Systems Factorial Technology*
 3349 (pp. 199–217). Elsevier. <https://doi.org/10.1016/B978-0-12-804315-8.00013-6>

3350 Ye, X., Zhu, R.-L., Zhou, X.-Q., He, S., & Wang, K. (2019). Slower and Less Variable Binocular
3351 Rivalry Rates in Patients With Bipolar Disorder, OCD, Major Depression, and
3352 Schizophrenia. *Frontiers in Neuroscience*, *13*. <https://doi.org/10.3389/fnins.2019.00514>
3353 Zhang, P., Bao, M., Kwon, M., He, S., & Engel, S. A. (2009). Effects of Orientation-Specific Visual
3354 Deprivation Induced with Altered Reality. *Current Biology*, *19*(22), 1956–1960.
3355 <https://doi.org/10.1016/j.cub.2009.10.018>
3356 Zhang, P., Jamison, K., Engel, S., He, B., & He, S. (2011). Binocular Rivalry Requires Visual
3357 Attention. *Neuron*, *71*(2), 362–369. <https://doi.org/10.1016/j.neuron.2011.05.035>
3358 Zhou, H., Schafer, R. J., & Desimone, R. (2016). Pulvinar-Cortex Interactions in Vision and
3359 Attention. *Neuron*, *89*(1), 209–220. <https://doi.org/10.1016/j.neuron.2015.11.034>
3360 Zhou, J., Clavagnier, S., & Hess, R. F. (2013). Short-term monocular deprivation strengthens the
3361 patched eye's contribution to binocular combination. *Journal of Vision*, *13*(5), 12–12.
3362 <https://doi.org/10.1167/13.5.12>
3363 Zhou, J., He, Z., Wu, Y., Chen, Y., Chen, X., Liang, Y., Mao, Y., Yao, Z., Lu, F., Qu, J., & Hess, R. F.
3364 (2019). Inverse Occlusion: A Binocularly Motivated Treatment for Amblyopia. *Neural*
3365 *Plasticity*, *2019*, 1–12. <https://doi.org/10.1155/2019/5157628>
3366 Zhou, J., Reynaud, A., & Hess, R. F. (2014). Real-time modulation of perceptual eye dominance
3367 in humans. *Proceedings of the Royal Society B: Biological Sciences*, *281*(1795), 20141717.
3368 <https://doi.org/10.1098/rspb.2014.1717>
3369 Ziminski, J. J., Frangou, P., Karlaftis, V. M., Emir, U., & Kourtzi, Z. (2023). Microstructural and
3370 neurochemical plasticity mechanisms interact to enhance human perceptual decision-
3371 making. *PLoS Biology*, *21*(3). <https://doi.org/10.1371/JOURNAL.PBIO.3002029>
3372